Dipartimento di Informatica, Bioingegneria,
Robotica ed Ingegneria dei Sistemi

Optimization and Control of Energy Communities in the Energy Market

by

Virginia Casella

Theses Series **DIBRIS-TH-2026-XX**

DIBRIS, Università di Genova
Via Opera Pia, 13 16145 Genova, Italy http://www.dibris.unige.it/

Università degli Studi di Genova

Dipartimento di Informatica, Bioingegneria,

Robotica ed Ingegneria dei Sistemi

Ph.D. Thesis in Computer Science and Systems Engineering
Computer Science Curriculum

Optimization and Control of Energy Communities in the Energy Market

by

Virginia Casella

May, 2026

Dottorato di Ricerca in Informatica ed Ingegneria dei Sistemi
Indirizzo Informatica
Dipartimento di Informatica, Bioingegneria, Robotica ed Ingegneria dei Sistemi
Università degli Studi di Genova

DIBRIS, Univ. di Genova
Via Opera Pia, 13
I-16145 Genova, Italy
http://www.dibris.unige.it/

Ph.D. Thesis in Computer Science and Systems Engineering
Computer Science Curriculum
(S.S.D. INF/01)

Submitted by Virginia Casella
DIBRIS, Università di Genova

Date of submission: February 2026

Title: Optimization and Control of Energy Communities in the Energy Market

Advisor: Michela Robba Dipartimento di Informatica, Bioingegneria, Robotica ed Ingegneria dei Sistemi
Università di Genova

External Reviewers:

Prof. Mazaher Karimi, University of Vaasa, Finland.

Prof. Vlad Muresan, Technical University of Cluj-Napoca, Romania

A Gin e Rum,
le mie bimbe pelose.
Per sempre.

Abstract

The large-scale integration of renewable energy sources represents the starting point for the energy transition aimed at reducing greenhouse gas emissions and mitigating climate change. However, the increasing penetration of non-programmable and intermittent renewable generation introduces significant challenges for power system operations. In this context, Renewable Energy Communities (RECs) have emerged as a promising solution to foster local renewable integration, enhance self-consumption, and eventually contribute to grid support through coordinated energy management. To address the challenges related to their operational management and maximize their potential, some optimization tools must be developed.

In this context, this thesis focuses on the operational and management aspects of RECs within the Italian regulatory framework. Optimization-based methodologies are developed to support efficient and regulation-aware management of both internal and external REC operations. Internal operations address the management of a single community and its members, integrating traditional objectives, such as cost minimization, with community-level goals, most notably the maximization of shared energy. External operations investigate the participation of RECs in flexibility and balancing mechanisms through demand-side management strategies, considering the coordination of multiple RECs by an aggregator to provide grid services. Then, the last two chapters of this thesis are devoted to modeling and optimal management of complex REC participants, such as smart parking lots and hydrogen-based multi-vector energy hubs, whose flexibility potential can be further enhanced through appropriate control strategies.

The multi-actor and multi-objective nature of RECs is addressed in this thesis by adopting multi-level optimization approaches, which are a valid solution when the problem involves multiple decision makers. To allow for scalable coordination, decentralized algorithms are developed to ensure efficient operation even when the size of the REC increases and in real-time applications.

The results demonstrate that optimization-based Energy Management Systems can effectively support RECs in maximizing shared energy, improving economic performance, and providing flexibility services to the grid. Overall, the proposed approaches contribute to bridging the gap between regulatory frameworks, technological integration, and real-world operations, highlighting the role of RECs as active and flexible entities in future low-carbon energy systems.

Table of Contents

List of Figures

List of Tables

Acronyms

ADMM	Alternating Direction Method of Multipliers
ARERA	*Autorità di Regolazione per Energia Reti e Ambiente*
BADMM	Bregman Alternating Direction Method of Multipliers
CAPEX	Capital Expenditure
CEC	Citizen Energy Community
DSM	Demand Side Management
DR	Demand Response
DSO	Distribution System Operator
EC	Energy Community
ECA	Energy Community Aggregator
ECM	Energy Community Manager
ECP	Energy Community Participant
EMS	Energy Management System
ESS	Energy Storage System
EU	European Union
EVA	Electric Vehicle Aggregator
EV	Electric Vehicle
GHG	Greenhouse Gas
GSE	*Gestore dei Servizi Energetici*
KKT	Karush–Kuhn–Tucker
ICT	Information and Communications Technology
IEA	International Energy Agency
MASE	*Ministero dell'Ambiente e della Sicurezza Energetica*
MISE	*Ministero delle Imprese e dello Sviluppo Economico*
MILP	Mixed-Integer Linear Programming
MINLP	Mixed-Integer Nonlinear Programming
MPC	Model Predictive Control
OPEX	Operational Expenditure
POD	Point of Delivery
PNRR	*Piano Nazionale di Ripresa e Resilienza*
PV	Photovoltaic
QP	Quadratic Programming
REC	Renewable Energy Community
RED II	Renewable Energy Directive (EU) 2018/2001
RES	Renewable Energy Source
SPL	Smart Parking Lot
TIAD	*Testo Integrato Autoconsumo Diffuso*
V2G	Vehicle-to-Grid

Chapter 1

Introduction and motivation

Sustainability has become one of the most popular concepts in recent years, covering economic, social, and environmental sectors. Focusing on the latter, a key challenge is reducing Green-House Gas (GHG) emissions. To achieve this, a deep integration of Renewable Energy Sources (RES) in the electrical grid is essential; however, their intrinsic non-programmable and intermittent nature introduces significant challenges for the power grid, ranging from congestion and voltage fluctuations to the need for additional flexibility. Consequently, innovative strategies are required to foster the integration of RES, while preserving the efficiency of energy systems and enhancing its flexibility. In this context, Renewable Energy Communities (RECs) have emerged as a promising solution because, besides increasing citizen engagement in the energy transition, they promote local production from renewable plants (typically photovoltaic), while enhancing local consumption of that same renewable energy. This "*energy sharing*" would reduce the reverse power flow on the electrical grid and therefore contribute to mitigate the stress on the grid, lower distribution/transmission losses, and limit the need for costly infrastructure reinforcements. Despite their potential, REC integration and operation introduce several challenges. On the users' side, regulatory complexity, investment costs, and uncertainty about economic returns may hinder participation. On the technical side, coordinating distributed energy resources, storage systems, and flexible loads requires advanced management strategies and optimization tools to ensure reliability and economic efficiency while achieving community-level goals. These aspects become even more crucial as RES penetration increases and the need for flexible operation intensifies.

In a landscape where the research community is increasingly focused on identifying solutions that are environmentally sustainable and technologically viable, significant sources of flexibility that might be also included in RECs have gained attention: smart parking lots and multi-vector energy hubs. Smart parking lots (SPLs) are a direct consequence of the widespread mobility electrification and are viewed as strategic nodes in future distribution systems as they couple the energy sector with the transportation sector. Despite representing a significant and concentrated load, SPLs can provide effective flexibility services to the grid if properly controlled; indeed, when equipped with smart charging, vehicle-to-grid (V2G) strategies and real-time energy management, they can help absorb excess renewable production, reduce peak demand, and enhance local self-consumption. Multi-vector hubs integrate different energy carriers (such as electricity, heat, and hydrogen) enabling sector coupling and providing additional flexibility for the energy system. Hydrogen is emerging as a key vector thanks to its potential for balancing renewable generation, serving as a long-term energy storage, and supporting mobility and industrial applications. These systems can therefore foster RES integration as the interaction between different energy carries can compensate for their intermittent and variable nature reducing curtailment and enhancing the overall resilience of local energy infrastructures. Smart parking lots and multi-vector energy hubs can naturally be framed within the REC paradigm. The load represented by SPLs can be integrated with RES and satisfied locally, in line with the key purpose of RECs. Multi-vector energy hubs, managing the inherent flexibility provided by different energy carrier, can either participate in existing RECs or establish dedicated energy communities, enabling local

energy sharing while reducing dependence on the main grid. This integration would open new opportunities for reducing emissions, alleviating stress on the distribution grid, and promoting more democratic and participatory models of energy governance.

This thesis addresses the challenges associated with the integration of RECs, by investigating operational and management aspects of energy communities, also modeling the regulatory framework in Italy. Optimization-based methodologies are developed to optimally manage internal and external operations of a single and multiple energy communities, respectively. Internal operations refer to the management of a single community and its members: in addition to minimizing costs while respecting technical constraints for each participant, the community-level objective of shared energy maximization is also integrated. External operations, on the other hand, investigate the participation of RECs in the balancing market, with a focus on Demand Response (DR); to increase the flexibility capacity and the effectiveness of the service, several RECs coordinated by an aggregator are managed to track the reference power target coming from the system operator. In particular, the thesis chapters address the optimal management problem of a RECs from the perspective of the various actors operating in the REC context: starting with the manager for internal operations, the figure of the aggregator is integrated for market participation. Then, the focus shifted to the participants and the configurations that could potentially form a REC: optimization models for the optimal management of SPLs and multi-vector energy hubs are presented because their potential as RECs (or their participants) can be further enhanced if these entities are properly controlled at the grassroots level. Then, once usual energy management systems are efficient, they could be integrated with community-level constraints, regulation-aware equations and energy sharing maximization objectives.
As regards solution methods, in contrast to conventional energy management systems which are mainly centralized, this thesis adopts multi-level and decentralized optimization frameworks. Multi-level approached are adopted because of the multi-actor nature that characterizes energy community, while decentralized algorithms are developed to ensure efficient operations even for large scale problems.

1.1 Main Contributions

The main contribution of this Ph.D. thesis can be summarized as:

- Analysis of the regulatory and legislative framework on renewable energy communities in Italy.
- Modeling of the real incentive scheme recently introduced by the most recent Italian legislation.
- Development of novel optimization models for the optimal management of a REC internal and external operations.

- Development of optimization models for the optimal management of potential participants in a REC, such as smart parking lots and multi-vector energy hubs.
- Design of decentralized algorithms applied to these problems to ensure efficient operation even in real-time contexts.

1.2 Thesis Organization

The chapters of this thesis address various aspects of REC optimal management (internal and external operations, and potential participants) through various models and methods that we developed during my PhD. Specifically, the chapters are mainly based on journal and conference papers, which are either published or currently under review. This thesis consists of seven Chapters, namely:

Chapter 2 presents the introduction about the renewable energy communities, focusing on the Italian legislation framework and highlighting the main actors within a REC.

Chapter 3 is devoted to the operational management of a REC internal operations and presents two different methods to approach this problem.

Chapter 4 presents an optimization problem where multiple RECs are coordinated for efficient participation in balancing market, with a focus on demand response. KKT are applied to solve the problem.

— From this chapter on, the focus is on entities that can form or join a REC —

Chapter 5 is dedicated to the optimal management of a smart parking lot, solved with an extended version of Newton-base Bregman ADMM.

Chapter 6 presents the optimal energy scheduling of a multi-vector microgrid, where the degradation of hydrogen components is prevented by implementing manufacturer recommended operational limits such as temperature bounds and ramp rates. To solve the problem, the Augmented Lagrangian Method enhanced with a switching matrix for selective constraint enforcement is proposed.

Chapter 7 concludes this thesis and proposes some possible future developments.

1.3 List of publication and editorial activity

The list of publications, organized special sessions, special issues and open invited tracks is hereafter reported, as well as editorial activities such as associate editor. My indexes are:

- H index Scopus **5**
- H index Scholar **6**

1.3.1 Journal papers

J1. **V. Casella**, D. Fernandez Valderrama, G. Ferro, R. Minciardi, M. Paolucci, L. Parodi, M. Robba "Towards the Integration of Sustainable Transportation and Smart Grids: A Review on Electric Vehicles' Management" **Energies 2022**

J2. **V. Casella**, G. Ferro, M. Robba, "A decentralized optimization approach to the power management of electric vehicles parking lots", **Sustainable Energy, Grids and Networks 2023** (Special Issue: Electric Vehicle Management in Multi-Energy Systems)

J3. **V. Casella**, A. La Fata, S. Suzzi, R. Barilli, G. Barbero "The UK electricity market mechanism: a tool for a BESS optimal dispatching", **Renewable energies 2024**

J4. **V. Casella**, G. Ferro, A. Parisio, M. Robba, M. Rossi, "A novel decentralized cooperative architecture for energy storage systems providing frequency support services", **Control engineering practice 2025**

J5. **V. Casella**, G. Ferro, L. Parodi, M. Robba, "Maximizing shared benefits in renewable energy communities: A Bilevel optimization model", **Applied Energy 2025**

Under review

J6. **V. Casella**, G. Ferro, L. Glielmo, L. Parodi, M. Robba, "Renewable Energy Communities Cooperation for Demand Response Services"

J7. **V. Casella**, G. Ferro, L. Parodi, M. Robba, "Real-Time Energy Management in Smart Parking Lots Using Newton-Based BregmanADMM"

J8. **V. Casella**, G. Ferro, R. Minciardi, L. Parodi, M. Robba, "Optimal charging of electric buses: a new bi-level architecture for periodic scheduling"

J9. A. Annaswamy, **V. Casella**, Y. Ennassiri, G. Ferro, K. Y. Lee, L. Parodi, M. Robba "Optimized Energy Scheduling in MultiVector Microgrids: A Comprehensive Model for Hydrogen Integration and Operational Constraints"

1.3.2 Conference papers

C1. **V. Casella**, G. Ferro, R. Minciardi, L. Parodi, M. Robba "Optimal charging of electric buses: a periodic discrete event approach." 2021 29th Mediterranean Conference on Control and Automation **IEEE MED2021**

C2. M. Aicardi, **V. Casella**, G. Ferro, R. Minciardi, L. Parodi, M. Robba "Optimal control of electric vehicles charging in a smart parking.", IFAC Conference on Integrated Assessment models for environmental systems, Tarbes, **IFAC IAMES2022**

C3. **V. Casella**, G. Ferro, R. Minciardi, L. Parodi, and M. Robba, "Optimization of electric buses charging station with multiple sockets: The case of Genoa Municipality", **IFAC WC 2023** Yokohama

C4. **V. Casella**, A. La Fata, S. Suzzi, G. Barbero, R. Barilli, "A Tool to Optimize the Participation of BESS to the UK Ancillary Services Market", 3rd IFAC Workshop on Integrated Assessment Modeling for Environmental Systems, **IFAC IAMES2024**

C5. **V. Casella**, R. Minciardi, L. Parodi, "Optimization of Electric Bus Charging: Integrating Discrete Event Modeling in Public Transportation Systems", 3rd IFAC Workshop on Integrated Assessment Modeling for Environmental Systems, **IFAC IAMES2024**

C6. **V. Casella**, G. Ferro, L. Parodi, e M. Robba, "Energy Community Optimal Management: A Bilevel Approach", presented at 2024 IEEE 20th International Conference on Automation Science and Engineering, **IEEE CASE2024**

C7. **V. Casella**, L. Farina, G. Ferro, L. Parodi, M. Robba "Operational management of multiple energy communities in the energy market: a bilevel optimization-based approach", **IFAC SENSYS2025**

C8. **V. Casella**, M. Gallo, F. Graffione, M. Robba, F. Silvestro "An Energy Management System for Green Ports", **IEEE CASE2025**

1.3.3 Organization of Special Session

- IFAC IAMES 2024 "Sustainable Districts' Optimization and Control", V. Casella, Y. Ennassiri, L. Parodi (University of Genoa)
- IEEE CASE 2024 "Energy Communities: optimization and control for sustainability", L. Parodi, **V. Casella**, M. Robba, G. Ferro, R. Sacile (University of Genoa), R. Carli, P. Scarabaggio (University of Bari), L. Glielmo (University of Sannio), G. Notarstefano (University of Bologna).

- IFAC SENSYS 2025 “Advanced Methods for Sustainable Energy and Mobility Integration”, **V. Casella**, G. Ferro, M. Javad Jafari, C. León, A. Parejo, L. Parodi, M. Robba.

1.3.4 Organization of Special Issues for international journals

- IFAC Journal of Systems and Control IAMES, “Modelling, optimization, and control for managing energy and environment transitions”, M. Robba, G. Ferro, **V. Casella** (University of Genoa), M. Volta (Università di Brescia), G. Guariso (Polytechnic University of Milan), R. Van Nooiyen (Technical University Delft), F. Perès (University of Toulouse), E. Ratnam (Australian National University), H. Dagdougui (Polytechnique de Montréal).

1.3.5 Organization of Open Invited Track

- IFAC CPES 2024 ”Optimal Control, Management, and Scheduling in Energy Hubs” **V. Casella**, Y. Ennassiri, G. Ferro, L. Parodi, M. Robba (University di Genoa)

1.3.6 Associate Editor for international conferences

- Associate Editor at IFAC IAMES 2024
- Associate Editor for Invited Sessions “Advanced Methods for Sustainable Energy and Mobility Integration” at IFAC SENSYS 2025
- Associate Editor at IFAC WC 2026

1.4 Projects

During my Ph.D. activities I participated in the following projects:

- PRIN (2022) – ECODREAM: Energy Community management: Distributed Algorithms and toolboxes for efficient and sustainable operations. Activities involve the use of distributed algorithms for the optimization of renewable energy communities for both planning and management (internal and external).
- RAISE - Spoke 3: Robotics and AI for Socio-economic Empowerment - Smart and sustainable ports. Activities involve the definition of operational strategies for properly managing a multi-energy port hub. In particular, models for energy efficiency in the port environment

will be considered including energy scheduling and predictive maintenance tools. Port system logistics will also be included, with the ultimate goal of implementing active demand management policies (demand response).

- DUT (2023-2026) - OPEN4CE: Service-oriented Open Platform for Citizen Energy Communities a collaborative platform. The project is funded by the European Commission (Grant No. 101069506) for the Driving Urban Transitions (DUT) call. Activities involve the development of optimization models to be integrated within an innovative service-oriented platform to facilitate citizen participation and integration of energy communities.

Chapter 2

Introduction to energy communities

The growing concern about climate change and the environmental impact of traditional energy systems has made the reduction of GreenHouse Gas (GHG) emissions one of the highest priorities for the European Union [6]. To achieve this common goal, all the most polluting and energy-consuming sectors need to undergo a transition towards more sustainable configurations. The energy sector plays a central role in this transition since it is the one contributing most to anthropogenic CO_2 emissions (Figure 2.1); therefore, achieving the EU long-term climate neutrality target requires a significant change in how energy is produced and consumed. On the production side, a massive deployment of Renewable Energy Sources (RES) is crucial to replace fossil-based generation [7]; on the consumption side, since projections indicate that further electrification of end-use sectors is expected to contribute to a rise in electricity demand in the European Union [8], adopting more energy-aware and efficient consummation patterns is increasingly important. Nevertheless, the increasing share of non-programmable and intermittent resources and the continuous growth in electricity demand introduces significant challenges for the electrical grid, including congestions, voltage fluctuations, reverse power flows and asset aging acceleration [9]. These technical issues arise because traditional grid architectures were not designed for such high penetration of distributed generation and such high electrical demand, and, as RES continue to expand [10] and electric load to grow, the system requires new models able to coordinate decentralized resources, mitigate stress on distribution networks, maximize self-consumption and exploit the available flexibility where possible. Enhancing local self-consumption of renewable energy seems to be a valid strategy to address these issues as it not only contributes to emission reduction, but also reduces the reverse power flow, mitigates losses and limit the need for costly infrastructure reinforcements.

Within this context, energy communities have emerged as one of the most promising solutions for supporting the decarbonization process, enabling local actors to participate directly in energy

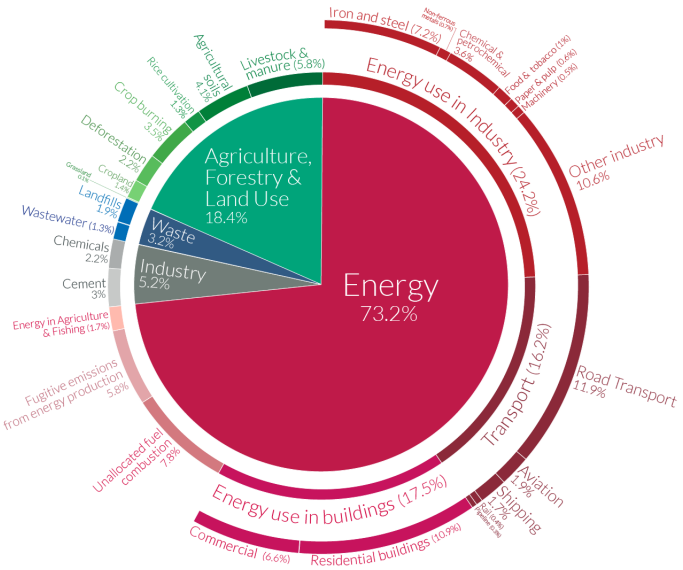

Figure 2.1: Global greenhouse gas emissions by sector - year 2016 [1]

Table 2.1: Comparison between citizen and renewable energy communities [4], [5]

	CEC	**REC**
Legal basis	Directive (EU) 2019/944	Directive (EU) 2018/2001
Membership	**Any** entity	Natural persons, local authorities, or SMEs **No** large enterprises
Control	Natural persons, local authorities, or small/micro enterprises (no medium enterprises)	Natural persons, local authorities, SMEs provided that participation does not constitute the primary commercial activity
Perimeter	**No** proximity requirement	Members must be **located in proximity of the renewable projects**
Energy	**Electricity only** but from **any**-source (Technology neutral)	**Multi-vector** but **100%** renewable sources
Purpose	Provide environmental, economic, or social community benefits for members or local area	

generation and management while promoting and incentivizing local energy consumption. The concept of energy communities was formally introduced by the European Union through the Clean Energy for All Europeans Package [11], adopted between 2018 and 2019. This comprehensive legislative package redefined the operations of the European energy market and placed citizens at the center of the energy transition. Within this framework, the EU established two distinct legal entities: Citizen Energy Communities (CECs) and Renewable Energy Communities (RECs). Both are designed to promote a bottom-up approach to the energy transition by enabling collective and citizen-driven energy actions to support the clean energy transition, by increasing public acceptance of renewable energy projects and by making easier to attract private investments in the clean energy transition. Energy communities can be an effective means of reshape our energy systems, by empowering citizens to drive the energy transition locally and directly benefit from better energy efficiency, lower bills, reduced energy poverty and increased local green job opportunities. Moreover, recent literature and institutional analyses highlight that energy communities are not only mechanisms for enhancing RES integration, but also tools for promoting consumer empowerment, social innovation, and local economic development [12]. In fact, according to the European Union, the main purpose of an Energy Community is to "provide environmental, economic or social community benefits to its members or shareholders or to the local areas where it operates rather than to generate financial profits".
Although both CECs and RECs aim to promote decentralized, participatory, and socially-oriented energy models, they differ in some aspects (Table 2.1) and intentionally serve different regulatory goals [13]: CECs expand the participation of citizens and small actors across all electricity market activities, while RECs focus specifically on strengthening local participation in renewable generation and empowering local communities to produce and share renewable energy. Together, they establish the legal foundation for citizen-driven, decentralized energy systems across the European Union. Citizen energy communities were introduced under Directive (EU) 2019/944 [14].

CECs are legal entities "based on voluntary and open participation and are controlled by members or shareholders that are natural persons, local authorities, or small enterprises". CECs are technology-neutral and may engage in a broad range of electricity-related activities such as "generation (including from renewable sources), distribution, supply, consumption, aggregation, energy storage, energy efficiency services or charging services for electric vehicles". CECs may operate across a distribution system area (without any perimeter restrictions) and are not required to restrict their activities to renewable sources. Renewable energy communities were defined under Directive (EU) 2018/2001 [15], also known as RED II, which focuses specifically on promoting energy from renewable sources. RECs are defined as legal entities "based on open and voluntary participation and are controlled by shareholders or members *located in the proximity* of the renewable energy projects that are owned and developed by that legal entity". RECs are therefore more restrictive in scope: their members must be located in geographical proximity to the renewable assets they own or manage, and they are allowed to engage only in activities related to renewable energy. In fact, the Directive points outs that "in multi-fuel plants using renewable and non-renewable sources, only the part of electricity produced from renewable sources shall be taken into account".
Although the European directives provide a common legal framework at the European level for CECs and RECs, their practical implementation is not uniform across the European Union. Indeed, in accordance with EU law, directives set the results to be achieved, while leaving Member States the responsibility to transpose their provisions and guidelines into national legislation. As a consequence, each Member State must adopt specific legal, regulatory, and technical measures to assimilate the requirements of the European Directives, defining in detail the rules governing community membership, governance structures, geographical constraints, incentive mechanisms, and interactions with the electricity grid. While the core principles established at the European level are preserved, this transposition process has led to heterogeneous national frameworks: the resulting implementations of energy communities exhibit significant variability across countries, highlighting the importance of analyzing national contexts when assessing their technical and operational performance.

Within this heterogeneous European framework, this thesis focuses specifically on renewable energy communities; therefore, from this point onward, all regulatory considerations will refer exclusively to Directive (EU) 2018/2001 (RED II) and renewable energy communities unless otherwise stated. Due to the significant heterogeneity across EU Member States, particular attention is devoted to the regulatory, technical, and operational implementation of RECs in the Italian context, which represents a relevant and well-defined case study within the European landscape.

2.1 Renewable energy communities in the Italian context

This section focuses on the Italian context, which is indeed the subject of this thesis. Therefore, after a brief analysis of Italy's progress in transposing the European Directive RED II, it presents

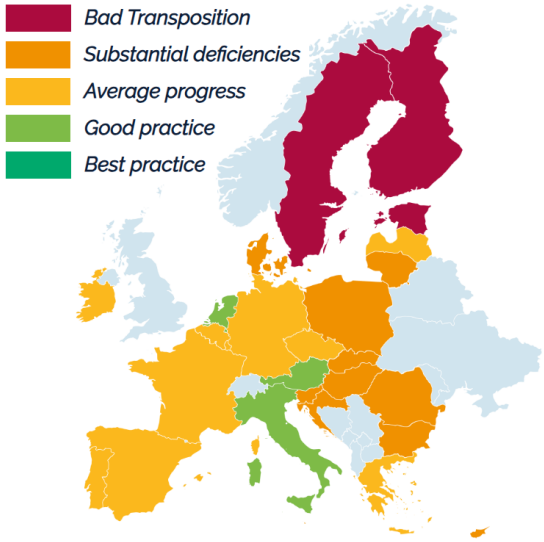

Figure 2.2: Progress status of the transposition of REC definitions in the European Member States [2]

the evolution of the Italian regulatory framework regarding RECs and how a key concept of RECs, namely shared energy, is assimilated.

Even though RED II establishes a harmonized definition of RECs, the directive leaves substantial flexibility regarding implementation. As a result, the level of REC transposition across the EU is highly heterogeneous. According to the Transposition Tracker in Figure 2.2, most EU Member States have formally introduced the REC definition into their legal systems; yet, only a limited number have developed a comprehensive enabling framework. In many cases, regulatory barriers persist, including complex authorization procedures, insufficient remuneration for shared energy, and lack of long-term policy certainty. These shortcomings significantly affect the scalability and economic viability of RECs and demonstrate that the mere legal recognition of RECs is not sufficient. Effective implementation requires coherent enabling frameworks, stable support schemes, and alignment between regulatory design and local technical conditions. Among EU Member States, Italy represents one of the most advanced examples of REC implementation. Through the final transposition of RED II into national legislation (Legislative Decree 199/2021), Italy has established a clear legal definition of renewable energy communities and introduced a structured incentive mechanism for energy sharing. The operational framework, managed by the national energy service operator (GSE), defines collective self-consumption within defined geographical boundaries and provides economic remuneration for shared renewable energy. This positions Italy within the "Good Practice" category in the European landscape, especially when compared to countries where REC legislation remains partial or poorly defined. Nevertheless, despite this advanced regulatory setup, challenges remain related to administrative complexity, grid integration constraints, effective operational management, and the long-term financial sustainability of community-based energy projects.

2.1.1 The Italian regulatory framework

Following the adoption of the European Directive RED II at the European level, Italy has progressively developed a national regulatory framework for renewable energy communities through a phased and evolving transposition process, summarized in Table 2.2. In Italy, the regulatory framework for RECs follows a hierarchical and sequential logic that ensures coherence between European objectives and national implementation. As said, the European Directive RED II establishes the general principles and binding goals for renewable energy communities, but does not directly prescribe their operational implementation. These principles and goals must be formally transposed into national law through a legislative decree, which provides the legal definition of renewable energy communities, identifies eligible actors, and sets the foundation rules for governance and participation. On this basis, ministerial decrees translate the legislative framework into practical policy instruments by establishing eligibility conditions, incentive schemes and the allocation of public funds, including those related to the National Recovery and Resilience Plan (PNRR). To ensure compatibility with the operation of the electricity system, technical and regulatory aspects of energy sharing and distributed self-consumption are then specified by the national energy regulator ARERA. ARERA issues resolutions to regulate smart metering, grid-related procedures and participation in energy markets. Finally, the national energy service operator (GSE) makes this framework fully operative by issuing detailed technical and operational rules, by managing application procedures, and by supervising verification and remuneration processes. The GSE technical rules are the final element in the chain, but they are of fundamental importance because all those who wish to apply must submit their application on the GSE website and in accordance with the GSE operational rules.
This layered approach ensures that RECs are legally grounded, technically regulated, economically supported, and operationally implementable, while preserving alignment with the European regulatory framework. This general logic has been applied throughout the evolution of the Italian regulatory framework, although with different degrees of maturity across distinct phases.

In the experimental phase, the legal basis was provided by Article 42-bis of Decree-Law No. 162/2019 [16] (also known as *Decreto Milleproroghe*). The Ministry for Economic Development (MISE) translated this legislative framework into concrete policy instruments through the Ministerial Decree MISE of 16 September 2020 [17], mainly defining the incentive schemes. Then, ARERA Resolution 318/2020 [18] and the first GSE technical rules completed this regulatory framework with more technical and practical instructions. This early transposition of the European directive enabled pilot configurations of collective self-consumption and energy communities. This early framework was intentionally limited in scope and aimed at testing the feasibility of energy sharing in real distribution networks. In particular, RECs were characterized by limited plant size, strict proximity constraints and by a simple premium tariff on shared energy: in particular, installed capacity should not exceed 200[kW], all production and consumption points were required to be connected under the same secondary substation, and the premium tariff was fixed to 110[€/MWh]. Moreover, energy storage systems were not allowed

as their energy was considered non-renewable. Despite these restrictions, the experimental phase represented a crucial milestone, as it introduced for the first time the formal concept of shared renewable energy in Italy and served to highlight the main critical issues. Therefore, the preliminary phase was updated over the years until the final version of the Italian regulatory framework; this transition phase has been characterized by various drafts and amendments, which are not reported for simplicity. Instead, only official documents are reported.
The Legislative Decree 199/2021 [19] marked the beginning of the final phase of the regulatory process for transposing of RED II in the Italian legislation. This decree laid the legal foundations for RECs as stable components of the Italian energy system and introduced some substantial changes compared to the previous phase by increasing the maximum power of renewable plants and extending the connection perimeter: in particular, RES plants must have a total capacity not exceeding 1[MW] and all production and consumption points must be connected to the electricity grid through the same primary substation. Moreover, the integration of energy storage systems is allowed to foster greater programmability of sources. In 2022, ARERA resolution 727/2022 [20] (also known as TIAD) laid the groundwork for a harmonized technical regulation of distributed self-consumption; this document expanded the scope of eligible technologies: in addition to production plants that came into operation after the date of entry into force of D.lgs 199/21, those that came into operation before that date are also eligible, provided that their total nominal power does not exceed the limit of 30% of the total power belonging to the renewable energy community. The Italian regulatory framework reached full maturity with the Ministerial Decree MASE Decree 414/2024 [21], which established a structured and long-term incentive scheme, as a variable premium tariff depending on hourly market price and plant size. The ARERA resolution 15/2024 [22] finalized the technical rules for energy sharing and grid interaction, while the final GSE operational rules [23] enabled full operational deployment. The final phase also introduced a capital grant funded under the National Recovery and Resilience Plan, which is intended to support the integration of renewable generation and storage systems serving RECs by reducing upfront investment costs; indeed, this capital grant applies to eligible investment costs of newly installed renewable generation plants (and possible associated storage systems) serving the REC, and amounts to 40% of the total capital expenditures. The Ministerial Decree MASE Decree No. 414/2024 assigned this economic contribution to municipalities with fewer than 5.000 inhabitants. Then, in 2025 the Ministry of the Environment and Energy Security issued another decree (MASE No. 127/2025), which constitutes a targeted amendment aimed at extending the eligibility criteria for the PNRR-funded capital grant to municipalities with fewer than 50.000 inhabitants, without altering the overall regulatory architecture of renewable energy communities.

Table 2.2: Italian regulatory framework for renewable energy communities

Act	**Date** mm/yy	**Description**
EU Directive 2018/2001	12/18	Introduction at the European level of renewable energy communities and the principle of shared renewable energy
		Preliminary phase
D.lgs 162/2019	12/19	Early transposition of the EU Directive "*Decreto Mille proroghe*"
DM MISE 2020	09/20	Implementing decree defining the remuneration of shared energy for pilot configurations as a fixed premium tariff (110€/MWh)
D. ARERA 318/2020	08/20	Technical rules for distributed self-consumption and shared energy
GSE rules	12/20	GSE operational rules for access to incentives and management of shared energy, written in accordance with DM MISE and Delibera ARERA 318/2020
		Final phase
D.lgs 199/2021	11/21	Final transposition of the EU Directive into Italian law; definitive legal recognition and definition of RECs
D. ARERA 727/2022	12/22	Technical rules for distributed self-consumption and shared energy TIAD *Testo Integrato dell'Autoconsumo Diffuso*
DM MASE 414/23	01/24	Implementing decree defining incentive levels, technical constraints, and eligible installations for RECs. PNRR funds for municipalities with fewer than 5.000 inhabitants.
D. ARERA 15/24	01/24	Amendment and integration of the TIAD in accordance with DM MASE 414
GSE rules	04/24	GSE operational rules for access to incentives and management of shared energy, written in accordance with DM MASE 414 and Delibera ARERA 15/24
DM MASE 127/2025	05/25	Specific amendment to DM MASE 414, extending the range of beneficiaries of the PNRR funds to municipalities with a population of less than 50.000 inhabitants
GSE rules	07/25	GSE operational rules for access to incentives and management of shared energy, written in accordance with DM MASE 127/2025

Under the current Italian regulatory framework for renewable energy communities, following the full transposition of RED II and the subsequent implementing measures, a REC must be established as an autonomous legal entity and must include at least two members: a consumer and a production plant, with two distinct connection points that must fall within the area beneath the same primary substation. All REC participants retain their rights as end customers. As legal entity, each REC needs a statute, which specifies that a REC must be: (a) based on open

Table 2.3: Comparison of the main regulatory phases for RECs in Italy

	Preliminary phase	**Final phase**
Governance	Basic and simplified governance requirements	Full RED II-compliant governance framework (autonomy, non-profit orientation, local control)
Perimeter	Secondary substation	Primary substation
Eligible plants	Renewable plants with installed capacity $\leq$**200kW**; newly installed or commissioned after the reference date	Renewable plants with installed capacity $\leq$**1MW**; installed before the reference date provided that they do not exceed **30%** of the total power; **storage systems** explicitly eligible
Shared energy	Hourly-based definition as the minimum between injected and withdrawn energy	$\equiv$
Incentive scheme	ARERA valorization on shared energy + **Fixed** premium tariff applied to incentivized energy	ARERA valorization on shared energy + **Variable** premium tariff applied to incentivized energy, combined with PNRR capital contributions

and voluntary participation, autonomous, and effectively controlled by shareholders or members that are located in the proximity of the renewable energy projects that are owned and developed by that legal entity, (b) whose members are natural persons, enterprises or local authorities, including municipalities, and (c) with the primary purpose to provide environmental, economic or social community benefits for its members or for the local areas where it operates, rather than financial profits. The statute also indicates a representative, who is defined as the person to whom technical and administrative management of the REC is entrusted, and as the legal counterpart in the contractual relationship with the GSE, for the application and the administration of the incentive provided for RECs. An insight on requirements and characteristics of participants in a REC are provided in the following.
Despite the differences across these phases (highlighted in Table 2.3) and the various regulatory amendments, the central role of shared energy as the operational basis of RECs have remained consistent throughout the evolution of the Italian framework in accordance with the RED II. Indeed, by incentivizing energy sharing, RECs promote local consumption of renewable energy; this alleviates the grid stress, and contributes to the reduction of distribution and transmission losses by shortening the distance electricity must travel from generation to consumption.

2.1.2 Shared Energy

Despite the numerous potential configurations for a REC depending on the legislative framework of each country, a key and central concept in the Directive (EU) 2018/2001 is that of shared energy. RED II grants members of a REC the right to generate, consume, store, and sell renewable

energy, and explicitly allows the internal allocation of renewable electricity among community participants, provided that such activities do not constitute the community primary commercial purpose. While the directive does not impose a uniform technical definition of energy sharing, it establishes the principle that renewable electricity produced by community-owned or community-controlled installations may be collectively assigned to the Points Of Delivery (PODs) associated with the consumption units of the members participating in the renewable energy community. Consequently, the notion of shared renewable energy constitutes a common and mandatory element across all national REC frameworks derived from RED II. Heterogeneity among member states arises only at the transposition level, where national authorities define the operational rules for measuring, allocating, and remunerating shared energy, while preserving the core European objective of promoting collective self-consumption and facilitating the integration of distributed renewable generation.

Within the Italian regulatory context, a REC operates through the collective production and sharing of renewable electricity, with shared energy formally defined as the portion of renewable generation that is injected into and simultaneously withdrawn from the distribution grid by community members within the same reference area. In Italian legislation, shared energy is defined as the "minimum between the electricity globally injected and the electricity globally withdrawn" (2.1).

$$e_t^{sh} = \min \left\{ \sum_{i \in S^N} p_{i,t}^{G,out}, \sum_{i \in S^N} p_{i,t}^{G,in} \right\} \Delta \quad t \in S^T \tag{2.1}$$

where $p_{i,t}^{G,out}$[kW] and $p_{i,t}^{G,in}$[kW] are the power flows injected into/withdrawn from the grid by each user i in each time interval. In this equation, S^N is the set of energy community participants, S^T is the set of time instants, while Δ[h] is the length of each time interval. Figure 2.3 graphically shows the definition of shared energy for a basic example with three production plants and three points of delivery in two different cases: surplus of consumption and surplus of production. From the figure, it is evident that the minimum is always taken. This quantity is calculated hourly ($\Delta = 1$[h]) and according to an ex-post calculation based on the members' smart meters. Electricity sharing occurs using the existing distribution network, and all energy exchanges are virtual, meaning there is no electrical grid modeling like in microgrids (MGs) or sustainable energy districts.

The legislation places energy sharing at the center of the Italian REC model, making it both the technical foundation for community operation and the basis for economic incentives. From a technical perspective, shared energy is important because the greater the shared energy, the greater local consumption and therefore the less stress on the grid. From an economic viewpoint, shared energy matters as the community obtains some incentives based on how much energy is shared. Specifically, two economic contributions are associated with shared energy:

a. valorization for shared self-consumed electricity

b. premium tariff for incentivized energy

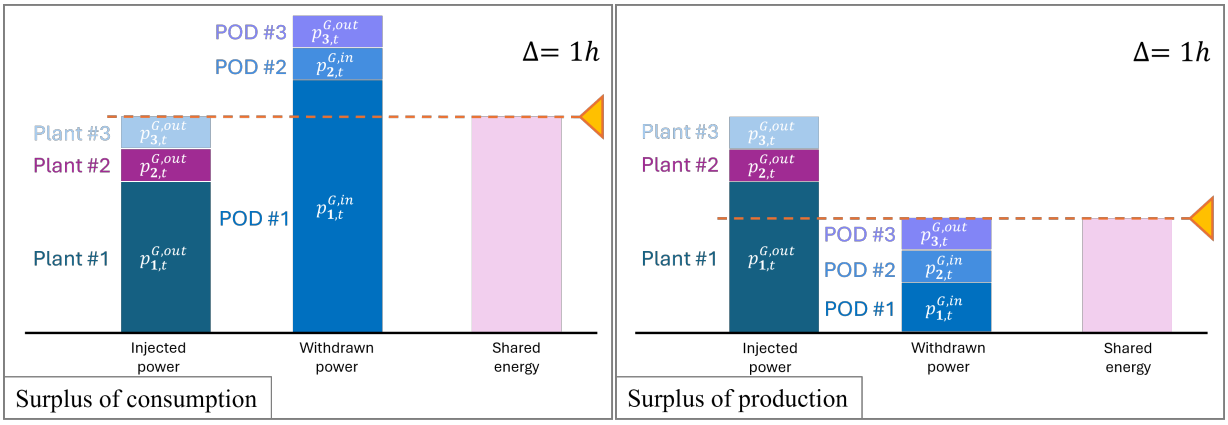

Figure 2.3: Graphical representation of the shared energy calculation [3]

As far as the incentive at point a), it is the economic compensation recognized by ARERA which accounts for the avoided network and system costs associated with local consumption. This valorization fee varies every year (in 2024 it was equal to 10.57[€/MWh] [24]). Regarding the valorization in point b), it is first necessary to distinguish between shared self-consumed energy and incentivized energy. Shared self-consumed energy is the energy defined in equation (2.1), while incentivized energy is a portion of shared self-consumed energy, but produced by eligible plants only. In particular, access to the premium tariff is subject to constraints on the commissioning date, installed capacity, and grid connection perimeter of the plants, as well as to the absence of incompatible support mechanisms. While renewable plants that do not meet all incentive requirements may still participate in the community and count for shared self-consumed energy, only those fulfilling the eligibility conditions contribute to the calculation of incentivized energy. In most configurations, shared self-consumed energy and incentivized energy coincide, but according to the legislation they are potentially two distinct quantities (Figure 2.4). Therefore, the premium tariff is awarded only for incentivized energy; it is a policy-driven incentive expressed in [€/MWh]. In the preliminary phase, this incentive was a fixed tariff, but in the final regulatory framework it is determined through a formula in Annex1 of the Ministerial Decree MASE 414/23, that makes this incentive depending on the hourly market price and on the size of the generation plant. Since modeling this incentive is the main focus of one of the two works presented in Chapter 3, the incentive at point b) is described in detail in the dedicated chapter (Section 3.2.1.2.2). In addition to these two contributions, all renewable energy produced but not self-consumed is injected into the grid and remains available to producers; hence, this energy may be withdrawn by the GSE and remunerated at market conditions, where requested.

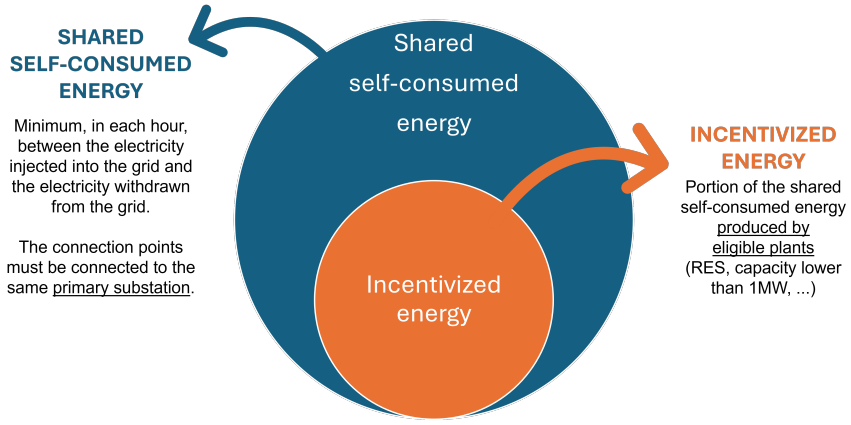

Figure 2.4: Shared self-consumed energy versus incentivized energy

2.2 REC main actors

This section provides an overview of the main actors in a REC, focusing on eligible participants and a potential manager. Then, the role of other potential members is investigated; specifically, smart parking lots and multi-vector energy hubs are considered. The paragraph dedicated to these entities introduces the reasons why they are establishing themselves in the energy landscape and why they are efficient candidates to participate in a REC, highlighting how their integration into a REC improves flexibility and coordination potential.

2.2.1 Participants

Under the current Italian regulatory framework, renewable energy communities may be established as autonomous legal entities composed of a wide range of local members. Eligible participants include physical persons, small and medium-sized enterprises, local authorities and territorial bodies (such as municipalities) as well as public non-economic entities, cooperatives, associations, foundations, and other third-sector organizations. From a technological perspective, RECs may include any electricity generation plants powered by renewable energy sources, such as photovoltaic, wind, hydroelectric, biogas, and solid biomass systems, provided that they comply with the criteria defined by national implementing decrees. However, access to the premium tariff on incentivized energy is granted only to those plants meeting the eligibility requirements. In addition, energy storage systems are explicitly admitted (D.lgs 199/2021) as part of the community infrastructure and may be owned either by the community or by individual members. Energy storage systems are crucial devices in a REC as they are the ultimate flexible devices. Given the earlier definition of RECs and energy sharing, it is clear that aligning consumption and production is fundamental for RECs to make a real impact on the network and provide significant

incentives. For this match to happen, it is necessary that ECPs have some flexibility available to shift in time their consumption/production to increase energy sharing. Storage systems have exactly this purpose: they do not generate shared energy per se, but they allow renewable electricity produced within the community to be shifted over time and subsequently contribute to shared energy when discharged and locally consumed. The treatment of electricity flows associated with storage systems, as well as their contribution to shared energy and incentive mechanisms, is defined at the regulatory and operational levels through ARERA resolutions and GSE technical rules [23].
Overall, this inclusive framework allows RECs to integrate a diverse set of participants and technologies within a localized energy system, fostering collective self-consumption, enhancing system flexibility, and supporting the efficient integration of distributed renewable energy resources into the distribution grid.

2.2.2 Manager

Since a REC is a complex entity from legislative, juridical and social perspectives, the presence of a coordinating figure can significantly enhance its overall effectiveness and long-term feasibility. A coordinating role, who will be referred to as 'Energy Community Manager' (ECM), may be introduced to support the organization and the operation of the community. Although this role is not formally required by the current regulatory framework, it has been proven increasingly relevant in REC real-world implementations, especially as their size, number of participants, and technological complexity increase. The main responsibility of the ECM is facilitating regulatory compliance and administrative coordination, acting as an intermediary between the community and external institutions such as the GSE, distribution system operators, and public authorities: this includes managing contractual relationships, monitoring compliance with evolving regulatory requirements, and ensuring the correct application of incentive mechanisms. In addition, the ECM has to support transparent communication among community members, and overseeing the allocation of economic benefits, such as the distribution of revenues derived from shared and incentivized energy, in accordance with the rules defined in the community statute.
While no specific qualifications are legally required to perform this role, the increasing technical complexity of RECs suggests that the role of a manager is becoming essential especially from a technical point of view. Most community members have limited expertise in the energy sector and may lack the technical expertise required to manage distributed generation assets, storage systems, and flexible loads in an optimal manner. Therefore, beyond its administrative functions, the ECM can contribute to improve the operational efficiency of the REC: the ECM could coordinate technical activities, oversee operation and maintenance tasks, and support strategic planning decisions to ensure operational efficiency and ensuring reliable operation over time. Indeed, having the overall energy consumption simultaneous with energy production is essential to increase shared energy. For this purpose, the manager could request an external consultation or use an optimization tool that would help coordinating all the players and technologies involved to

maximize local self-consumption, enhance flexibility, and achieve shared goals of sustainability and energy autonomy.

2.2.3 ECPs: focus on Smart Parking Lots and Multi-vector Energy Hubs

RECs are often associated with domestic users such as individual households or residential condominiums; however, the current regulatory framework also allows the participation of more complex and structured entities and aggregated energy systems. In this context, RECs can naturally extend beyond purely domestic settings to include infrastructures characterized by high power demand, flexible operation, and advanced energy management capacity. Among these, smart parking lots and multi-vector energy hubs represent two particularly relevant and emerging applications, which are explicitly addressed in the technical chapters of this thesis (Chapter 5 and Chapter 6, respectively).

Smart parking lots are typically associated with commercial areas, transportation hubs or public facilities. In practical implementations, SPLs are typically characterized by a single point of connection to the distribution grid; this configuration allows a parking lot to be treated as a single participant within a REC. Internally, the charging process of individual vehicles is managed through smart charging strategies, while externally the parking lot interacts with the REC as a unified entity. This makes smart parking lots particularly suitable as ECPs because of the simple interface with the public grid, while having considerable internal flexibility behind a single connection point. This aggregated electricity demand can act as a large and flexible energy consumer within a REC or, if renewable generation and/or storage systems are included, as a prosumer. In any case, this structure is particularly relevant for energy sharing since the EV charging demand can be scheduled in accordance with local renewable generation profiles to achieve community-level objectives. Aligning demand with local renewable generation becomes even more urgent given the aggregated nature of this type of load and considering that the number of parking lots is expected to increase together with the number of EVs [25].
The transportation sector has been shown to be one of the most impactful in terms of emissions and human footprint on our planet [26]. Therefore, in the last decade, it has undergone a significant transformation thanks to the widespread adoption of electric vehicles (EVs), which are recognized as a viable solution for reducing greenhouse gas emissions and meeting climate targets [27]. Nevertheless, the massive electrification of the transport system can have negative consequences on the grid: in fact, considering the high charging demand of each vehicle and the increasing number of EVs being promoted by governments, the resulting overall load on the grid could be significantly damaging. In order to avoid negative effects, it is crucial to properly control the EV charging in order to reduce their impact on the grid [28]. Indeed, it has been proven that the so called smart charging effectively relieves stress on the grid [29], especially when combined with demand response strategies and grid services. Indeed, EVs can be treated as mobile energy storage systems, whose charge/discharge process can be managed not only to pursue

smart charging strategies, but also to provide services to the grid [30]. Obviously, these kinds of strategies are effective if applied in a context where EVs are stationary for an extended period of time, such as a workplace parking or a park-and-ride parking. Indeed, since in these kind of SPLs EVs are typically parked for longer than the time required for charging, these idle periods can be exploited to allow the implementation of smart charging strategies aimed at achieving specific system objectives and providing some flexibility to the main grid. In SPLs, several EVs are concentrated in localized areas; because of that, carefully managing their charging process becomes even more urgent, as they represent a load of great intensity and concentrated in a single grid bus, which increases the stress on the power network. On the other hand, an aggregated load could intensify the effect of demand-side management (DSM) strategies and enhance an efficient coordination of charging and discharging activities, improving the provision of flexibility services [31]. Moreover, unlike stationary ESSs, EVs have additional constraints that depend on owners' needs, such as release time, deadline, and energy request satisfaction. Given the complexity of managing a SPL, a figure who coordinates and manages the charging and discharging process for each vehicle in order to achieve the desired overall objective is crucial: parking lot operators can assume the role of electric vehicle aggregators (EVAs) [32]. In the context of RECs, parking lot operators can act as intermediaries between electric vehicles and the community, managing the charging process of the fleet of parked electric vehicles to alleviate stress on the grid and pursue energy sharing objectives.

A similar concept applies to multi-vector energy hubs integrating hydrogen systems. Multi-vector energy hubs are often composed of multiple assets, such as renewable generation units, fixed and deferrable electric loads, electrolyzers, fuel cells, storage systems (both electrical and hydrogen-based), and eventually thermal systems. Unlike smart parking lots, which are typically characterized by a single point of connection to the electricity grid, these entities may be associated with multiple connection points; as a result, multi-vector energy hubs are not only compatible with the renewable energy community framework, but are naturally suited to form a REC as they already involve several energy assets within a geographically localized area. Multi-vector energy hubs turn out well as a REC because they are infrastructures integrating decentralized, flexible and controllable technologies: the presence of localized multiple connection points facilitates identifying potential ECPs, while the presence of multiple energy vectors enhances overall system flexibility. The REC would provide an organizational and regulatory framework that eases the coordinated management of these complex infrastructures to achieve efficient and reliable operations and, if a REC were formed, energy sharing maximization. In this sense, all flexible devices of the hub can be scheduled to match production from renewable sources with consumption. As an example, hydrogen-based hubs would support the decoupling of renewable generation from instantaneous electricity demand, enhancing energy sharing. In fact, renewable energy surplus can be absorbed by the electrolyzer, converted into hydrogen for medium-term storage and converted again into electricity by the fuel cell when other renewable sources are not available. The need to align energy demand and conversion processes across multiple vectors with local renewable generation is further reinforced by the increasing complexity and growing

deployment of multi-vector energy hubs within local energy systems.
The global energy sector is undergoing a deep transformation driven by three key trends: the accelerated development of renewable energy, the electrification of energy-intensive sectors, and the integration of multiple energy carriers [33]. Renewable capacity has expanded rapidly in recent years, with solar and wind accounting for over 80% of new electricity capacity additions in 2023 [34], [35]. According to the International Energy Agency, renewable sources are expected to provide 50% of global electricity by 2030 [7]. Despite these advances, RES are intrinsically uncertain and intermittent, posing significant challenges and barriers to energy system security and reliability [36], [37]. To address the challenges posed by a deep exploitation of renewable energy sources, multi-vector energy systems have emerged as a promising paradigm. These systems are a direct consequence to the need to find alternatives to fossil fuels and integrate multiple energy carriers, including unconventional energy sources, into a coordinated framework that maximizes efficiency, flexibility, and resilience [38], [39]. Among emerging energy carriers, hydrogen is particularly promising, with global demand projected to grow by 500% by 2050 [40], [41]. All these transformations need advanced approaches able to harmonize several energy sources, reduce operational costs, and foster resilience. Smart microgrids are among the most efficient implementations of multi-vector energy systems, providing a cluster of innovative technologies that can be coordinated to mitigate the impact of RES on the main grid and provide flexible demand management. Indeed, in polygenerative and multi-vector infrastructures several technologies and energy carriers coexist; their integration significantly enhances system flexibility because each component has different operating principles, distinct operational characteristics, response capabilities and technical constraints [42]. This ability to reallocate energy across carriers and time scales helps compensating for the inherent variability of renewable generation and responding more effectively to fluctuations in demand, improving reliability and supporting grid stability. On the other hand, the interactions between heterogeneous energy sources, both conventional and unconventional, introduce an additional level of complexity leading to tightly coupled dynamics and competing operational objectives; all these aspects make the management of modern energy systems increasingly difficult and significantly challenging. In this context, traditional Energy Management Systems (EMS) are evolving to adapt to this new scenario where the all technologies must be coordinated to achieve efficient and reliable operations; indeed, setting up an comprehensive optimization of the entire system is essential to fully exploit the enhanced system flexibility, while ensuring stability, resilience, and compliance with grid requirements. In the context of RECs, EMSs implemented in multi-vector energy hubs can be integrated with community-level constraints, regulation-aware equations and energy sharing maximization objectives, and serve as a supporting tool for the energy community manager.

2.3 RECs in the Energy Markets

This section investigates why flexibility is crucial in modern energy systems and how it can be provided. Therefore, a brief overview on balancing markets is proposed, highlighting how RECs can provide some flexibility services to the system operator.
Renewable generation, while essential for the transition into a low carbon system, is inherently variable and only partially predictable, leading to imbalances between electricity supply and demand; at the same time, electricity consumption is growing and becoming more concentrated in time and space, leading to electricity surplus or deficit on the grid. Moreover, even though all agents in the energy market are expected to respect their contracted volume of electricity in each time slot, it can happen that suppliers (individual consumers buy electricity from a supplier of their choice) may have incorrectly forecast their electricity requirements, generators may be unable to generate the contracted amount, or there may be problems with electricity transmission/distribution. All these factors result in more frequent imbalances, an increased stress on distribution networks, which induce congestion and voltage violations, and a lower system inertia, which lead to system frequency deviating from its usual 50[Hz] much quicker than before. If any of this happens, the Distribution System Operator (DSO) needs to balance the system in real-time and solve any transmission or frequency issues; this is where flexibility comes into play. Flexibility refers to the ability of the power system to respond to variability and uncertainty by adjusting generation, consumption, or power exchanges over different time scales. Flexibility can be provided through a combination of different technologies and operational solutions. As regards technologies, every controllable and deferrable asset is capable of providing flexibility: ESSs are the flexible devices par excellence, but also shiftable loads, heat pumps, power-to-X systems and any technology able to modulate its power demand. In general, distributed energy resources are increasingly recognized as valuable sources of flexibility, as they can be coordinated through advanced control and optimization frameworks to actively support grid operation. As far as operational solutions are concerned, any controllable energy system can provide flexibility: such systems need to be scheduled based on grid conditions and signals from grid operators. The underlying concept is to extend traditional EMS beyond the objective of demand satisfaction while minimizing costs and to integrate new Key Performance Indicators (KPIs) that also consider network needs.
It is clear that the DSO has a range of flexibility services to balance supply and demand [43], to continually regulate frequency around the 50 Hz target [44] and to correct real-time deviations between scheduled and actual power injections and withdrawals [45]: balancing mechanism and ancillary services. Flexibility services are typically procured through market-based mechanisms, which are widely recognized as the most effective approach, as it ensures transparency and cost-efficiency. Usually, these markets are operated through auctions, where flexibility providers (i.e. prosumers or aggregators) submit bids specifying the flexibility capacity they can offer and the corresponding price. The market is then cleared once the DSO flexibility requirement is matched, selecting the winning bids according to predefined criteria such as minimum cost or network

constraint satisfaction. After market clearing, the successful providers are notified and subsequently activated by the DSO; usually, selected providers must follow a reference power signal proportional to the contracted capacity, when their flexibility service is required to alleviate grid congestion or maintain voltage and frequency stability [46], [47], [48].

While traditional balancing services have historically relied on large, centralized generation units, the growing penetration of DERs has shifted attention toward demand-side management strategies and demand response strategies as key sources of flexibility. These strategies typically involve the upward or downward modulation of active and/or reactive power exchanged with the grid by flexible loads and distributed resources to ensure compliance with distribution network constraints under normal operating conditions, as well as following reconfigurations due to faults and/or scheduled maintenance. By adjusting consumption patterns in response to system needs or price signals, these local flexibility services can contribute to real-time balancing and congestion management, including over-voltages and over-currents. In this context, microgrids are recognized as energy infrastructures that can help the DSO in managing the grid, by facilitating the integration of power production from renewable resources and distributed generation to satisfy a local demand. Moreover, MGs are a cluster of several and different technologies which allows them to offer a level of operational flexibility that cannot be achieved by individual resources acting independently. Indeed, aggregated demand response allows small-scale flexible resources to collectively provide services that would otherwise be inaccessible to individual consumers and intensifies the effect of these strategies. For this reasons, in the last years, the ability to deliver ancillary services to DSOs has been extended to a wide range of end-users [49], thanks to the emergence of new balancing service providers like *aggregators*, who can manage the flexibility of numerous small customers and offer it to the system operators. This aggregation is crucial for participation in balancing and ancillary service provision: while single distributed resources often lack sufficient flexibility capacity to meet market conditions or reliability to meet technical requirements, their coordinated operation enables the delivery of meaningful flexibility services, such as demand response and peak shaving.
The same concepts could potentially apply to renewable energy communities: like microgrids, RECs aggregate multiple flexible assets under a coordinated management framework and are therefore well suited to participate in balancing and ancillary services, complementing their primary role in promoting local renewable integration and energy sharing. However, while MGs have a single point of common coupling with the grid, RECs aggregate several end-users, each with their own POD. From an operational point of view, having several connection points would complicate the provision of these services; from a results point of view, the benefit to the grid would be considerable at the primary substation level. For these reasons, the provision of ancillary services and DSM strategies by RECs is not active yet, but it would be an excellent opportunity to exploit the intrinsic flexibility of these infrastructures. In any case, if implemented, providing flexibility services to the grid would improve the economic benefit of a REC, currently relying only on the incentive for energy sharing. From a control and optimization point of view, both shared energy maximization and flexibility provision compliance rely on controlling the

power exchange profiles with the grid; therefore, integrating DMS into an optimal management problem for RECs can be achieved without altering the structure of the optimization problem. Nevertheless, this integration introduces an additional layer of complexity, as the optimization problem must jointly address demand–generation matching at the community level, while satisfying external system requirements and grid service constraints.

2.4 Optimization Methods in the Energy Sector

This section discusses the role of modeling and optimization methods for the optimal management of RECs. First, an overview of energy management systems and how they can be classified is provided. Then, the last part of this section describes how these tools can be applied to RECs: why they are effective in achieving the shared energy maximization goal and which approaches are the most suitable to address the problem of optimal management of a REC.
The growing complexity of modern energy systems, characterized by increasing uncertainty and interdependence among resources and processes, introduces the need for structured management systems to support rational decisions, particularly when multiple objectives and constraints must be simultaneously addressed. Within the energy domain, this general concept translates into the so-called Energy Management Systems (EMSs), which are needed to exploit the full potential of energy-related assets and infrastructures. The progressive evolution of traditional power systems towards microgrids has further reinforced the central role of EMSs: a microgrid is a small-scale, decentralized power system that can operate in parallel with or independently from the main grid and typically consists of a combination of Distributed Energy Resources (DERs), such as solar panels, wind turbines, and energy storage systems. Within a microgrid, an EMS is responsible for monitoring and controlling the various components of the MG, and guarantees that the system operates in compliance with technical and physical constraints, such as balancing energy supply and demand. To achieve this, the EMS integrates hardware and software components such as in-field sensors, Supervisory Control and Data Acquisition (SCADA) systems and optimization-based dispatch algorithms: the EMS interprets the data collected in real-time by the sensors in the field and implements advanced algorithms based on optimization models and methods to solve complex decision-making problems. Generally, optimization models for MG management determine the optimal schedule that integrates RES and minimizes operational costs, emissions or other KPIs under constraints representing the system model. For MGs, the system model is achieved by employing a simple representation for each class of components and a single busbar representation for the electric infrastructure. In the last decade, decentralized paradigms such as microgrids and energy communities have significantly expanded the role of EMSs: as these systems have grown in size and complexity, management systems evolve from simple monitoring tools to advanced decision-support platforms capable of handling uncertainty, multi-objective trade-offs, and dynamic system behavior. Therefore, in addition to coordinating energy scheduling, modern EMSs are also tasked with multi-energy system integration across

different temporal and spatial scales, pursuit of system stability and reliability and DSM and DR strategies provision. To achieve that, they include advanced optimization methods and control algorithms, as well as data driven methods, including machine learning for forecasting. Forecasts of renewable generation, electrical demand and market signals allow to compute optimal data-driven operating strategies, which make advanced EMSs able to handle the increased complexity and size of energy systems with numerous DERs and energy vectors, and provide more accurate and reliable system control [50].

Generally, EMSs are characterized by a centralized architecture: the EMS collects information and data from each asset, solve a centralized optimization problem for the optimal dispatch of each unit and provides commands to field components and local controllers. To achieve this, all assets in the system share operational constraints, cost functions, and other pertinent information with the central controller, which the EMS uses to make decisions. Then, all goals are translated into coordinated operational actions that are then communicated to each unit, which actuates according to the coordinated schedule. Centralized EMSs are often solved by commercial optimization tools under an MPC scheme [51] and are usually implemented when the extension of the microgrid is limited since the EMS needs to collect information from each dispatchable asset to provide a centralized optimal schedule. The main advantage of centralized optimization lies in the capability of achieving the optimal solution to the problem. However, the centralized framework presents some drawbacks, such as data storage requirements, communication burden and delays, high computational load, lack of reliability and robustness to changes of the system, low resilience to cyberattacks. Moreover, the lack of privacy makes centralized approaches unattractive for agents that do not want to share detailed technical characteristics and costs with the central controller, thus reducing the participation of different devices in the system. For these reasons, non-centralized techniques may be better suited to provide the required functionality of an EMS [52], [53]. There are two main types of non-centralized methods [54]: (i) a decentralized approach where each agent independently solves an optimization subproblem but receives some aggregate information from a central node without communicating with other agents, and (ii) a distributed approach where each agent solves its own optimization problem by communicating information with its neighbors (see Figure 2.5). Decentralized architectures include a central controller that communicates with local devices, by sharing only a subset of variables. In this way, privacy is partly preserved and resilience is improved compared with the centralized approach. Parallel computation can be also implemented. Popular methods for decentralized optimization are the sub-gradient method and ADMM. A decentralized approach has a lower computational and communication burden (compared to centralized schemes) and, if well designed, can be robust to failure modes (unlike centralized approaches, which have a single point of failure). In distributed architectures, nodes communicate only with their neighbors. This configuration still implies the need of an ICT infrastructure, but characterized by low communication needs. Distributed architectures reduce the computational effort in large-scale systems via parallel computation and offer privacy and resilience advantages, although commercial tools applying these techniques are still lacking. In current literature, the most popular distributed

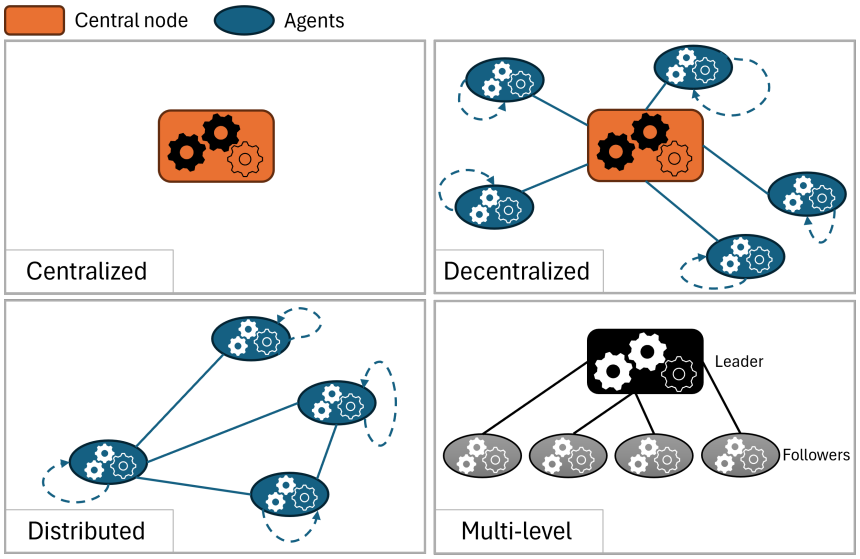

Figure 2.5: EMS optimization methods

optimization methods are distributed dual decomposition, distributed ADMM (dADMM), and the distributed primal dual interior point method. In addition to centralized and non-centralized paradigms, EMSs may also be structured according to multi-level optimization frameworks [55], in which decision-making authority is hierarchically structured across different agents. In these settings, upper level agents take strategic decisions while explicitly anticipating the reactions of lower level agents, giving rise to Stackelberg leader–follower games. Such problems are naturally formulated as bi-level optimization problems, where the leader's objective is optimized subject to the optimal response of the followers. Under suitable convexity and regularity assumptions, the followers' optimization problems can be replaced by their Karush–Kuhn–Tucker (KKT) optimality conditions, allowing the bi-level formulation to be reformulated as a Mathematical Program with Equilibrium (or Complementarity) Constraints, which can be efficiently embedded within optimization-based EMS frameworks. This structure improves computational tractability and facilitates the integration of heterogeneous actors and technologies within complex energy systems. The main advantages of multi-level optimization lie in its scalability and in the ability to explicitly represent coordination mechanisms among different decision makers, while preserving local autonomy at lower levels. At the same time, this approach introduces additional challenges, as the overall performance depends on the consistency of information exchanged across levels: misalignment between upper level objectives and lower level operational constraints may lead to suboptimal or conservative solutions.

2.4.1 Energy Management Systems for RECs

Like all initiatives for a more sustainable future, renewable energy communities also present technical, economic, regulatory, and social challenges [56]. To address these challenges, dedicated management systems and optimization models are required to ensure efficient and reliable operation, while complying with legislative constraints. Successful REC projects recognize and address challenges at both planning and management stages to ensure long-term sustainability and efficiency. In this context, modeling techniques and optimization methods [57] play a crucial role as they provide a comprehensive framework to design resilient and adaptive energy systems during the planning stage, while offering real-time solutions for managing the dynamic nature of renewable energy resources in the operational phase. In this context, the literature addressing optimization of energy communities generally distinguishes between planning problems, which focus on long-term strategic decision, and operational management problems, which concern real-time energy management under technical, economic, and regulatory constraints. Planning problems typically address optimal device sizing and integration of renewable energy resources [58] as well as the overall configuration of the community. Scheduling problems instead focus on shorter time horizons and determine optimal power exchanges, charging and discharging profiles, and energy sharing strategies. This distinction is particularly relevant for addressing the complexities of renewable energy communities under evolving legislative frameworks.

In this thesis, the focus is on the second class of decision problems, namely management decision problems applied to renewable energy communities.
Compared to common EMSs develop for microgrids, energy management systems designed for RECs build upon largely similar optimization models: the main objectives remain unchanged , while constraints still describe the technical and physical characteristics of the considered technologies. However, EMSs for RECs integrate additional objectives and constraints that come from the specific regulatory and organizational nature of energy communities. In particular, in addition to the traditional goals, such as optimizing the operation of ESSs to balance intermittent energy production and reduce peak load, coordinating distributed energy sources to maximize the overall efficiency and ensure reliable operation, and developing effective DSM strategies to provide flexibility services to the grid, EMSs for REC optimal management must explicitly include the maximization of shared energy, which represents a central performance indicator directly linked to both economic incentives and grid-related benefits. Moreover, the optimization problem is further constrained by legislative requirements, such as the definition of eligible assets, the perimeter of the community, incentive mechanisms, and rules governing energy allocation among members. As a result, while the underlying optimization structure remains similar to that of microgrid EMS, REC-oriented management frameworks require an extended formulation that integrates regulatory constraints and community-level objectives, thereby reflecting the distinctive operational logic of renewable energy communities. As said, when properly applied to a REC context, management decision problems focus on how to constantly match demand and production curves thereby increasing the amount of shared energy and improving the economic

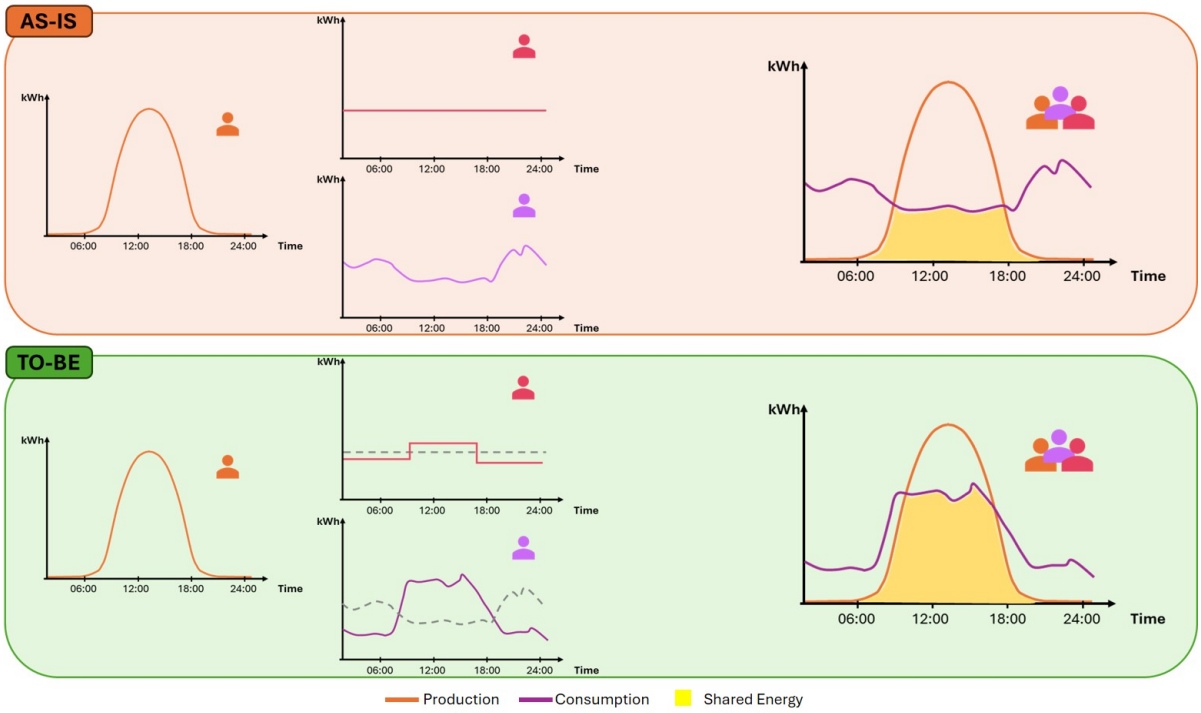

Figure 2.6: Effect of optimization considering community-level goal of shared energy maximization

and technical performance of the REC. Figure 2.6 shows a very simple example to illustrate how optimization can really make the difference in this context. A REC with three users is considered, including one photovoltaic plant and two consumers. The AS-IS scenario represents the one without optimization, while the TO-BE scenario occurs when an optimization algorithm is implemented. For both scenarios, cumulative production and consumption curves are overlapped ; the area subtended by both curves, highlighted in yellow, graphically represents shared energy. The shared energy is not zero even when optimization is not implemented, demonstrating that RECs lead to an advantage anyway; however, if an optimization algorithm is implemented, the exchange profiles of the users can be optimized to maximize energy sharing. To achieve this, the flexibility of each member must be exploited so that consumption is concentrated when there is some photovoltaic production.

As regards optimization methods, the main architectures discussed for traditional EMSs, namely centralized, decentralized and distributed approaches, can also be applied to renewable energy communities, preserving the same advantages and limitations. Centralized approaches allow for globally optimal solutions at the cost of higher computational and organizational complexity; as the size of the community increases, as it is likely to happen given the geographical perimeter of the primary cabin, classical solution methods may not be efficient enough to enable real-time control. On the other hand, decentralized and distributed optimization techniques have gained increasing attention as they enhance scalability, preserve data privacy, and improve practical imple-

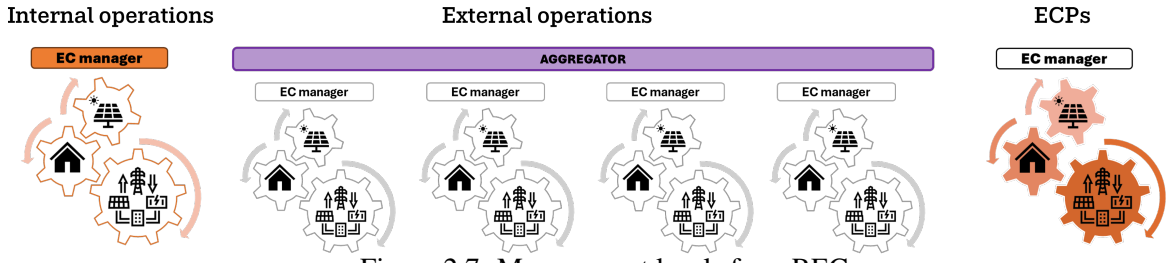

Figure 2.7: Management levels for a REC

mentation. At the same time, renewable energy communities are characterized by the presence of multiple actors (individual participants, a manager, and, in some cases, an aggregator), each with distinct and potentially conflicting objectives and different operational constraints. This structure of the problem is particularly suited to adopt multi-level optimization approaches, which are a valid solution when the problem involves multiple decision makers. In this context, higher levels may focus on community-wide objectives, such as energy sharing maximization or compliance with regulatory requirements, while lower levels address the operational optimization of individual resources. A potential resolution method is integrating the different optimization problems into a single one by analytically solving the lower-level problems and embedding these solutions as constraints within the higher-level problem. The analytical solution of each lower-level optimization problem can be found through KKT conditions, which are applied in some works presented in this thesis. As in microgrid applications, the choice of the optimization architecture for a REC depends on the size of the system, the heterogeneity of its assets, and the degree of coordination required. In this thesis, optimal management strategies for renewable energy communities are developed by adopting decentralized and multi-level optimization architectures, in accordance with the specific characteristics and coordination requirements of each case study.

The following chapters of the thesis address the problem of optimal management of a REC from the perspective of the various actors operating in the REC context: indeed, the optimal management of renewable energy communities can be approached at different levels, which will essentially form the chapters of this thesis (Figure 2.7). The ”base” level considers the optimal management of internal operations, where the goal is to maximize shared energy by acting on each ECP’s exchange profile. Two different approaches have been applied to analyze this problem: multi-level and decentralized, as explained in Chapter 3. At a higher level, multiple RECs coordinated for efficient participation in balancing markets, specifically DR, are considered: the figure of the aggregator is integrated for market participation. In this case, tracking the reference power value from the DSO is obtained by acting on the power exchange of each REC, and KKT conditions are applied to solve the problem. Finally, at a microscopic level, the focus is on individual participants or on configurations that could potentially form an REC: in fact, their potential as RECs (or participants) can be further enhanced if these entities are properly controlled at the grassroots level. Therefore, once normal EMSs are efficient, they could be integrated

with community-level constraints, regulation-aware equations, and energy sharing maximization objectives. As EPCs, smart parking lots and multi-vector energy hubs are analyzed. SPLs are typically characterized by a single point of connection to the distribution grid; this configuration allows a parking lot to be treated as a single participant within a REC. Multi-vector energy hubs instead are usually associated with multiple connection points; as a result, multi-vector energy hubs are not only compatible with the REC framework, but are naturally suited to form a REC as they already involve several energy assets within a geographically localized area.

Chapter 3

Optimal management of a renewable energy community: internal operations

This chapter is dedicated to the operational management of a REC internal operations. A renewable energy community, being defined by its collaborative approach, involves several actors that must be properly coordinated to ensure long-term sustainability and efficiency. Moreover, the definition of shared energy and its valorization rules make REC operation a regulation-aware optimization problem. All these issues make the resulting optimization problems complex to model and solve: that is where modeling techniques and optimization tools come into play. Specifically referring to management decision problems, in the context of RECs they can offer real-time solutions to increase self-consumption and improve energy sharing: they examine how to constantly match demand and production curves to maximize the shared energy and the relative incentive, how to optimize the operation of an ESS for balancing intermittent energy production and reducing peak load, how to coordinate the various distributed energy sources to maximize the overall system efficiency and how to develop effective demand-response strategies to provide flexibility services to the grid.
For these reasons, in the last years there was a rapid evolution in the field of energy management systems (EMSs) for energy communities (ECs) and community microgrids. Research contributions range from centralized optimization frameworks to decentralized, and hierarchical schemes aimed at maximizing community welfare, economic efficiency, or self-sufficiency under technical and regulatory constraints. Even thought most works do not explicitly formalize the notion of shared energy as in equation (2.1), many of them pursue equivalent goals of collective energy use, cost minimization, and sustainable cooperation among prosumers. In [59], the optimal management of an energy community is extended by introducing a new entity that manages a fleet of EVs for rent. Authors in [60] present a stochastic MPC to optimize EC operations with a proper control strategy of ESS by adopting a Time Delay Neural Network to forecast the future values of the energy features in the community. In [61], authors propose a novel community control approach for EMS that utilizes deep reinforcement learning to manage multiple appliances and energy storage systems; the final solution balances energy profitability for operators and user comfort. In [62], authors propose a hierarchical energy-sharing mechanism where end-users and producers perform a self-scheduling to minimize costs; then, the EC manager optimizes the energy trades with the external suppliers and then performs a sharing mechanism based on three different energy classes. Authors in [63] propose a methodology to optimize energy management in prosumer energy communities with the primal focus on maximizing self-consumption and self-sufficiency within the community by managing prosumers' batteries for community purposes. In [64], [65], [66], [67] an energy community is meant as a group of users that share technologies, mainly PV and ESS. In [64], PV and ESS are considered as decentralized and centralized technologies in the community; a MILP framework is developed for the community optimal operation dispatch with the option of transferring renewable energy between the EC participants. In the remaining three papers, community energy storage systems (CESSs) are considered. The decentralized control mechanism based on noncooperative game theory presented in [67] allows users to effectively determine the optimal charging and discharging strategies of a CESS in such a way that user costs and CESS degradation are minimized. In [65], the considered CESS is integrated with HVACs; authors propose a decentralized method based on

multi-block proximal Jacobian alternating direction method of multiplier that minimizes the total expected energy costs while ensuring the occupants' thermal comfort. In [66] EC users shared both a CESS and renewable energy resources; to cope with the uncertainties, a stochastic MPC approach aiming at minimizing the community energy costs is developed. The energy sharing model proposed in [68] exploits the Shapley Value to distribute the community-owned renewable energy among the members in a fair and costless approach. Another possible way to intend an energy community is considering the possibility that users exchange energy; if this possibility is considered, community-based market models should be investigated to increase the community sustainability. [69] develop a Nash equilibrium problem, solved in a distributed fashion, to solve an energy market setup where the community members have private cost functions coupled with each other through the monetary price at which each member sells its energy. In [70], an innovative user-centered framework is proposed: users exchange energy by specifying their individual preferences thanks to weighting coefficients. Based on carbon trading (CT) policies, authors in [71] propose a two-stage optimization model for a hybrid renewable energy systems: the first stage is the cost-benefit model that is associated with different cooperation modes while the second stage is the benefit-sharing model. The results show that the benefits of inclusion in a large alliance increase compared to independent decision-making and partial alliances, and the basic Shapley value method is preferred.
From the conducted literature review emerge that renewable energy communities, as defined by European Directive [15], are not properly investigated; indeed, none of the above-mentioned papers considers this regulation framework, proving that there still is a research gap about RECs. Nevertheless, REC management problems need to be addressed to make European policies really effective. The following papers provide an insight on RECs management decision problems where the concept of energy sharing is also investigated with a specific focus on the Italian regulation framework already introduced in Chapter 2. In [72], authors propose a cooperative distributed optimization framework for Italian energy communities; according to the results, this approach can yield financial benefits of 14.53% using the shared energy concept. In [73] a centralized mixed-integer linear programming optimization scheme is proposed to optimally coordinate prosumers' ESS and thermostatically controlled loads to reduce the overall energy cost for the community considering cost minimization and shared energy maximization. Authors in [74] propose a model to optimally manage an EC through reversible solid oxide cells: REC operations are optimized by maximizing the overall incentive proportional to "shared energy" and minimizing the aggregated cost for energy exchange with the grid. [75], a three-module strategy for the optimal scheduling of an ESS in a REC is proposed to minimize operation costs and optimize economic revenues, considering the possibility to share energy within the community to take advantage of the existing incentives. Authors in [76] propose a MILP model for the optimal operation of an energy community maximizing a social welfare term, including the incentives received for energy sharing at the community level. Authors in [77] propose a stochastic linear programming model to find the optimal control strategies for air conditioning systems and ESSs, which meet users' comfort requirements while maximizing the expected revenue from energy sharing with the incentives established by the Italian regulation.

Summarizing, the performed literature research reveals a diverse set of EMS paradigms applied to energy communities. Despite the different architectures and solution methods, these works share a common objective: to coordinate distributed resources to achieve collective efficiency and sustainability. However, the integration of regulatory concepts, such as "shared energy" and its valorization incentive, into these frameworks remains limited. Addressing this gap is where this PhD thesis aims to contribute, by combining regulation-aware optimization and community-level coordination.

3.1 REC internal operations: actors and objectives

This chapter examines the problem of optimal management of a REC from the "base" level of internal operations: the management of a single community and its members. In addition to minimizing costs while respecting technical constraints for each participant, the community-level objective of shared energy maximization is also integrated. To properly define the problem settings and framework, it is necessary to identify the main actors operating at this level:

- the energy community participants (ECPs)
- the energy community manager (ECM)

The ECPs are the final customers who form the community and who need to actively participate in energy generation and consumption, while the ECM is the figure coordinating all participants to make the community more efficient in several ways. Since the main characteristics and requirements of ECPs and ECM have already been outlined in the introductory chapter (2.2.3 and 2.2.2, respectively), for the sake of brevity they will not be repeated here.

As regards the objectives, this chapter focuses on maximizing the economic benefit that the REC can obtain, while considering ECPs' costs. As a community, this economic benefit mainly comes from the incentive for energy sharing (Section 3.2); however, it may not be enough to encourage ECPs to form a REC. To make the community more profitable also from an economic point of view, ECPs could also provide ancillary services to the grid through the ECM (Section 3.3). Therefore, the ECM has to coordinate the participants to maximize shared energy and guarantee a proper service provision. To do that, the ECM acts on the flexibility that each participant makes available to the community to modify their power exchange profile with the grid with the final purpose of achieving community goals. It must be considered that the ECM's actions could alter these profiles to such an extent that they result in additional costs for participants. To avoid this and for the community to be stable and solid, ECPs' requirements should be taken into account by minimizing their costs.
This specific problem is addressed in this chapter. In particular, among the various methods analyzed in the literature, two different approaches have been applied to the optimal management of the internal operations of a REC:

1. the first approach considers a multi-level architecture to encode the presence of the different actors that form a community. To solve the problem, KKT conditions are applied (Section 3.2)

2. in the second approach, a suited decentralized optimization algorithm is developed. The participation in demand response programs is also implemented as an equality coupling constraint (Section 3.3)

As said, shared energy maximization goal is achieved by acting on the power that ECP exchanges with the main grid and the same holds true for ancillary service provision to the grid. Therefore, the flexibility that each ECP puts at disposal of the community is exploited by the manager to modify power absorption/injection from/to the grid to make the overall production and consumption curves match and to guarantee a proper provision of ancillary services. All this considering the operational constraints of each participant. Since the operational constraints of each ECP are common to both approaches, for sake of brevity they are reported at the beginning of this chapter. Then, each of the two approaches is detailed in a dedicated section.

3.1.1 The proposed ECP operational Constraints

The most common technologies admitted by the legislation are considered when modeling the ECPs. On the production side, the renewable energy source to be considered is photovoltaic as this technology is the most installed RES in Italy in the last years [78], [79] and has confirmed as the main generation technology for this type of entity due to its characteristics of cost-effectiveness and versatility. On the consumption side, fixed and flexible loads are considered as well as electric vehicles (EVs). ESSs are also considered as they represent the ultimate flexible devices. Indeed, flexibility is essential for a community to achieve its goal because to maximize energy sharing the ECM needs to match demand and production curves and this matching can only be achieved if ECPs have some flexibility the manager can act on. Among these technologies, few of them have some limitations related to shared energy calculation which must be totally from renewable. As regards EVs, only the charging mode is considered (V2G mode is discarded) as in RECs the only energy resource allowed is from RES; therefore, EVs cannot work in V2G mode because in this case there would be no guarantee that such discharging energy is fully renewable. As concerns ESSs, they can be charged by withdrawing power from the main grid but its discharge must be always and only used to satisfy the internal loads and never sold back to the to the grid because it cannot be proven with certainty what the energy mix is composed of. This condition is verified as long as the buying cost from the grid is greater than the benefits (energy selling and EC incentive); indeed, in this case buying energy from the grid to charge the storage and sell the stored energy back is never convenient, but it may be convenient to charge the storage and use the stored energy later to satisfy internal loads and maximize the shared energy. All of these technologies have been considered for all ECPs; then, data are set

such that the right technologies are considered for each ECP.
Given the above considerations, the operational constraints of each ECP are reported in the following equations, whose variables and parameters are shown in Table 3.1. S^N is the set of ECPs while S^T is the set of time instants; therefore, in the formalization that follows, subscript $(\cdot)_{i,t}$ refers to quantities in time instant t for the ECP i. Moreover, upper and lower bounds are not explicitly defined as they are well recognizable from notation: they are characterized by an upper bar ($\bar{\cdot}$) and lower bar ($\underline{\cdot}$), respectively.

$$p_{i,t}^{G,in} - p_{i,t}^{G,out} + P_{i,t}^{PV} + p_{i,t}^{S,dch} - p_{i,t}^{S,ch} = P_{i,t}^{L,fix} + p_{i,t}^{L,flex} + p_{i,t}^{EV} \quad i \in S^N, t \in S^T \tag{3.1}$$

$$0 \leq p_{i,t}^{G,out} \leq \overline{P}_i^G \quad i \in S^N, t \in S^T \tag{3.2}$$

$$0 \leq p_{i,t}^{G,in} \leq \overline{P}_i^G \quad i \in S^N, t \in S^T \tag{3.3}$$

$$x_{i,t}^S = x_{i,t-1}^S + \frac{\Delta}{CAP_i^S}\left(\Gamma_i^{S,ch} p_{i,t}^{S,ch} - \frac{1}{\Gamma_i^{S,dch}} p_{i,t}^{S,dch}\right) \quad i \in S^N, t \in S^T \tag{3.4}$$

$$0 \leq p_{i,t}^{S,ch} \leq \overline{P}_i^S \quad i \in S^N, t \in S^T \tag{3.5}$$

$$0 \leq p_{i,t}^{S,dch} \leq \overline{P}_i^S \quad i \in S^N, t \in S^T \tag{3.6}$$

$$\underline{X}_i^S \leq x_{i,t}^S \leq \overline{X}_i^S \quad i \in S^N, t \in S^T \tag{3.7}$$

$$\sum_{t \in S^T} p_{i,t}^{L,flex} \Delta \geq E_i^{L,flex} \quad i \in S^N \tag{3.8}$$

$$0 \leq p_{i,t}^{L,flex} \leq \overline{P}_i^{L,flex} \quad i \in S^N, t \in S^T \tag{3.9}$$

$$x_{i,t}^{EV} = x_{i,t-1}^{EV} + \frac{\Delta}{CAP_i^{EV}} \Gamma_i^{EV} p_{i,t}^{EV} \quad i \in S^N, t \in S^T \tag{3.10}$$

$$0 \leq p_{i,t}^{EV} \leq \overline{P}_i^{EV} \quad i \in S^N, t \in S^T \tag{3.11}$$

$$\underline{X}_i^{EV} \leq x_{i,t}^{EV} \leq \overline{X}_i^{EV} \quad i \in S^N, t \in S^T \tag{3.12}$$

$$x_{i,t}^{EV} \geq X_i^{EV*} \quad i \in S^N, t = T_i^{EV*} \tag{3.13}$$

Constraint (3.1) is the power balance for each user, where $P_{i,t}^{PV}$ is power from photovoltaic plant, $p_{i,t}^{S,ch}$ and $p_{i,t}^{S,ch}$ are the power flows relevant to charging and discharging the storage, $P_{i,t}^{L,fix}$ is the fixed power load which cannot be controlled, $p_{i,t}^{L,flex}$ is the flexible power load portion, i.e. the load that can be shifted along the day, and $p_{i,t}^{EV}$ is the charging power of the electric vehicle.

Constraints (3.2) and (3.3) operate the power exchange with the main grid: the two positive terms defining $p_{i,t}^{G}$ are upper bounded by the maximum exchangeable power according to each ECP's contract. The constraints relevant to the energy storage system are (3.4)-(3.7). (3.4) is the ESS dynamic equation where $x_{i,t}^{S}$ is the ESS state of charge, CAP_i^S its capacity, $\Gamma_i^{S,ch}$ and $\Gamma_i^{S,dch}$ its charging and discharging efficiencies. Then, constraints (3.5)-(3.7) represent upper and lower bounds of ESS power flows and states of charge. Equations (3.8) and (3.9) operate the deferrable loads. Equation (3.8) imposes that the energy required by this kind of load is delivered over the entire optimization horizon. Please note that using the greater equal is preferred over the equal to alleviate the problem; this choice is further justified if one considers that the buying price from the network is always greater than the overall benefit (selling price + EC incentive) thus the solver for sure tends to satisfy $E_i^{L,flex}$ as much as enough without exceeding it. Then, the power devoted to feed the flexible loads is bounded in (3.9). The constraints relevant to electric vehicles are (3.10)-(3.13). (3.10) is the EV dynamic equation, where $x_{i,t}^{EV}$ is the EV state of charge, CAP_i^{EV} its capacity and Γ_i^{EV} its charging efficiency. Constraints (3.11) and (3.12) represent the upper and lower bounds of EV power flows and states of charge. Finally, constraint (3.13) ensures that the desired value for the EV state of charge is reached (and possibly exceeded) at the desired time instant T_i^{EV*}.

Table 3.1: Nomenclature

Symbol	Unit	Description
Sets		
$S^T = \{1, \dots, T\}$		Set of time instants
$S^{DR} \subseteq S^T$		Set of time instants where the DSO requires DR services
$S^N = \{1, \dots, N\}$		Set of energy community participants
$S^P = \{1, \dots, P\}$		Sub-set of participants with a production plant
Variables		
β	[kW]	Auxiliary variable to avoid the $\max\min(\cdot)$ formulation in the ECM objective function
$p_{i,t}^{G,in}$	[kW]	Power absorbed from the grid by ECP i
$p_{i,t}^{G,out}$	[kW]	Power injected into the grid by ECP i
$p_{i,t}^{S,ch}$	[kW]	Charging power of the storage system
$p_{i,t}^{S,dch}$	[kW]	Discharging power of the storage system
$x_{i,t}^{S}$	[/]	State of charge of the storage system
$P_{i,t}^{L,flex}$	[kW]	Flexible load power consumption
$p_{i,t}^{EV}$	[kW]	Charging power of the electric vehicle
$x_{i,t}^{EV}$	[/]	State of charge of the electric vehicle
Parameters		

Symbol	Unit	Description
Δ	[h]	Time step
α	[/]	Weight in the objective function
C^{buy}	[€/kWh]	Grid cost for purchasing energy from the grid
C^{sell}	[€/kWh]	Grid cost for selling energy to the grid
$P_{i,t}^{PV}$	[kW]	Power generated by the photovoltaic plant
$P_{i,t}^{L,fix}$	[kW]	Fixed load power consumption
$\overline{P}_i^G$	[kW]	Maximum power exchangeable with the main grid
CAP_i^S	[kWh]	Capacity of the storage system
$\Gamma_i^{S,ch}$	[/]	Charging efficiency of the storage system
$\Gamma_i^{S,dch}$	[/]	Discharging efficiency of the storage system
$\overline{P}_i^S$	[kW]	Maximum power of the storage system
$\underline{X}_i^S, \overline{X}_i^S$	[/]	Minimum/Maximum state of charge of the storage system
$E_i^{L,flex}$	[kWh]	Energy required by flexible load over the horizon
$\overline{P}_i^{L,flex}$	[kW]	Maximum power deliverable to the flexible load
$\mathbf{CAP}_i^{EV}$	[kWh]	Capacity of the electric vehicle
$\Gamma_i^{EV,ch}$	[/]	Charging efficiency of the electric vehicle
$\overline{P}_i^{EV}$	[kW]	Maximum charging power of the electric vehicle
$\underline{X}_i^{EV}, \overline{X}_i^{EV}$	[/]	Minimum/Maximum state of charge of the EV
$X_{i,t}^{EV*}$	[/]	Desired value of the EV state of charge
T_i^{EV*}	[h]	Time instant at which the desired EV SoC must be reached
ζ	[/]	Parameter affecting the NLP approximation quality
$TIP_{p,t}$	[€/kWh]	Incentive for ECPs with a production plant ($p \in S^P \subseteq S^N$)
P_t^{DR}	[kW]	Demand response set point given by the DSO

3.2 Multi-level optimal management

This section investigates the first of the two approaches applied for the optimal management of a REC internal operations. As the community framework needs to consider two different perspectives - that of the participants and that of the manager - the proposed architecture consists of two distinct levels, described in Section 3.2.1. By considering both the ECPs and the ECM, the model considers potentially conflicting objectives, ensuring optimal operations of the ECPs by minimizing their costs, while maximizing shared energy.
The main novelty here lies in modeling the most up-to-date incentive scheme, that was introduced in the final phase (see Table 2.2) by DM MASE 414/23, also called as *Decreto CACER* [80], [21]. As emerged from the literature review, energy communities are mainly treated as classical energy districts and microgrids and, even when treated as indicated in the European Directive [15], the real incentive scheme is neglected. Table 3.2 compares the latest papers related to the optimal management of RECs in the Italian context[1] and highlights that this work is the only one that introduces the new incentive according to the newest legislation [80]. The newest tariff formula is very complex and needs to be approximated. To do that, two different approximation techniques are used and tested: one leads to a mixed-integer linear programming (MILP) problem, while the other ends up in a non-linear programming (NLP), which are described in Section 3.2.1.2.
Summarizing, the main contributions of this chapter are:

- A novel optimization model for the optimal management of a REC is presented. In particular, both the ECPs and the ECM objectives are considered by maximizing the shared energy while minimizing the participants costs.
- The real incentive scheme recently introduced by the Italian legislation is considered in the ECM problem. As this scheme has a very complex formulation, it is approximated using two different techniques. In the case study, the performances of the two formulations are tested.
- An accurate representation of a real EC is presented in the case study. The impact of participating in a EC is analyzed showing the real benefit received by the ECPs.

3.2.1 Decision problem definition

In this section, the optimization problems of the the two levels are formulated. At the low-level, the ECPs aim to minimize their costs , while the high-level encodes the ECM who aims to maximize the revenue generated by sharing energy. Each low-level optimization problem is

[1]The focus is kept on the Italian context because the regulations and the incentive mechanisms are still not homogeneous and each country has its own rules, as explained in Chapter 2.

Table 3.2: Literature research summary on RECs in the Italian context.

	Year	Problem class	Max{Shared-energy}	Min{ECP costs}	Updated Incentive [80]
[76]	2022	MILP	✓	✓	-
[74]	2023	MIQCP	✓	-	-
[60]	2022	MILP	✓	-	-
[72]	2024	LP	✓	✓	-
[73]	2024	MILP	✓	✓	-
This work		MILP/NLP	✓	✓	✓

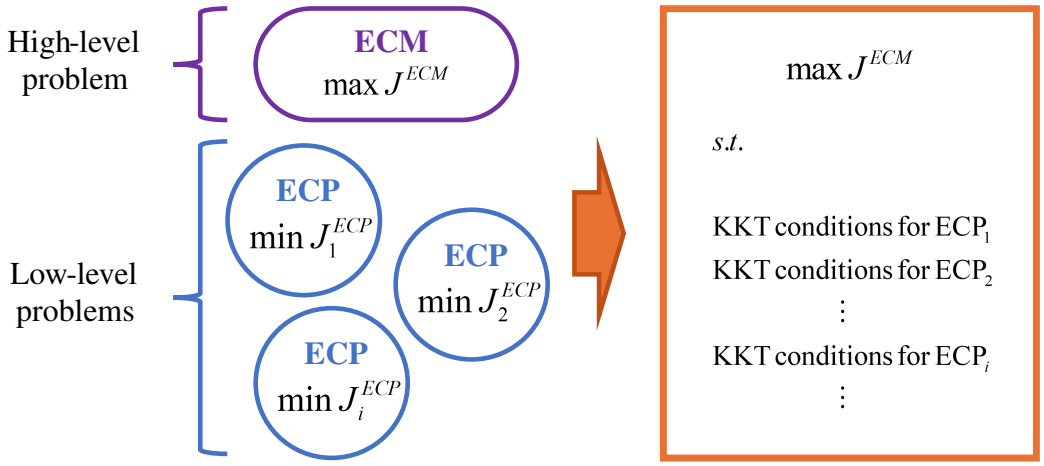

Figure 3.1: Schematic representation of the proposed bi-level approach

converted into constraints for the high-level problem by using the Karush-Kuhn-Tucker (KKT) conditions (Figure 3.1). The mathematical formulation of the two levels is presented in the following; when discussing the high-level, the overall framework relevant to the incentive scheme is presented.

3.2.1.1 Low-level: EC participants

The low-level of the proposed approach is focused on each EC participant, who aims to minimize its own costs. At this level, one optimization problem for each ECP, denoted with index i, is set and solved.
The objective function for each user is composed by two different terms

$$J_i^{ECP} = \Delta \sum_{t \in S^T} \left(C^{buy} p_{i,t}^{G,in} - C^{sell} p_{i,t}^{G,out} \right) + \alpha \left(x_T^S - x_0^S \right)^2 \quad i \in S^N \tag{3.14}$$

The first term is related to grid cost minimization, where C^{buy} and C^{sell} are the costs for purchasing/selling energy from/to the grid, respectively; please note that to evaluate costs and benefits

properly, the bidirectional power exchange with the main grid is split into two positive terms $p_{i,t}^{G,in}$ and $p_{i,t}^{G,out}$. In addition to grid costs, the second term is added to avoid exploiting the ESS 'for free', by minimizing the difference between the ESS state of charge at the end of the optimization horizon (x_T^S) and its value at the beginning of the optimization horizon (x_0^S).
Each ECP is characterized by different features and technologies, whose technical and physical constraints must be respected. Therefore, the operational constraints modeled in (3.1)-(3.13) must be included as constraints of the low-level problems. As already mentioned, all technologies are considered when modeling ECP constraints; then, data are set such that for each ECP only the suitable devices are actually implemented.

3.2.1.2 High-level: ECM

The high-level models the ECM problem, which is maximizing the overall REC benefits. To reach this goal, the energy community manager aims to maximize shared energy e_t^{sh} (2.1), which is rewarded according to the most up-to-date incentive scheme [80] by the GSE.

3.2.1.2.1 The considered incentive scheme As the goal of the ECM is shared energy maximization, the economic contribution to be analyzed in detail is the one regarding the incentive for energy sharing, contribution *b)* in Section 2.1.2.
The equation provided by the legislation is the following:

$$TIP_{i,t} = \left\{\min\left[CAP_i; TP_i^{base} + \max\left(0, 180 - PZ_t\right)\right] + FC^{zone}\right\} \cdot (1 - F) \quad i \in S^N, t \in S^T \tag{3.15}$$

This equation shows that the incentive is made up of a fixed and a variable part: the fixed part TP_i^{base} varies according to the size of each plant i (Table 3.3), the variable part according to the hourly market price of energy PZ_t. The fixed part decreases as the size of the plants increases, while the variable part fluctuates depending on the energy price (as the energy market price decreases, the variable part increases). For the incentive an upper bound is defined: CAP_i is the threshold value that the tariff can assume and is defined based on the size of each plant (Table 3.3). Then, to consider the lower productivity of photovoltaic systems in central-northern regions with respect to southern ones, the correction factor FC^{zone} has been introduced; in this way, for central-northern regions the tariff is increased as reported in Table 3.4. Finally, parameter F is linked to the possible payout of a capital contribution: in most cases, it varies linearly between 0, in the case in which no capital contribution is foreseen, and 0.5, in the case of a capital contribution equal to 40% of the investment. For more information about this, please refer to Part III of [80].

The calculation of the overall incentive requires further investigation; indeed, as presented above, each production plant has an incentive depending on its size. However, since shared energy can collect different contributions from the production plants, the overall incentive depends on which plants are considered in the definition of the shared energy. In fact, as presented in

Table 3.3: Base tariff and threshold value depending on the plant size

Size of the plant	TP^{base}	CAP
$P < 200\,\text{kW}$	0.08 [€/kWh]	0.12 [€/kWh]
$200\,\text{kW} < P < 600\,\text{kW}$	0.07 [€/kWh]	0.11 [€/kWh]
$P > 600\,\text{kW}$	0.06 [€/kWh]	0.10 [€/kWh]

Table 3.4: Correction factor for PV productivity

Zone	FC^{zone}
Central Italy	+0.004 [€/kWh]
Northern Italy	+0.010 [€/kWh]

the right side of Figure 2.3, some plants or a portion of them can be excluded. The rule coming from the legislation is that the plants are ordered according to the date of the first connection to the grid. In Figure 3.2, an example of how the tariff is calculated in case of production surplus is reported. In this example, two different production plants are considered: plant $\#1$ was connected to the grid on January 2024, while plant $\#2$ was connected to the grid on April 2024. Considering the data of connection to the grid, the energy produced by plant $\#1$ is counted first; then plant $\#2$ receives an incentive not on the total produced energy but on how much it contributed to the energy sharing. In this way, each plant receives the incentive based on how much it actually contributes to energy sharing and the EC obtains an incentive equal to the sum of the incentives obtained by each plant.

Modeling the new incentive scheme is complex because the incentive depends on the plant size and therefore each plant has its own incentive value. Therefore, it is necessary to consider how much each plant actually contribute to sharing energy, because they are incentivized on this amount of energy. To calculate the energy that each plant contributes to share, it is necessary to consider how much load has already been covered by the other plant that count first by date of first connection to the grid. Figure 3.3 provides a simple example of two production plants and three points of delivery to better understand how this incentive scheme has been modeled. As imposed by the Italian legislation, plants are ordered according to the date of the first connection to the grid. Therefore, starting from Plant $\#1$, its production is compared with the overall withdrawn power and the minimum is taken (remember that shared energy is the minimum between electricity injected and the electricity withdrawn). Then for Plant $\#2$, its production is not compared with the overall withdrawn power but with the residual one, i.e. is the overall one minus that already covered by Plant $\#1$. Again, the minimum must be taken; however, in this case the production of Plant $\#2$ exceeds the residual withdrawn power, because most of the consumption is already covered by Plant $\#1$ which is counted first. In this way, taking the minimum, the second plant is not incentivized on its total production but on how much it actually contributes to energy sharing.

In order to model this incentive scheme, it is necessary to compare the power produced by each

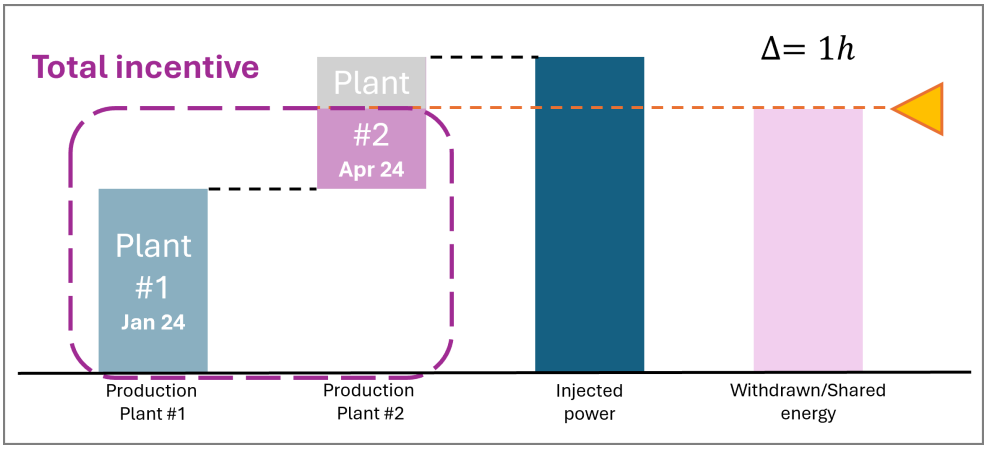

Figure 3.2: Tariff calculation in case of surplus of production [3]

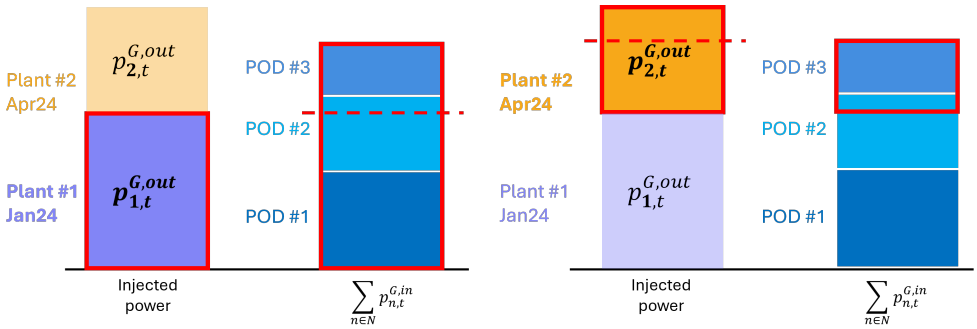

Figure 3.3: Comparison between injected and withdrawn power for the incentive scheme modeling

production plant p (ordered by their date of first connection) with the residual withdrawn energy, which is the total one minus that already covered by plants $\{1, \ldots, p-1\}$. Hence, the remaining load when analyzing production plant p can be written as:

$$\sum_{n \in S^N} p_{n,t}^{G,in} - \sum_{i=1}^{p-1} p_{i,t}^{G,out} \tag{3.16}$$

This difference takes a negative value if the total consumption is already satisfied by the production. Since it is not possible to generate more shared energy, the maximum between the value of this difference and zero is considered.
Moreover, the result of this maximum, i.e. the load that can be virtually satisfied, must be compared with the power injected by plant p into the grid ($p_{p,t}^{G,out}$). This comparison is made by taking the minimum between the two terms recalling the definition of shared energy in (2.1) and ensures that plants are not incentivized on total production but on how much they actually contribute to energy sharing.

The result is that for each hour the incentive is:

$$\sum_{p \in S^P} TIP_{p,t} \Delta \cdot \min \left\{ p_{p,t}^{G,out}, \max \left[0, \sum_{n \in S^N} p_{n,t}^{G,in} - \sum_{i=1}^{p-1} p_{i,t}^{G,out} \right] \right\} \tag{3.17}$$

where

- $TIP_{p,t}$ is the incentive expressed in [€/kWh], calculated for each member as in (3.15). Since the final value of the incentive depends on fixed and a-priori known parameters, this can be calculated in pre-processing;
- $S^P \subseteq S^N$ is the sub-set of participants with a production plant that, depending on production and consumption, could potentially inject some power;
- $p_{p,t}^{G,out(in)}$ is the power injected (withdrawn) in (from) the main grid by the $p-th$ participant.

3.2.1.2.2 The proposed ECM Objective Function The community manager aims at maximizing the overall incentive obtained by the REC over the entire optimization horizon, therefore the ECM objective function would be:

$$\max \ J^{ECM} \tag{3.18}$$

with

$$J^{ECM} = \sum_{t \in S^T} \left\{ \sum_{p \in S^P} TIP_{p,t} \Delta \cdot \min \left\{ p_{p,t}^{G,out}, \max \left[0, \sum_{n \in S^N} p_{n,t}^{G,in} - \sum_{i=1}^{p-1} p_{i,t}^{G,out} \right] \right\} \right\} \tag{3.19}$$

Since the objective function in (3.19) is highly nonlinear and very complicated from a computational viewpoint, it cannot be implemented as it is. To cope with this issue, it has been simplified thanks to some approximation and linearization techniques.
First, the inner $max(\cdot)$ function can be substituted by introducing a variable β such as:

$$J^{ECM} = \sum_{t \in S^T} \left\{ \sum_{p \in S^P} TIP_{p,t} \Delta \cdot \min \left\{ p_{p,t}^{G,out}, \beta_{p,t} \right\} \right\} \tag{3.20}$$

$$\beta_{p,t} \geq \sum_{n \in S^N} p_{n,t}^{G,in} - \sum_{i=1}^{p-1} p_{i,t}^{G,out} \tag{3.21}$$

$$\beta_{p,t} \geq 0 \tag{3.22}$$

Then, by applying the well-known rule $min(x_1, x_2) = -max(-x_1, -x_2)$, the $min(\cdot)$ function in (3.20) can be rewritten as a $max(\cdot)$ function obtaining:

$$J^{ECM} = \sum_{t \in S^T} \left\{ \sum_{p \in S^P} TIP_{p,t} \Delta \cdot \left[- \max \left\{ -p_{p,t}^{G,out}, -\beta_{p,t} \right\} \right] \right\} \tag{3.23}$$

At this point, the max function in (3.23) can be substituted with two techniques.

T1. MILP formulation The first approximation technique involves the absolute value as in (3.24). In fact, the $max(\cdot)$ function can be written as

$$\max(x_1, x_2) = \frac{(x_1 + x_2) + |x_1 - x_2|}{2} \tag{3.24}$$

By substituting this expression in (3.23), the following ECM objective function is obtained

$$J^{ECM} = \sum_{t \in S^T} \left\{ \sum_{p \in S^P} TIP_{p,t} \Delta \cdot \left[- \frac{\left(-p_{p,t}^{G,out} - \beta_{p,t} \right) + \left| -p_{p,t}^{G,out} - \beta_{p,t} \right|}{2} \right] \right\} \tag{3.25}$$

With this technique, a MILP problem is defined.

T2. NLP formulation The second approximation technique is the one presented in [81], where authors describe how the Gaussian error function

$$erf(x) = \frac{2}{\sqrt{\pi}} \int_0^x e^{-t^2} dt \tag{3.26}$$

can be used to approximate the max function such as

$$\max(x_1, x_2) = f(x_1, x_2, \zeta) = \frac{(x_1 + x_2) + (x_1 - x_2)\, erf\left(\zeta\,(x_1 - x_2)\right)}{2} \tag{3.27}$$

The quality of the approximation depends on the value of the parameter ζ; in Figure 3.4, a comparison of different values is reported. As clearly represented, the higher the parameter value, the better the approximation quality.
By using this technique, the following ECM objective function is obtained and a NLP problem is defined.

$$J^{ECM} = \sum_{t \in S^T} \left\{ \sum_{p \in S^P} TIP_{p,t} \Delta \cdot \left[- \frac{\left(-p_{p,t}^{G,out} - \beta_{p,t} \right) + \left(-p_{p,t}^{G,out} + \beta_{p,t} \right) erf\left(\zeta \left(-p_{p,t}^{G,out} - \beta_{p,t} \right) \right)}{2} \right] \right\} \tag{3.28}$$

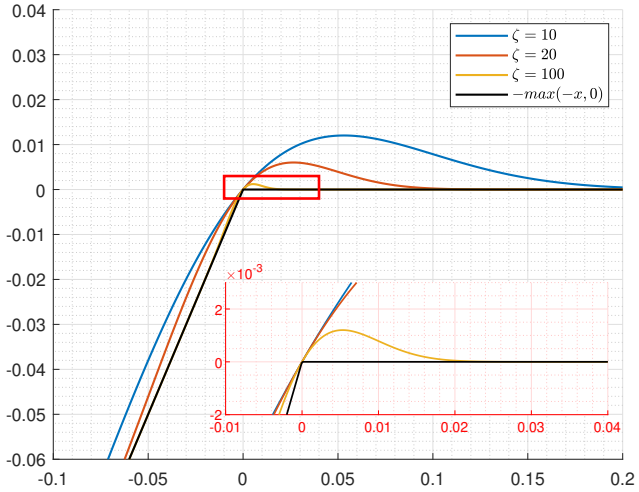

Figure 3.4: Comparison of the second approximation by changing the parameter ζ

As a final remark, the different techniques applied to remove the $max(min(max(\cdot)))$ structure should be used this specific combination. In fact, it is possible to use them in different orders; however, due to the particular structure of the functions, using the two techniques in **T1.** and **T2.** before using the variable β, would define a problem where the two approximations **T1.** and **T2.** are in the constraints of the problem. This solution is harder to solve and leads to numerical issues even in small instances. Instead, with the proposed order, the approximations remain in the cost function resulting in a run-time reduction.

3.2.2 Overall Optimization Problem

To consider the multi-agent framework, a multi-level approach is adopted. In this section, the problems relevant to the low-level are rewritten in the canonical form and then converted into the corresponding KKT conditions. Before that, in the following paragraph, the basic notions of multi-level optimization are reported, which will then be implemented to solve the problem.

3.2.2.1 Multi-level programming

Many decision problems involve multiple decision makers with different objectives; therefore, decision makers have their own optimization goals, but share aspects of the system model and/or certain constraints. It could happen that decisions are structured hierarchically across various levels, meaning that the choices of some decision makers affect the others'; this is the case when multilevel programming can be applied. The most common structure is the bi-level problem,

where two hierarchical levels are considered: it involves a leader (upper level) and one or more followers (lower level), who pursue their individual goals while considering the decisions of the leader above. In this context, a potential resolution method is to integrate the different optimization problems into a single one by analytically solving the lower-level problems and embedding these solutions as constraints within the leader's problem. The general formulation of a multi-level programming problem is provided by:

$$\begin{aligned} &\underset{x}{\text{Min}}\, f\left(x, x_1, ..., x_N\right) \\ &s.t. \\ &g\left(x, x_1, ..., x_N\right) = 0 \\ &h\left(x, x_1, ..., x_N\right) \leq 0 \end{aligned} \tag{3.29}$$

$$\begin{cases} \underset{x_1}{\text{Min}}\, f_1\left(x, x_1, ..., x_N\right) \\ s.t \\ g_1\left(x, x_1, ..., x_N\right) = 0 \\ h_1\left(x, x_1, ..., x_N\right) \leq 0 \end{cases} \quad \ldots \quad \begin{cases} \underset{x_N}{\text{Min}}\, f_N\left(x, x_1, ..., x_N\right) \\ s.t \\ g_N\left(x, x_1, ..., x_N\right) = 0 \\ h_N\left(x, x_1, ..., x_N\right) \leq 0 \end{cases} \tag{3.30}$$

where vector $x \in \mathbb{R}^n$ includes the set of optimization variables of the upper level problem, vector $x_i \in \mathbb{R}^m$ includes the set of optimization variables of constraining problem i, and $\lambda_i \in \mathbb{R}^m$ and $\mu_i \in \mathbb{R}^m$ are the dual variable vectors of problem i associated with the equality and inequality constraints. The analytical solution of each follower' optimization problem can be found through KKT conditions:

$$\begin{aligned} &\underset{x}{\text{Min}}\, f\left(x, x_1, ..., x_N\right) \\ &s.t. \\ &g\left(x, x_1, ..., x_N\right) = 0 \\ &h\left(x, x_1, ..., x_N\right) \leq 0 \\ &KKT_1 \\ &\vdots \\ &KKT_N \end{aligned} \tag{3.31}$$

It is reminded that the KKT conditions of a general problem 3.32:

$$\begin{aligned} &\min_x \quad f(x) \\ &s.t. \\ &h(x) = 0 \\ &g(x) \leq 0 \end{aligned} \tag{3.32}$$

are

$$\begin{aligned} &\nabla_x f(x) + \lambda^T \nabla_x h(x) + \mu^T \nabla_x g(x) = 0 \\ &h(x) = 0 \\ &g(x) \leq 0 \\ &\mu^T g(x) = 0 \\ &\mu \geq 0 \end{aligned} \tag{3.33}$$

The first KKT condition, known as the *stationarity condition*, ensures that the derivative of the objective function with respect to any admissible direction, considering the constraints, must be zero i.e. no local improvement is possible. The second and third KKT conditions are related to *primal feasibility*: both the equality and inequality constraints must be satisfied for the optimal solution to lie within the feasible region. The fourth condition is the *complementary slackness* condition, ensuring that if the constraint is active the associated multiplier μ is positive, or if the constraint is inactive $\mu = 0$. The last condition, known as *dual feasibility* condition, prevents negative Lagrange multipliers associated with the inequality constraints; this would suggest that violating a constraint improves the solution, which contradicts the very definition of constraints.

3.2.2.2 Low-level problems reformulation

With the notions just reviewed, the overall problem is given by the high-level objective function and the low-level problems converted into the corresponding KKT. To do this, the ECPs problems must be reformulated, as shown in this paragraph.
Since the problem statement is the same for each participant, for the sake of simplicity, the index relevant to each ECP is omitted in this section. Moreover, the bold characters in the following will denote vectors and matrices.
By substituting the power balance (3.1) in (3.14) and rearranging, the objective function becomes

$$J^{ECP} = \Delta \left[\left(\mathbf{C^{buy}} - \mathbf{C^{sell}} \right)^{\mathbf{T}} \mathbf{p^{G,out}} + \left(\mathbf{C^{buy}} \right)^{\mathbf{T}} \left(\mathbf{p^{S,ch}} - \mathbf{p^{S,dch}} + \mathbf{p^{L,flex}} + \mathbf{p^{EV}} \right) \right] + \alpha \cdot \left(x_T^S - x_0^S \right)^2 \tag{3.34}$$

where the five variables represent the control variables such

$$\mathbf{u} = \begin{bmatrix} \mathbf{u_1} \\ \mathbf{u_2} \\ \mathbf{u_3} \\ \mathbf{u_4} \\ \mathbf{u_5} \end{bmatrix} = \begin{bmatrix} \mathbf{p^{G,out}} \\ \mathbf{p^{S,ch}} \\ \mathbf{p^{S,dch}} \\ \mathbf{p^{L,flex}} \\ \mathbf{p^{EV}} \end{bmatrix} \tag{3.35}$$

Then, (3.34) can be written as a function of $\mathbf{u}$

$$J^{ECP} = \Delta \left[\left(\mathbf{C}^{buy} - \mathbf{C}^{sell}\right)^T \quad \left(\mathbf{C}^{buy}\right)^T \quad \left(-\mathbf{C}^{buy}\right)^T \quad \left(\mathbf{C}^{buy}\right)^T \quad \left(\mathbf{C}^{buy}\right)^T \right] \mathbf{u} + \alpha \cdot \mathbf{\Theta}^T \mathbf{\Theta} \mathbf{u} \tag{3.36}$$

where:

$$\mathbf{\Theta} = \begin{bmatrix} \mathbf{0} & \mathbf{K^{ch}} & \mathbf{K^{dch}} & \mathbf{0} & \mathbf{0} \end{bmatrix} \tag{3.37}$$

Equality constraints are rewritten in matrix form to be substituted in the inequality constraints, so that the overall optimization problem becomes an inequality constrained convex optimization problem. The power balance in (3.1) could be written as

$$\begin{bmatrix} \mathbf{I} & \mathbf{I} & -\mathbf{I} & \mathbf{I} & \mathbf{I} \end{bmatrix} \mathbf{u} = \mathbf{P}^{PV} - \mathbf{P}^{L,fix} + \mathbf{p}^{G,in} \tag{3.38}$$

Then, the ESS and EV state equations in (3.4) and (3.10) could be written as

$$\mathbf{x}^S = \begin{bmatrix} \mathbf{0} & \mathbf{K^{ch}} & \mathbf{K^{dch}} & \mathbf{0} & \mathbf{0} \end{bmatrix} \mathbf{u} + \mathbf{1} X_0^S \tag{3.39}$$

$$\mathbf{x}^{EV} = \begin{bmatrix} \mathbf{0} & \mathbf{K^{ch}} & \mathbf{K^{dch}} & \mathbf{0} & \mathbf{0} \end{bmatrix} \mathbf{u} + \mathbf{1} X_0^{EV} \tag{3.40}$$

where terms $\mathbf{K}^*$ are TxT matrices defined as:

$$\begin{aligned} \mathbf{K}^{ch} &= \begin{cases} k_{i,j} = 0 & \text{if} \quad i < j \\ k_{i,j} = \frac{\Gamma^{S,ch}\Delta}{CAP^S} & \text{if} \quad i \geq j \end{cases} \\ \mathbf{K}^{dch} &= \begin{cases} k_{i,j} = 0 & \text{if} \quad i < j \\ k_{i,j} = -\frac{\Delta}{\Gamma^{S,dch} CAP^S} & \text{if} \quad i \geq j \end{cases} \end{aligned} \tag{3.41}$$

$$\mathbf{K}^{EV} = \begin{cases} k_{i,j} = 0 & \text{if} \quad i < j \\ k_{i,j} = \frac{\Gamma^{EV}\Delta}{CAP^{EV}} & \text{if} \quad i \geq j \end{cases} \tag{3.42}$$

Note that the formulation in (3.39)-(3.42) represents the conversion of the dynamic problem to a static one. Then, making appropriate substitutions and some algebraic manipulations, inequality constraints (3.2)-(3.3) (3.5)-(3.9), (3.11)-(3.13) can be written in matrix form such as

$$\mathbf{\Omega u} + \mathbf{\Psi} \leq \mathbf{0} \tag{3.43}$$

with

$$\boldsymbol{\Omega} = \begin{bmatrix} \mathbf{0} & -\mathbf{I} & \mathbf{0} & \mathbf{0} & \mathbf{0} \\ \mathbf{0} & \mathbf{I} & \mathbf{0} & \mathbf{0} & \mathbf{0} \\ \mathbf{0} & \mathbf{0} & -\mathbf{I} & \mathbf{0} & \mathbf{0} \\ \mathbf{0} & \mathbf{0} & \mathbf{I} & \mathbf{0} & \mathbf{0} \\ \mathbf{0} & -\mathbf{K}^{\mathbf{ch}} & -\mathbf{K}^{\mathbf{dch}} & \mathbf{0} & \mathbf{0} \\ \mathbf{0} & \mathbf{K}^{\mathbf{ch}} & \mathbf{K}^{\mathbf{dch}} & \mathbf{0} & \mathbf{0} \\ -\mathbf{I} & \mathbf{0} & \mathbf{0} & \mathbf{0} & \mathbf{0} \\ \mathbf{I} & \mathbf{0} & \mathbf{0} & \mathbf{0} & \mathbf{0} \\ -\mathbf{I} & -\mathbf{I} & \mathbf{I} & -\mathbf{I} & -\mathbf{I} \\ \mathbf{I} & \mathbf{I} & -\mathbf{I} & \mathbf{I} & \mathbf{I} \\ \mathbf{0} & \mathbf{0} & \mathbf{0} & -\mathbf{I} & \mathbf{0} \\ \mathbf{0} & \mathbf{0} & \mathbf{0} & \mathbf{I} & \mathbf{0} \\ \mathbf{0} & \mathbf{0} & \mathbf{0} & -\mathbf{1}\boldsymbol{\Delta} & \mathbf{0} \\ \mathbf{0} & \mathbf{0} & \mathbf{0} & \mathbf{0} & -\mathbf{I} \\ \mathbf{0} & \mathbf{0} & \mathbf{0} & \mathbf{0} & \mathbf{I} \\ \mathbf{0} & \mathbf{0} & \mathbf{0} & \mathbf{0} & -\mathbf{K}^{\mathbf{EV}} \\ \mathbf{0} & \mathbf{0} & \mathbf{0} & \mathbf{0} & \mathbf{K}^{\mathbf{EV}} \\ \mathbf{0} & \mathbf{0} & \mathbf{0} & \mathbf{0} & -\mathbf{K}^{\mathbf{EV}}_{\mathbf{T^{EV*},:}} \end{bmatrix}; \boldsymbol{\Psi} = \begin{bmatrix} \mathbf{0} \\ -\overline{\mathbf{P}}^{\mathbf{S}} \\ \mathbf{0} \\ -\overline{\mathbf{P}}^{\mathbf{S}} \\ \mathbf{X}^{\mathbf{S}} - \mathbf{1}X_0^S \\ -\overline{\mathbf{X}}^{\mathbf{S}} + \mathbf{1}X_0^S \\ \mathbf{0} \\ -\overline{\mathbf{P}}^{\mathbf{G}} \\ \mathbf{P}^{\mathbf{PV}} - \mathbf{P}^{\mathbf{L,fix}} \\ -\overline{\mathbf{P}}^{\mathbf{G}} - \mathbf{P}^{\mathbf{PV}} + \mathbf{P}^{\mathbf{L,fix}} \\ \mathbf{0} \\ -\overline{\mathbf{P}}^{\mathbf{L,flex}} \\ E^{L,flex} \\ \mathbf{0} \\ -\overline{\mathbf{P}}^{\mathbf{EV}} \\ \mathbf{X}^{\mathbf{EV}} - \mathbf{1}X_0^{EV} \\ \mathbf{1}X_0^{EV} - \overline{\mathbf{X}}^{\mathbf{EV}} \\ X^{EV*} \end{bmatrix}$$

where double inequalities have been split to present the constraints explicitly. Again, please note that the low-level equality constraints do not explicitly enter into the definition of these matrices as they are substituted into the objective function and other constraints.

3.2.2.3 Deriving KKT conditions

Once the ECPs problems are properly reformulated, it is possible to define the KKT conditions as

$$\left[\left(\mathbf{C}^{buy} - \mathbf{C}^{sell}\right)^T \quad \left(\mathbf{C}^{buy}\right)^T \quad \left(-\mathbf{C}^{buy}\right)^T \quad \left(\mathbf{C}^{buy}\right)^T \quad \left(\mathbf{C}^{buy}\right)^T \right] \Delta + \mu^T \boldsymbol{\Omega} = \mathbf{0} \tag{3.44}$$

$$\mu^T \left\{ \boldsymbol{\Omega}\mathbf{u} + \boldsymbol{\Psi} \right\} = \mathbf{0} \tag{3.45}$$

$$\mu \geq \mathbf{0} \tag{3.46}$$

where μ is the Lagrange multiplier associated with inequality constraints. Of course, also (3.43) must be considered among KKT conditions.

Table 3.5: Problem data

T	Δ [h]	$\overline{P}^{L,\text{flex}}$ [kW]	$\overline{P}^{G}$ [kW]	$\Gamma^{S,\text{ch}}$ [/]	$\Gamma^{S,\text{dch}}$ [/]	$\underline{X}^{S}$ [/]	$\overline{X}^{S}$ [/]	$\overline{P}^{EV}$ [kW]	Γ^{EV} [/]	$\underline{X}^{EV}$ [/]	$\overline{X}^{EV}$ [/]
24	1	2	30	0.95	0.95	0.2	1	3	0.95	0.2	1

Note that, to obtain a MILP problem, (3.45) can be linearized by introducing a binary variable δ and substituting the constraints with

$$\{\mathbf{\Omega u} + \mathbf{\Psi}\} + (\mathbf{1} - \delta) \cdot M \geq \mathbf{0} \tag{3.47}$$

$$\mu - \delta M \leq \mathbf{0} \tag{3.48}$$

where M is a sufficiently big number.

Finally, depending on the considered approximation technique (MILP or NLP) the overall optimization problem becomes:

- MILP formulation : (3.18),(3.25) s.t. (3.21)-(3.22), (3.43)-(3.44), (3.46)-(3.48)
- NLP formulation : (3.18),(3.28) s.t. (3.21)-(3.22), (3.43)-(3.46).

3.2.3 Application to a Case Study

This section presents the case study and discusses the main results. Then, the comparison between the two approximation techniques introduced in Section 3.2.1.2.2 is presented in order to show their performances. A scalability analysis is also presented to prove the suitability of this approach for larger scenarios. Finally, in the last part of this section, a sensitivity analysis on the most important parameters is described.

3.2.3.1 Problem data

Here, the main data relevant to the analyzed EC are presented; in particular, a medium-size case study is tested, where an EC with 10 ECPs ($N = 10$) is considered. Table 3.5 reports the general data relevant to the optimization problem, while Table 3.6 shows the data relevant to each ECP. Please note that selecting a one-hour time step is coherent with the legislation, according to which shared energy is calculated ex-post on an hourly basis.

In addition to these data, it is necessary to specify the selling and buying price for exchanging power with the main grid: C_t^{sell} is set to 0.08[€/kWh], while C_t^{buy} is reported in Figure 3.5. Moreover, Figure 3.6 depicts the power profiles relevant to the PV production and the fixed load for each ECP. By analyzing data in Table 3.6 and Figure 3.6, one can notice how generation and consumption are allocated: as an example, only ECP 1-2-4-6-9 need to charge their EVs, while

Table 3.6: ECP data

	CAP^S [kWh]	X_0^S [/]	$\overline{P}^S$ [kW]	$E^{L,\text{flex}}$ [kWh]	CAP^{EV} [kWh]	X_0^{EV} [/]	X^{EV*} [/]	T^{EV*} [h]
ECP1	/	/	/	3.21	10	0.4	0.8	8
ECP2	30	0.2	10	7.01	10	0.5	0.8	11
ECP3	20	0.2	10	11.31	/	/	/	/
ECP4	/	/	/	8.31	10	0.2	0.8	16
ECP5	/	/	/	6.56	/	/	/	/
ECP6	15	0.2	10	5.14	10	0.3	0.9	21
ECP7	/	/	/	3.20	/	/	/	/
ECP8	/	/	/	12.76	/	/	/	/
ECP9	/	/	/	6.50	10	0.35	0.8	13
ECP10	/	/	/	13.78	/	/	/	/

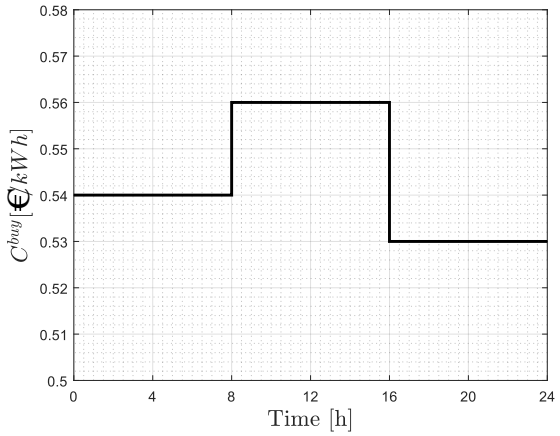

Figure 3.5: Energy buying price

ECP 2-3-6 are the only ones to have a production plant and are the ones that could potentially injected some power into the grid.

The incentive value must also be specified, referring to the equation provided by the legislation as in (3.15). In this paper, all the production plants are assumed to be smaller than 200[kW], which is consistent with small PV plants that are installed on the roofs of independent homes and condominiums. Therefore, according to Table 3.3, $CAP_i = 0.1$[€/kWh] and $TIP_i^{base} = 0.08$[€/kWh] for all plants. As far as the correction factor is concerned, it is assumed that the considered EC is in the north of Italy and so $FC^{zone} = 0.010$[€/kWh]. Then, since the disbursement of the possible payout of a capital contribution does not affect the optimal solution, parameter F is assigned a value equal to zero. Finally, considering the values just defined for the parameters in equation (3.15) and the energy price in Figure 3.5, the final value for the incentive $TIP_{i,t} = 0.11$[€/kWh] for all plants and in every time interval.

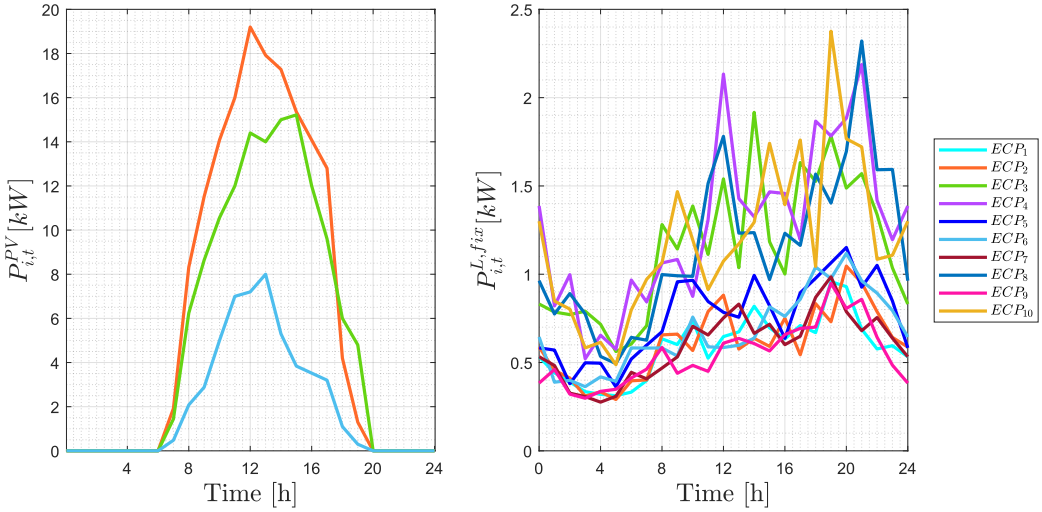

Figure 3.6: ECP profiles on PV production and consumption

Table 3.7: ECP Cost [€]

ECP1	ECP2	ECP3	ECP4	ECP5	ECP6	ECP7	ECP8	ECP9	ECP10	$\sum$ ECPs
11.75	-10.26	-7.18	24.27	13.45	-1.71	9.51	21.94	13.11	22.82	97.71

3.2.3.2 Optimization results

The proposed methodology is tested on the instance just described and a detailed description of the main results is provided. It is relevant to highlight that the results illustrated below are obtained by applying the second approximation technique and therefore are relevant to a NLP problem, whose solution is obtained via IPOPT solver within the YALMIP toolbox [82] in MATLAB on an AMD Ryzen 7 5800H, 3.2 GHz, 8 core processor, 16GB RAM in about 28 seconds. This approximation method is preferred over the one leading to a MILP formulation because it performs better, as will be explained in a dedicated section 3.2.3.3.

In Table 3.7 the total cost for each user is reported. Figure 3.7 reports the amount of shared energy in each hour. As presented in equation (2.1), this quantity (yellow line the figure) is always equal to the minimum between the overall power absorption (red bars) and the overall power injection (blue bars). Please note that energy and power coincide in this specific case, where the selected Δ is one hour. This figure allows also to appreciate that in the extreme hours of the day, when there is no production from PV (remember that, by law, RES generation is the only one allowed), the shared energy is null as no EPC is selling power to the grid. This means that for the shared energy to be non-zero, there must be simultaneous consumption and production. The total shared energy corresponds to 107.84[kWh], resulting in an overall incentive (for the whole EC) of 11.86€. This incentive could seem not very high but, considering the costs in Table VI, it is possible to see that the overall expenses for the EC members is 97.71€ and thus

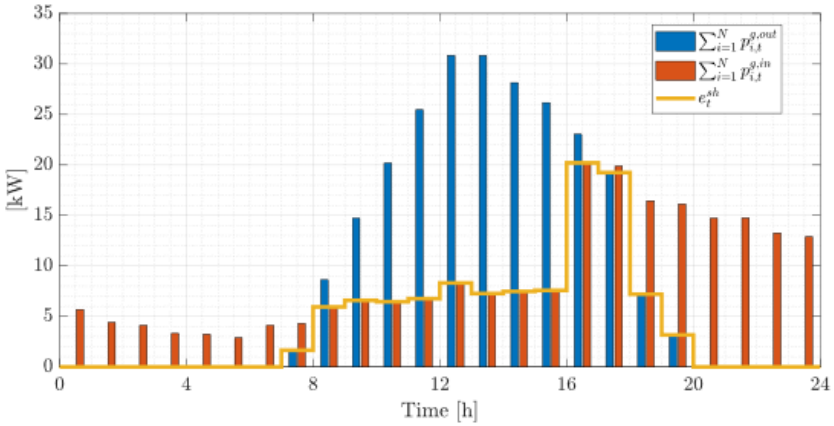

Figure 3.7: Power exchange with the grid and resulting shared energy

the incentive corresponds to a 12.14% reduction in the total electricity bill. Moreover, note that the actual benefit for each ECP depends on the splitting rules of each REC. Figure 3.8 reports the power balance for each ECP. In addition to verifying that the balance is respected at any time step, this figure allows also to verify how the ESS is exploited for those participants who have it: the storage is charged during the central hours of the day (excess of PV production) and discharged to satisfy the load. This is the usual operation of ESS in generic households since this approach can reduce the costs of the owner. This figure also allows to see that the storage is only charged by renewable energy. This behavior complies with the regulation of RECs even if the use of the storage does not provide any contribution to the shared energy since the stored energy is used only to satisfy the load of the same user; indeed, this represents a more convenient solution in terms of operation costs. In Figure 3.9, the EV charging profiles are reported. The figure, allows to verify that constraint (3.13) is respected: the desired state of charge is reached within the predefine time instant T^{EV*}. Of course, the plotted profiles always increase since for EVs vehicle-to-grid mode is discarded to comply with the request for only renewable energy production.

Another interesting analysis is relevant to the impact of the shared energy incentive on the optimal energy management for the users, i.e. how the ECP scheduling changes whether the objective of shared energy maximization is considered or not. In fact, it should be considered that even in the case where the objective function (3.19) is not considered and the only cost to be minimized is that of the members, there is still a certain amount of shared energy provided by the optimal scheduling of ECPs. In particular, when (3.19) is disregarded the shared energy amounts to 96.5[kWh]. As already presented, by introducing the shared energy maximization it is possible to obtain an increase of 10.17[kWh] (+10.53%) without changing the cost for the ECPs.

In order to provide more insights about the behavior of the system, in particular about the impact of the storage system, a comparison between the presented scenario and a situation where the ECPs do not have any storage is presented in Table 3.8. The huge advantage brought from the storage (-11.15% of the total ECPs' costs) is particularly evident within this system configura-

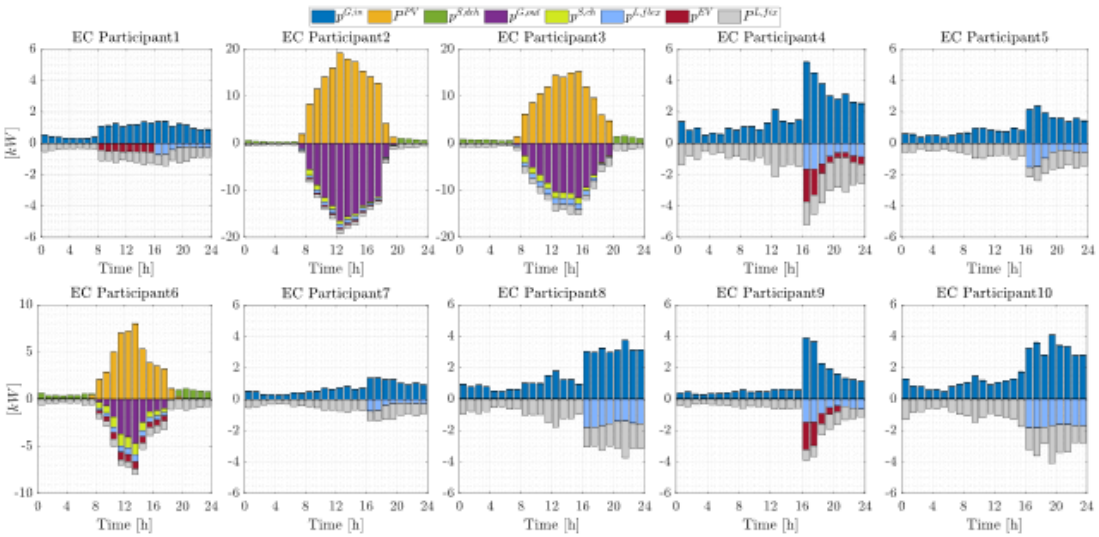

Figure 3.8: Power balance of each ECP

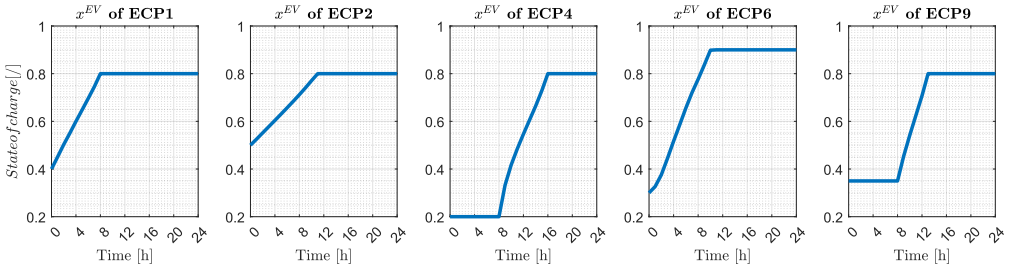

Figure 3.9: EV state of charge for each ECP

tion due to the nature of the considered renewable plants which can benefit from the flexibility induced by the storage. On the shared energy side, it is possible to find that without the ESS the total value increases from 107.84[kWh] to 115.20[kWh], corresponding to an increase of 0.75€ (+6.8%) in the received incentive. This behavior confirms that the savings due to the avoided purchase of energy influence the solution more than the incentives relevant to the shared energy.

Table 3.8: ECP Costs comparison with and without the ESS [€]

	ECP1	ECP2	ECP3	ECP4	ECP5	ECP6	ECP7	ECP8	ECP9	ECP10	$\sum$ ECPs
ESS	11.75	-10.26	-7.18	24.27	13.45	-1.71	9.51	21.94	13.11	22.82	97.71
No ESS	11.75	-7.49	-2.49	24.27	13.45	1.74	9.51	21.94	13.11	22.82	108.61

Table 3.9: Comparison of the two analyzed approximation techniques

	T=24, N=3		T=24, N=6		T=24, N=10		T=24, N=15		T=24, N=20		T=24, N=30		T=24, N=50	
	MILP	NLP	MILP	NLP	MILP	NLP	MILP	NLP	MILP	NLP	MILP	NLP	MILP	NLP
Solver time [s]	21.17	4.58	285.31	12.32	> 1000	27.99	> 1000	79.81	> 1000	79.75	> 1000	175.52	> 1000	699.7
Obj	28.27	28.27	28.64	28.64		28.64	——	31.03	——	31.03	——	59.04	——	89.44
Err %		$-5.69 \cdot 10^{-5}$		$-1.08 \cdot 10^{-4}$										

3.2.3.3 Comparison of approximation techniques and scalability analysis

This section tests the performance of the two proposed approximation techniques. Since they lead to two different classes of problems, two different solvers are used: GUROBI for the approximation leading to a MILP and IPOPT for the one resulting in a NLP.
The two analyzed techniques are compared by running the proposed model considering problems of increasing size. For the case study, a value of $\zeta = 100$ is selected for the second approximation technique using the Gaussian error function because it is sufficient for an acceptable approximation. From the results reported in Table 3.9, it is clear that the second method, using the Gaussian error function, has the best performances: the result for the optimization problem is about the same, but it performs better from a runtime point of view. An interesting result of this comparison is that the proposed model can be solved quickly even for complex systems with many ECPs. Even if the existing ECs are very small nowadays, they are expected to grow in the next years, leading to the development of very large and complex systems with the need of a very fast optimization, able to run online to provide an optimal management of the whole REC. The proposed model can be a valid candidate to play this role.

3.2.3.4 Sensitivity analysis

In this section, a sensitivity analysis on two of the most impacting parameters is conducted. First, the results obtained by different electricity prices are considered. Then, the role of renewable production is investigated.

3.2.3.4.1 Energy buying price As energy buying price is probably the most important parameter, especially from the ECPs viewpoint. To analyze its impact the price already presented in Figure 3.5 is modified such as the lower tier is the one corresponding to the central hours of the day, i.e. those where PV generation is concentrated (Figure 3.10).
Of course, this scenario represents a more favorable situation for EC operations in terms of shared energy, in fact the best hours for purchasing electricity are also those where the higher value for renewable power production is reached. Figure 3.11 presents the resulting power balance. As expected, the power consumption is concentrated in the central hours, as a consequence the values for shared energy are higher with respect to the initial case. The behavior of the ESSs remains more or less the same. In the following, Figure 3.12 illustrates the overall power exchange and

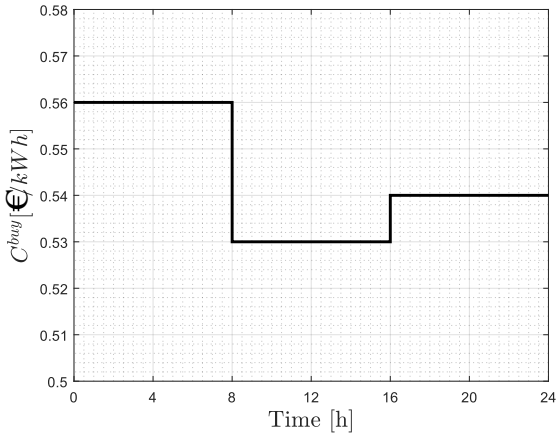

Figure 3.10: Modified energy buying price

the resulting shared energy calculation. In this case, both cost term and shared energy improve. The total costs for the ECPs decrease slight from 97.71€ to 97.28€ (-0.4%), while the total shared energy increase from 107.84[kWh] to 142.22[kWh] (+31.9%). This significant increase corresponds to an increase in the received incentive of 3.5€. This analysis clearly presents how a favorable cost structure can improve the results and then the effectiveness of ECs.

3.2.3.4.2 Renewable power variation Another critical parameter relevant to RECs can be identified as renewable production. Indeed, since shared energy is calculated based solely on renewable power production, the amount of power generated by renewable plants considerably impacts the results. To analyze the consequences of power production the forecasted power production is decreased and increased by different percentages, as illustrated in Figure 3.13. Note that in this analysis the installation costs and the physical limits for the PV plants are not considered since the goal is to analyze the trend in the shared energy and the ECPs costs. On the left side it is possible to see how the progressive reduction of renewable power leads to an increase in the overall costs and to a total absence of shared energy. On the right side, while increasing the power production, the costs decrease while the total shared energy reaches a plateau that is due to the total satisfaction of the load. In that case, even increasing production, the value of the shared energy cannot increase due to the definition given by the law. This trend in shared energy proves that the structure and the design of a REC should not be static but rather dynamic: if production increases, consumption should increase accordingly (and vice versa). This would increase the incentive obtained from energy sharing, thereby reducing the payback period of the investment, and would increase local consumption, thereby reducing the stress on the grid.

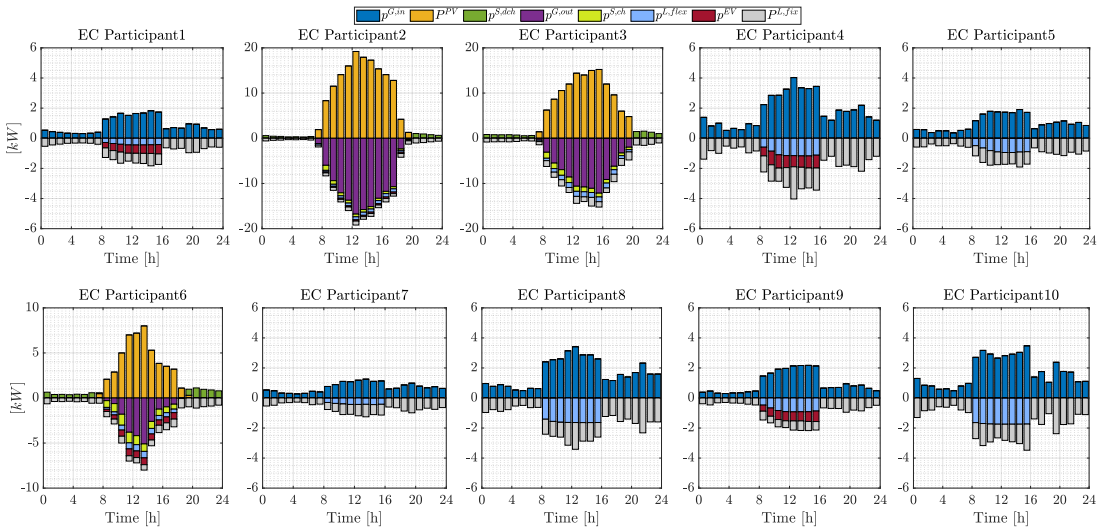

Figure 3.11: Power balance of each ECP (Modified-energy-pricing framework)

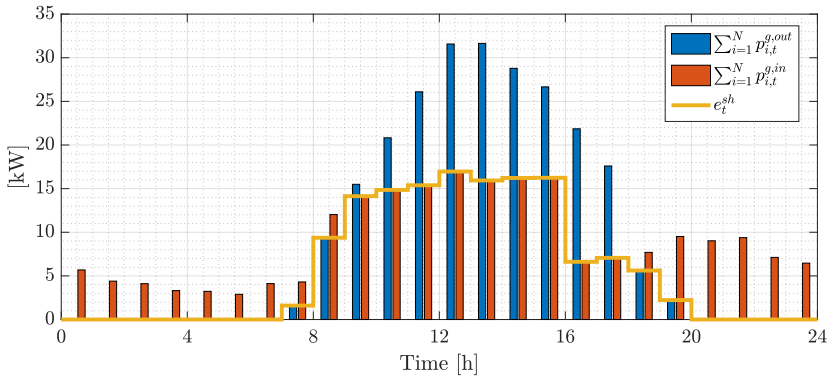

Figure 3.12: Power exchange with the grid and resulting shared energy (Modified-energy-pricing framework)

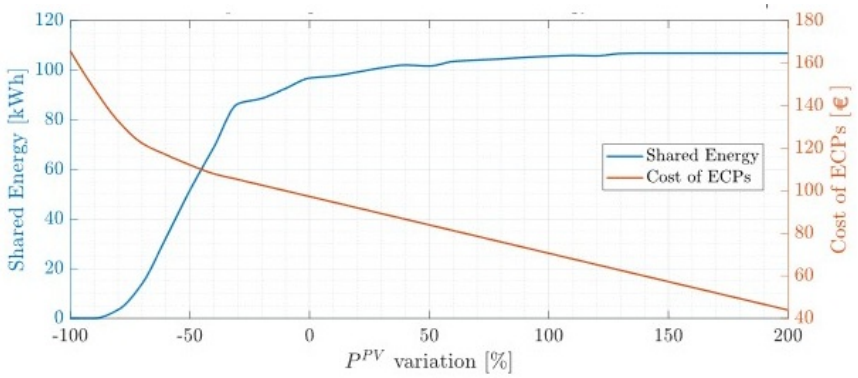

Figure 3.13: Effect of renewable power variation on shared energy and ECPs' cost

3.3 Decentralized optimal management for DR provision

In this section, the second approach used to address the optimal management problem of a REC internal operations is investigated. Unlike the approach described in the previous section, here the problem is formalized in a unique level, which considers both ECM and ECP goals in the same objective function. This approach adopts a suited decentralized optimization algorithm that exploits second-order information [83] to achieve fast convergence by keeping privacy among ECPs. In addition to shared energy maximization, the participation to DR service is also considered because demand side management (DSM) strategies can help improve the economic benefit for the REC, which currently only relies only on the incentive for shared energy. To compensate it, a REC may also provide ancillary services, such as demand response (DR), for a greater collective benefit. The participation in DR programs is implemented as an equality coupling constraint: all ECPs are involved and have to comply with the DR provision with their power exchange with the main grid.
Most of the papers cited in the literature review at the beginning of this chapter consider only the operational management of RECs, without addressing the possibility of providing flexibility services to the system operator. Few papers investigate DR strategies in the context of energy community optimal management, but they do not focus on the regulation framework that defines renewable energy communities [80]. [84] assesses the role of DSM on an energy community, showing that the lower the heterogeneity of the composition, the higher the impact of the demand side management. Moreover, DSM allows to increase savings and to decrease investment costs. The EMS proposed in [85] integrates the possibility of participating to the aFRR-market for a community-clustered solar plus battery prosumers. Authors in [86] integrate curtailable and shiftable loads as DSM strategies in the day-ahead scheduling problem of a smart microgrid with wind energy. According to the results, implementing DSM strategies decreases the total operation cost and the emission pollution and increases the customer's satisfaction and wind penetration indices. From a modeling perspective, the novelty lies in integrating the provision of flexibility services into regulation-aware EMSs for renewable energy communities. Another novelty lies in the development of a new decentralized algorithm, based on second-order update, which is able to keep privacy between the ECPs while achieving fast convergence. Several studies have explored second-order methods for decentralized optimization. In [87], a decentralized Newton method is proposed for global consensus optimization problems and compared with state-of-the-art algorithms such as ADMM. Similarly, [88] introduces a decentralized reinforced Newton method for unconstrained consensus problems. While second-order information, such as the Hessian, can enhance optimization, its computation can be prohibitively expensive for certain cost functions, especially in machine learning contexts. Some works address this challenge. For instance, [89] presents a decentralized second-order algorithm utilizing an approximate Newton step, whereas [90] develops a parameterized approximate inverse Hessian based on matrix splitting techniques and a truncated Neumann series. Notably, these methods primarily focus on accelerating primal convergence and are centralized in nature. In the realm of distributed applica-

Table 3.10: Comparison with state of the art works and their features

	REC regulatory focus	DSM/DR	Decentralized/Distributed	Problem class/Solution method	II-order information
[76]	✓	-	-	MILP	-
[74]	✓	-	-	MIQCP	-
[60]	✓	-	-	MILP	-
[72]	✓	-	-	LP	-
[73]	✓	-	-	MILP	-
[86]	-	✓	-	MINLP	-
[94]	-	✓	-	MILP	-
[88]	-	-	✓	Newton-based	✓
[87]	-	-	✓	Newton-based	✓
[89]	-	-	✓	Newton-based	✓
[90]	-	-	✓	Dual-Descent	✓
This work	✓	✓	✓	II-order dual update	✓

tions, [91] applies second-order distributed MPC to optimize the control of autonomous vehicles at intersections, with a particular focus on energy consumption. [92] proposes an enhanced dual decomposition method for quadratic programming, solving subproblems locally and ensuring coupling constraints through a distributed non-smooth Newton iteration on dual variables. Additionally, [93] introduces a parallelizable algorithm for implementing a primal-dual interior point method in MPC problems by leveraging the problem's specific structure. Table 3.10 summarizes the literature review conducted above and highlights the features offered by the proposed study.
Summarizing, the main contributions of this chapter are:

- A novel architecture for the participation of RECs to DR programs.
- A new decentralized algorithm that exploits second order information to achieve fast convergence by keeping privacy among ECPs.
- The case study represents realistic configuration for a REC within a residential area.

3.3.1 Decision problem definition

This section describes the overall optimization problem for a REC optimal management considering the participation in DR programs (Figure 3.14). Unlike the approach presented in the previous section, here the problem is structured in a unique level. Therefore, the objective function considers both ECM and ECP goals: the ECM pursues shared energy maximization, while ECPs aim to minimize their own costs. In addition to the ECP operational constraints (Section 3.1.1), a constraint is implemented to meet the DSO request.

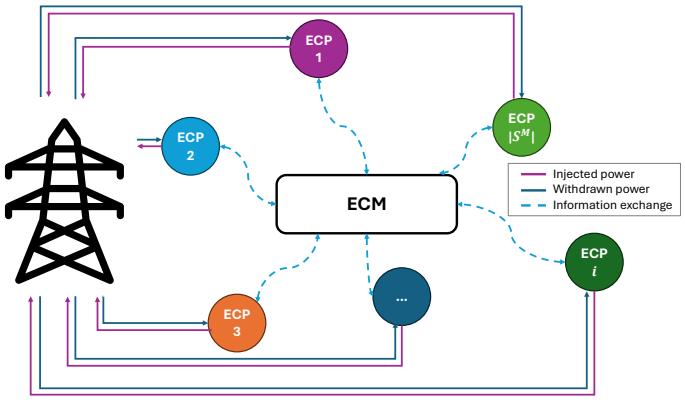

Figure 3.14: A representation of a REC with ECM and ECPs

3.3.1.1 Objective function

Since the overall problem is structured in a unique level, the objective function considers both ECM and ECP goals.
As concerns the ECM objective, its goal is again related to the maximization of shared energy, defined in equation (2.1). Since this function is not globally differentiable, we propose a differentiable reformulation of the shared energy objective that is more manageable from an algorithmic point of view

$$J^{ECM} = \sum_{t \in S^T} \left[\alpha_1 \left(\sum_{i \in S^N} \frac{p_{i,t}^{G,\text{in}} - p_{i,t}^{G,\text{out}}}{\overline{P}_i^G} \right)^2 - \alpha_2 \sum_{i \in S^N} \left(\frac{p_{i,t}^{G,\text{out}}}{\overline{P}_i^G} \right) \right] \tag{3.49}$$

where $\overline{P}_i^G$[kW] is the maximum power that participant i can exchange with the grid. The key idea behind this alternative formulation is that, to achieve shared energy maximization, the overall production and consumption (considering all the ECPs) must be the highest possible and simultaneously. Thus, we want to minimize the overall exchange with the grid, while maximizing each ECP absorption/injection in each time interval.
Regarding the ECPs, their goal is to minimize their own costs, due to power withdrawal from the grid:

$$J^{ECP} = \sum_{t \in S^T} \left[\alpha_3 \sum_{i \in S^N} \left(C_{i,t}^{\text{buy}} p_{i,t}^{G,\text{in}} - C_{i,t}^{\text{sell}} p_{i,t}^{G,\text{out}} \right) \Delta \right] \tag{3.50}$$

Since the overall objective function of the problem considers both ECM and ECP objectives, we finally obtain

$$\min J = J^{ECM} + J^{ECP} \tag{3.51}$$

where α_* are weights for the three terms of the objective function.

3.3.1.2 Constraints

Constraints are related to the equations modeling the physical and technical operations of the technologies considered for each ECP. The general mix of technologies presented at the beginning of this chapter is still considered; most constraints are therefore given by the ECPs' operational constraints in equations (3.1)-(3.13).
In addition to these constraints, the coupling constraint for the DR service provision must be implemented. In particular, the REC must follow a particular time-varying power profile P_t^{DR} for a certain period $S^{\mathrm{DR}} \subseteq S^T$. All ECPs have to actively participate to guarantee that the DR service is correctly provided: the required value for the power exchange with the grid must be satisfied by the overall power flows from/to the ECPs.

$$\sum_{i \in S^N} \left(p_{i,t}^{G,\mathrm{in}} - p_{i,t}^{G,\mathrm{out}} \right) = P_t^{\mathrm{DR}} \qquad t \in S^{\mathrm{DR}} \subseteq S^T \tag{3.52}$$

Therefore, the overall optimization problem is given by (3.49)-(3.51) subject to (3.1)-(3.13), (3.52).

3.3.2 Optimization Algorithm

This section presents the proposed decentralized optimization algorithm, which is a dual ascent algorithm that employs a second-order dual update. First, the problem formulation in its canonical form is derived, then the proposed algorithm is presented.
The overall problem is implemented under a receding horizon approach using a one hour window to cope with uncertainties related to renewable generation forecasts and load; moreover, the optimization is carried out over the entire day, with rescheduling over each step.

3.3.2.1 Problem reformulation

To apply the designed decentralized algorithm, the problem formulated in the previous sections must be rewritten in canonical form. First of all, we define the decision variables vector as

$$\mathbf{u}_i = \begin{bmatrix} p^{G,\mathrm{out}} & p^{S,\mathrm{ch}} & p^{S,\mathrm{dch}} & p^{L,\mathrm{flex}} & p^{\mathrm{EV}} \end{bmatrix}_i \tag{3.53}$$

Thanks to some algebraic manipulations, the overall problem can be rewritten as

$$\begin{aligned} \min_{\mathbf{u}} \quad & f(\mathbf{u}) \\ s.t. \quad & \mathbf{A}\mathbf{u} = \mathbf{b} \\ & \mathbf{C}\mathbf{u} \leq \mathbf{d} \end{aligned} \tag{3.54}$$

where $\mathbf{A} \in \mathbb{R}^{P\times N}$, $\mathbf{b} \in \mathbb{R}^{P}$, $\mathbf{C} \in \mathbb{R}^{Z\times N}$, $\mathbf{d} \in \mathbb{R}^{Z}$ are suitable matrices and vectors with P and Z being the number of equalities and inequalities, respectively. $f(\mathbf{u}) : \mathbb{R}^N \rightarrow \mathbb{R}$ is a convex objective function given by

$$f(\mathbf{u}) = \frac{1}{2}\mathbf{u}^T\mathbf{Q}\mathbf{u} + \mathbf{q}^T\mathbf{u} \tag{3.55}$$

with

$$\mathbf{Q} = \mathrm{diag}(\mathbf{Q}_i) \qquad \mathbf{Q}_i = \frac{2}{\left(\overline{P}_i^G\right)^2}\begin{bmatrix} 0 & 0 & 0 & 0 & 0 \\ 0 & \mathbf{I} & -\mathbf{I} & \mathbf{I} & \mathbf{I} \\ 0 & -\mathbf{I} & \mathbf{I} & -\mathbf{I} & -\mathbf{I} \\ 0 & \mathbf{I} & -\mathbf{I} & \mathbf{I} & \mathbf{I} \\ 0 & \mathbf{I} & -\mathbf{I} & \mathbf{I} & \mathbf{I} \end{bmatrix} \tag{3.56}$$

$$\mathbf{q}^T = \mathrm{row}(\mathbf{q}_i)$$

$$\mathbf{q}_i^T = \tfrac{1}{\overline{P}_i^G}\left(\mathbf{P}^{L,fix} - \mathbf{P}^{PV}\right)^T \begin{bmatrix} 0 & \mathbf{I} & -\mathbf{I} & \mathbf{I} & \mathbf{I} \end{bmatrix} - \begin{bmatrix} \frac{1}{\overline{P}_i^G} & 0 & 0 & 0 & 0 \end{bmatrix} + \begin{bmatrix} (C_i^{\mathrm{buy}} - C_i^{\mathrm{sell}}) & C_i^{\mathrm{buy}} & -C_i^{\mathrm{buy}} & C_i^{\mathrm{buy}} & C_i^{\mathrm{buy}} \end{bmatrix} \tag{3.57}$$

3.3.2.2 Decentralized Optimization Algorithm

Here, a decentralized approach based on second order dual update is proposed to solve the problem in (3.54). The Lagrange function of this problem defined as

$$L(\mathbf{u}, \boldsymbol{\nu}, \boldsymbol{\mu}) = f(\mathbf{u}) + \boldsymbol{\nu}^T(\mathbf{A}\mathbf{u} - \mathbf{b}) + \boldsymbol{\mu}^T(\mathbf{C}\mathbf{u} - \mathbf{d}) \tag{3.58}$$

in which $\boldsymbol{\nu}$ is the multiplier for the equality coupling constraints and $\boldsymbol{\mu} \geq 0$ is the multiplier for the inequality local constraints. Inspired by the works in [95]- [96], we propose an alternative way to augment the Lagrange function without increasing the overall computational complexity. To increase the speed of convergence, we augment the Lagrange function through a diagonal switching matrix $\mathbf{I}^\rho$ whose elements are defined as

$$\mathbf{I}^\rho_{i,i} = \rho > 0 \quad \text{if} \quad \mu_i > 0 \qquad i \in R(\mathbf{C}) \tag{3.59}$$

where $R(\mathbf{C})$ is the set of rows of the inequality constraint matrix $\mathbf{C}$. The diagonal elements of $\mathbf{I}^\rho$ are equal to ρ iff their corresponding constraints are active, i.e. they are satisfied as equality, otherwise are zero. Furthermore, the objective function $f(\mathbf{u})$ is a convex function, but may not be strongly convex. To ensure strong convexity, we use a proximal augmentation term, where $\mathbf{u}_\tau$ denotes the primal variable at the previous iteration. According to these considerations, the augmented Lagrangian becomes

$$\mathcal{L}(\mathbf{u}, \boldsymbol{\nu}, \boldsymbol{\mu}) = L(\mathbf{u}, \boldsymbol{\nu}, \boldsymbol{\mu}) + \frac{1}{2}(\mathbf{u}^T\mathbf{C}^T - \mathbf{d}^T)\mathbf{I}^\rho(\mathbf{C}\mathbf{u} - \mathbf{d}) + \frac{1}{2}\mathbf{d}^T\mathbf{I}^\rho\mathbf{d} + \frac{1}{2\rho}\left\|\mathbf{u} - \mathbf{u}_\tau\right\|_2^2 \tag{3.60}$$

First of all, we analyze the properties of the first order conditions of (3.60)

$$\nabla_u \mathcal{L}\left(\mathbf{u}, \boldsymbol{\nu}, \boldsymbol{\mu}\right) = \nabla_u f\left(\mathbf{u}\right) + \mathbf{A}^T\boldsymbol{\nu} + \mathbf{C}^T\boldsymbol{\mu} + \mathbf{C}^T\mathbf{I}^\rho\mathbf{C}\mathbf{u} - \mathbf{C}^T\mathbf{I}^\rho\mathbf{d} + \frac{1}{\rho}\left(\mathbf{u} - \mathbf{u}_\tau\right) = 0 \quad (3.61)$$

In view of the implicit function theorem, the solution of the first order conditions system (3.61) -$\mathbf{u}\left(\boldsymbol{\nu}, \boldsymbol{\mu}\right)$- is a continuous and differentiable function of the parameters $\boldsymbol{\mu}$ and $\boldsymbol{\nu}$ if the Jacobian of (3.61), i.e. the Hessian matrix of (3.60) with respect to $\mathbf{u}$, is invertible in a neighbourhood of the optimal value $\mathbf{u}^*$. Such Jacobian is given by

$$\nabla_{uu} \mathcal{L}\left(\mathbf{u}, \boldsymbol{\nu}, \boldsymbol{\mu}\right) = \nabla_{uu} f\left(\mathbf{u}\right) + \mathbf{C}^T\mathbf{I}^\rho\mathbf{C} + \frac{1}{\rho}\mathbf{I} \quad (3.62)$$

that is positive definite since $\nabla_{uu} f\left(\mathbf{u}\right) \geq 0$, $\mathbf{C}^T\mathbf{I}^\rho\mathbf{C} \geq 0$ from the convexity of objective function and inequality constraints, and $\rho > 0$ by assumption.
We next derive the second order dual update step. First, we formulate the dual function while holding $\boldsymbol{\mu}_\tau$ constant:

$$\mathcal{D}(\boldsymbol{\nu}, \boldsymbol{\mu}_\tau) = \mathcal{L}\left(\mathbf{u}\left(\boldsymbol{\nu}, \boldsymbol{\mu}_\tau\right), \boldsymbol{\nu}, \boldsymbol{\mu}_\tau\right) \quad (3.63)$$

The gradient of the dual function $\mathcal{D}(\boldsymbol{\nu}, \boldsymbol{\mu}_\tau)$ can be obtained as

$$\nabla_\nu \mathcal{D}(\boldsymbol{\nu}, \boldsymbol{\mu}_\tau) = \frac{\partial}{\partial \nu}\mathbf{u}(\boldsymbol{\nu}, \boldsymbol{\mu}_\tau)\nabla_u \mathcal{L}\left(\mathbf{u}\left(\boldsymbol{\nu}, \boldsymbol{\mu}_\tau\right), \boldsymbol{\nu}, \boldsymbol{\mu}_\tau\right) + \mathbf{A}\mathbf{u}(\boldsymbol{\nu}, \boldsymbol{\mu}_\tau) - \mathbf{b} = \mathbf{A}\mathbf{u}(\boldsymbol{\nu}, \boldsymbol{\mu}_\tau) - \mathbf{b} \quad (3.64)$$

where we used (3.61). From this we can compute the Hessian of the dual function

$$\nabla^2_{\nu\nu} \mathcal{D}(\boldsymbol{\nu}, \boldsymbol{\mu}_\tau) = \mathbf{A}^T \frac{\partial}{\partial \nu}\mathbf{u}(\boldsymbol{\nu}, \boldsymbol{\mu}_\tau) \quad (3.65)$$

where $\frac{\partial}{\partial \nu}$ is the Jacobian with respect to variable $\boldsymbol{\nu}$. To obtain $\frac{\partial}{\partial \nu}\mathbf{u}(\boldsymbol{\nu}, \boldsymbol{\mu}_\tau)$ we start by differentiating (3.61) with respect to $\boldsymbol{\nu}$

$$\nabla_\nu \left[\nabla_u f\left(\mathbf{u}(\boldsymbol{\nu}, \boldsymbol{\mu}_\tau)\right) + \mathbf{A}^T\boldsymbol{\nu} + \mathbf{C}^T\boldsymbol{\mu} + \mathbf{C}^T\mathbf{I}^\rho\mathbf{C}\mathbf{u}(\boldsymbol{\nu}, \boldsymbol{\mu}_\tau) - \mathbf{C}^T\mathbf{I}^\rho\mathbf{d} + \frac{1}{\rho}\left(\mathbf{u}(\boldsymbol{\nu}, \boldsymbol{\mu}_\tau) - \mathbf{u}_\tau\right)\right] =$$
$$\mathbf{A} + \left(\nabla_{uu} f\left(\mathbf{u}(\boldsymbol{\nu}, \boldsymbol{\mu}_\tau)\right) + \frac{\mathbf{I}}{\rho} + \mathbf{C}^T\mathbf{I}^\rho\mathbf{C}\right)\frac{\partial}{\partial \nu}\mathbf{u}(\boldsymbol{\nu}, \boldsymbol{\mu}_\tau) = 0 \quad (3.66)$$

Thanks to the previous equation it is possible to obtain the Hessian of the dual function as

$$\nabla^2_{\nu\nu} \mathcal{D}(\boldsymbol{\nu}\boldsymbol{\mu}_\tau) = -\mathbf{A}^T(\nabla_{uu} \mathcal{L}\left(\mathbf{u}(\boldsymbol{\nu}, \boldsymbol{\mu}_\tau), \boldsymbol{\nu}, \boldsymbol{\mu}_\tau\right))^{-1}\mathbf{A} \quad (3.67)$$

Finally, the proposed algorithm can be stated as

$$\mathbf{u}_{\tau+1} = \underset{\mathbf{u}}{\operatorname{argmin}}\ \left\{\mathcal{L}\left(\mathbf{u}, \boldsymbol{\nu}_\tau, \boldsymbol{\mu}_\tau\right)\right\} \quad (3.68)$$

$$\boldsymbol{\mu}_{\tau+1} = \max\left\{0, \boldsymbol{\mu}_\tau + \rho\left(\mathbf{C}\mathbf{u}_{\tau+1} - \mathbf{d}\right)\right\} \quad (3.69)$$

$$\boldsymbol{\nu}_{\tau+1} = \boldsymbol{\nu}_\tau + \left[\mathbf{A}^T(\nabla_{uu} \mathcal{L}\left(\mathbf{u}_{\tau+1}, \boldsymbol{\nu}_\tau, \boldsymbol{\mu}_\tau\right))^{-1}\mathbf{A}\right]^{-1}\left(\mathbf{A}\mathbf{u}_{\tau+1} - \mathbf{b}\right) \quad (3.70)$$

The dual update in (3.70) uses second-order information from the Hessian performing a Newton-like iteration rather than the classical gradient iteration of the dual function.

At this point, analyzing the overall optimization problem is important to understand a possible decomposition. The objective function is separable among each ECP subject to individual inequality constraints and a unique coupling equality constraint, that is the DR one represented by the ECM. Therefore, it is possible to split the updates (3.68) and (3.69) into $\left|S^M\right|$ parallel updates corresponding to each ECP, and then perform a unique dual update through the ECM. The concept is described as follows

$$\mathbf{u}_{i,\tau+1} = -\left(\mathbf{Q}_i + \frac{\mathbf{I}}{\rho} + \mathbf{C}_i^T \mathbf{I}^\rho \mathbf{C}_i\right)^{-1} \left(\mathbf{q}_i + \left[\mathbf{A}^T \boldsymbol{\nu}_\tau\right]_i + \mathbf{C}_i^T \boldsymbol{\mu}_{i,\tau} - \frac{\mathbf{u}_{i,\tau}}{\rho} - \mathbf{C}_i^T \mathbf{I}^\rho \mathbf{d}_i\right), \tag{3.71}$$

$$\boldsymbol{\mu}_{i,\tau+1} = \max\left\{0, \boldsymbol{\mu}_{i,\tau} + \rho\left(\mathbf{C}_i \mathbf{u}_{i,\tau+1} - \mathbf{d}_i\right)\right\}, \tag{3.72}$$

$$\text{Communicate} \quad \mathbf{u}_{i,\tau+1} \quad \text{to the ECM}, \tag{3.73}$$

$$\boldsymbol{\nu}_{\tau+1} = \boldsymbol{\nu}_\tau + \left[\mathbf{A}(\nabla_{uu}\mathcal{L}\left(\mathbf{u}_{\tau+1}, \boldsymbol{\nu}_\tau, \boldsymbol{\mu}_\tau\right))^{-1}\mathbf{A}^T\right]^{-1}\left(\mathbf{A}\mathbf{u}_{\tau+1} - \mathbf{b}\right), \tag{3.74}$$

$$\text{Communicate} \quad \boldsymbol{\nu}_{\tau+1} \quad \text{to the ECPs}. \tag{3.75}$$

Using of a decentralized solution becomes useful from a resilience and privacy point of view: since the main computation is shared among each ECP, there is no variable sharing among them and a possible failure can be addressed without replacing the central computational unit.

3.3.3 Application to a Case Study

This section presents the case study and discusses the main results. First, to evaluate the correctness of the alternative differentiable formulation for shared energy maximization, an analysis of the objective function in (3.49) is performed with respect to the state-of-the-art formulation in equation (2.1). Then, the results for the actual case study are presented and discussed. A scalability analysis is also performed to validate the proposed approach for larger instances. Finally, the effect of parallelizing the update is investigated in the last part of this section.
All the results presented in this section have been retrieved by using MATLAB on an AMD Ryzen 7 5800H, 3.2 GHz, 8 core processor, 16GB RAM.

3.3.3.1 Problem Data

Here, the considered data are presented. The actual case study is relevant to a REC with 10 ECPs optimized over a 24-hour horizon. Table 3.11 reports the data relevant to each ECP, while Figure 3.15 reports the power production and demand profiles. Please note that both profiles have been obtained by scaling the renewable production in [97] and the average domestic user profiles present in [98]. By analyzing data in Table 3.11 and Figure 3.15, it is possible to notice

Table 3.11: ECP data

	CAP^S [kWh]	X_0^S[/]	$\overline{P}^S$[kW]	$E^{L,flex}$[kWh]	CAP^{EV}[kW]	T^{EV*}[h]
ECP1	/	/	/	3.21	10	8
ECP2	30	0.2	10	7.01	10	11
ECP3	20	0.2	10	11.31	/	/
ECP4	/	/	/	8.31	10	16
ECP5	/	/	/	6.56	/	/
ECP6	15	0.2	10	5.14	10	21
ECP7	/	/	/	3.20	/	/
ECP8	/	/	/	12.76	/	/
ECP9	/	/	/	6.50	10	13
ECP10	/	/	/	13.78	/	/

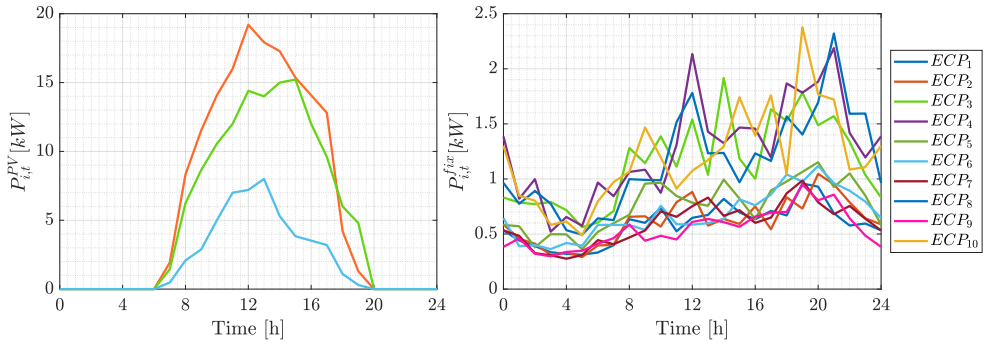

Figure 3.15: Renewables and Load input data for the 10 ECP case

how the different ECPs are characterized. In fact, only five ECPs (1-2-4-6-9) own EVs and therefore need to charge them; for EVs, $X_0^{EV} = \underline{X}^{EV}$ and $X^{EV*} = \overline{X}^{EV}$. On the other hand, only three ECPs (2-3-6) have a PV plant and an associated storage system, so they are the only that could potentially feed some electricity into the grid. A multi-rate pricing tariff is considered with a minimum of 0.53[€/kWh] from 9:00 to 18:00. The incentive relevant to shared energy is 0.108[€/kWh] as defined by the national regulation (preliminary phase). Moreover, DR is considered and the power level is imposed to 10[kW] (sold to the grid) from 11:00 to 13:00.

3.3.3.2 Objective function alternative formulation validation

To test if the proposed approach correctly maximizes shared energy, the objective function in (3.49) has been substituted in the high-level problem of [99] and then compared to the results obtained with the original formulation. Table 3.12 shows the results of this comparison and allows to appreciate that the difference between the optimal solutions is negligible.

Table 3.12: Comparison of the two objective functions

T	N	Obj in [99] with (2.1)	Obj in [99] with (3.49)	% Err
1	3	1.63	1.63	0.00
5	5	36.03	36.03	1.08E-05
10	8	85.19	85.19	1.96E-05
24	10	114.85	114.85	3.12E-05

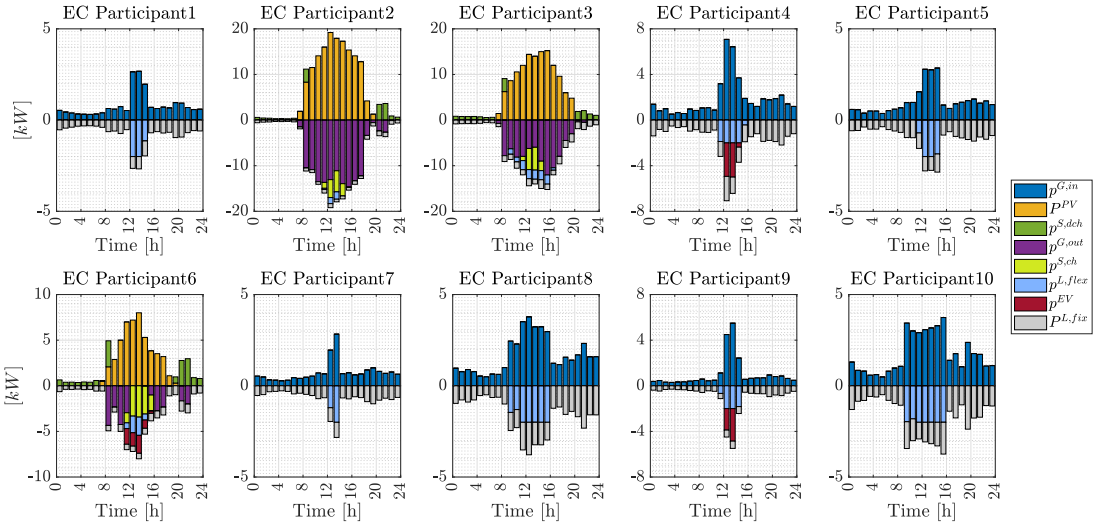

Figure 3.16: Optimal results for the case with 10 ECP

3.3.3.3 Optimization results

This section tests the proposed methodology on the instance just described and provides a detailed description of the main results. Figure 3.16 shows the power balance for each ECP. It is possible to see how the power consumption is concentrated in the central hours of the day to take advantage of the renewable production, both in terms of self-consumption and shared energy. In fact, the ECPs who own a PV plant charge the storage systems in these time intervals and all the flexible consumptions ($p^{L,\text{flex}}$ and p^{EV}) are grouped when there is a surplus sold to the grid. Of course, this behavior is also favoured by the energy price which is minimum in the central hours of the day.

The total amount of shared energy in each hour is reported in Figure 3.17. As presented in equation (2.1), this quantity (yellow line the figure) is always equal to the minimum between the overall power absorption (red bars) and the overall power injection (blue bars). Please note that energy and power numerically coincide in this specific case, where the selected Δ is one hour to be coherent with the legislation, according to which shared energy is calculated ex-post on an hourly basis. This figure also allows to see that in the extreme hours of the day, when there is no PV production (remember that by law only RES production is allowed), the shared energy

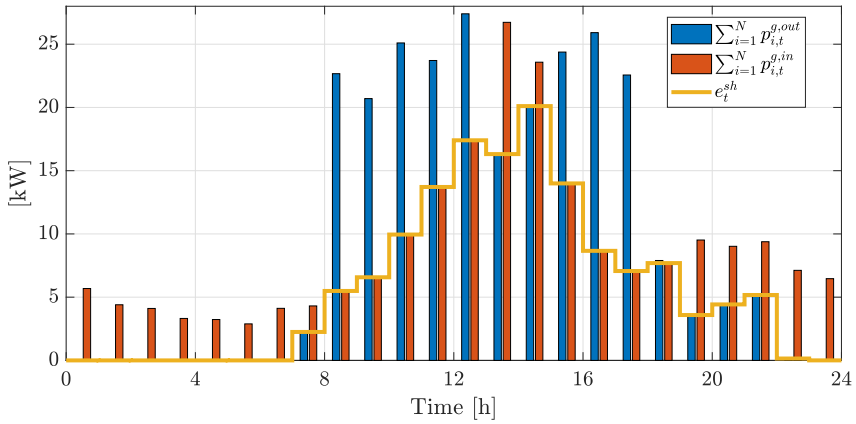

Figure 3.17: Shared energy for the 10 ECP case

is zero because no ECP is selling electricity to the grid. This means that for the shared energy to be non-zero, there must be simultaneous consumption and production. A last detail that can be observed in the figure is that the overall exchange with the grid (difference between blue and red bars) follows the DR request. The total shared energy corresponds to 140.41[kWh], resulting in an overall incentive of 15.44€. As the cost for purchasing energy (for the whole REC) is 96.53€, the incentive provide a reduction of 15.99% in the total electricity bill. Of course, it is noteworthy that the actual benefit for each ECP depends on the splitting rules determined in each REC statute.

3.3.3.4 Scalability analysis

To assess the scalability of the proposed approach, two new scenarios with 20 and 50 ECPs are devised, with data compliant with the ones used for the 10 ECPs case. The convergence and runtime plot are given in Figure 3.18. It is important to note that the convergence of each algorithm is plotted in terms of the optimality gap $[\%]$, that is the percentage distance between the algorithm solution and the optimal solution obtained by the Quadprog solver using the YALMIP interface [82]. All the converge plots show that the algorithm scales reasonably with the number of ECPs and, as a matter of fact, in the largest case, the algorithm takes less than 500 seconds to reach a reasonable gap (around $10^{-6}\%$). Notably, this runtime is compatible with the one-hour discretization step typical of REC applications.

3.3.3.5 Comparison with other algorithms

In order to show the effectiveness of the proposed second-order algorithm, it has been compared with two other different scenarios:

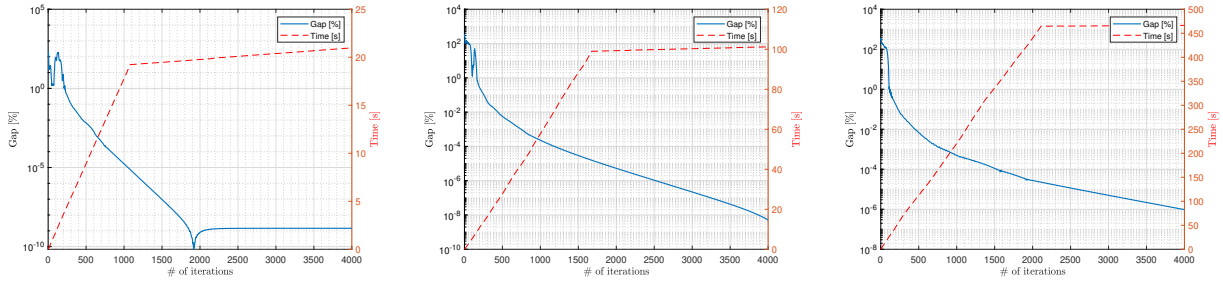

(a) 10 ECPs (b) 20 ECPs (c) 50 ECPs

Figure 3.18: Convergence and runtime

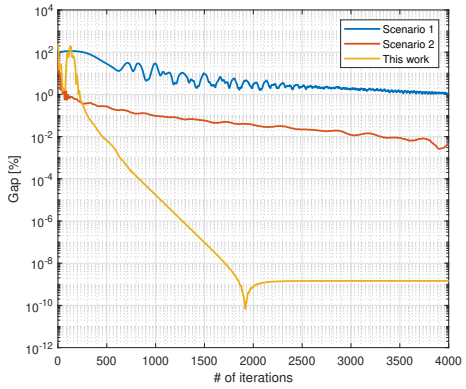

Figure 3.19: Comparison between different algorithms

- Scenario 1: the Lagrangian is not augmented, and a gradient-based dual update is employed;
- Scenario 2: as Scenario 1 but considering the Lagrangian augmented as in (3.60).

It is important to note that a comparison with the popular ADMM algorithm [100] would not be entirely correct, so it has not been reported. Indeed, the ADMM algorithm would use the consensus mechanism by broadcasting all primal variables among all agents [100]. On the contrary, our algorithm exchanges only dual variables with all ECPs while maintaining the privacy of the primary variables. Given the different communication structures, the comparison would not be fair between the algorithms.

All algorithms have been implemented using the decentralized architecture, and the optimality gap trajectory is presented in Figure 3.19 on the 10 ECP problem for 4000 iterations. The plot shows that the proposed algorithm achieves greater precision than the other scenarios ($10^0\%$ and $10^{-2}\%$ respectively), outperforming current state-of-the-art approaches.

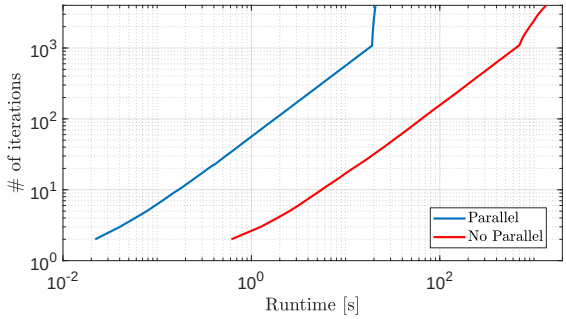

Figure 3.20: Logplot of the runtime with and without parallelisation

3.3.3.6 The effect of parallel computing

Finally, the last analysis is devoted to assessing the performances of the proposed algorithm according to the parallelization of the updates (3.71)-(3.72) instead of (3.68)-(3.69). This analysis is reported in Figure 3.20 for the 10 ECP case. This plot clearly shows that, to reach the same iterations and precision, the non-parallel implementation takes two orders of magnitude more runtime than the parallel one.

Chapter 4

Optimal management of multiple renewable energy communities: external operations

This chapter is dedicated to the operational management of a REC external operations. Considering the number of REC implementations, and the subsequent high penetration of non-programmable RES, new paradigms are needed for a safe and efficient management of electricity grids [101]. In fact, it is not certain that promoting RECs will lead to a positive outcome for the grid perspective because Italy already has an abundance of distributed generation and REC adoption with a high amount of local production could lead to worsening operating conditions [102], [103]. As an example, the simulations conducted in [104] demonstrate that RECs have a significant impact on LV networks: on one side distributed PV production locally consumed has a positive impact on the grid, one the other side the high participation levels of REC-involved elements may also create new and unforeseen contingencies, negatively affecting network operations. Nevertheless, the heterogeneous composition of RECs provides them with a flexibility that can be exploited to provide ancillary services to distribution grids. From an operational point of view, having several connection points would complicate the provision of these services; from a results point of view, the benefit to the grid would be considerable at the primary substation level. For these reasons, the provision of ancillary services and DSM strategies by RECs is not active yet, but it would be an excellent opportunity to exploit the intrinsic flexibility of these infrastructures. The use of flexibility to improve system stability is recognized as a key enabler for meeting Europe's long-term decarbonization goals [105] since long ago, but the recent advancements in ICT and the increased connection of distributed generation have prompted regulators and DSOs to explore flexibility services from small consumers and producers connected to LV networks as effective tools to support energy transition objectives. Indeed, LV systems can serve as valuable sources of flexibility for the operation of upstream systems (MV distribution network) by pooling small-scale resources scattered across that voltage level [106], [107].

Research in this field focuses on the possibility for RECs to provide flexibility services to the grid by participating in balancing markets like Demand Response (DR) programs, manual Frequency Restoration Reserve (mFRR), local flexibility markets. In this context, RECs play a crucial role within electricity markets since, if properly controlled, they are capable of efficiently managing distributed energy resources and technologies to provide useful services to the electricity grid, while supporting social, economic and environmental benefits for its members. As seen in the previous chapter, the optimal management of RECs is typically focused on the cost-based maximization of individual and collective self-consumption. This is achieved by acting on power profiles of each EPC thanks to energy scheduling tools that exploit users' flexibility: distributed energy resources, ESSs, deferrable loads and EV charging plans. Few papers in the literature treat RECs as entities able to provide ancillary services to the grid and use this flexibility for demand-side management strategies. Nevertheless, it is crucial to address this topic so that RECs can be properly integrated into the grid, especially considering that their integration at MV/LV nodes may alter the flexibility that these nodes can offer to the DSO, since demand shifting reduces the flexibility available to the upstream network by preemptively adjusting the demand profile [104]. For these reasons, developing optimization models for managing the external operations of RECs in the flexibility market is crucial to achieve a proper service provision, avoid

increasing the stress on the grid and, at the same time, meet the objectives of the community and its participants. Authors in [94] provided a two-stage EC management scheduling, considering balancing market (mFRR) participation and exploiting ESS and EV as flexibility sources. The study demonstrates that providing ancillary services offers benefits to the grid and increases community profits. Authors in [84] analyze the role of demand-side management in community operation, demonstrating that lower heterogeneity among members enhances the overall effectiveness of DSM, leading to greater savings and reduced investment costs. The energy management system proposed in [85] is capable of integrating the participation in the aFRR market, coordinating clustered solar + battery prosumers to jointly provide flexibility services. Similarly, [86] integrates curtailable and shiftable loads as DSM strategies in the day-ahead scheduling of a smart microgrid with high wind penetration. Their results confirm that implementing DSM reduces total operational costs and emissions while enhancing customer satisfaction and renewable energy utilization. The literature on EMSs for the optimal management of a REC that integrate the provision of flexibility services has already been reviewed in the previous chapter; therefore, please refer to Section 3.3, and specifically to Table 3.10. In particular, the conducted literature research shows that none of the analyzed papers consider the possibility of aggregating and managing multiple RECs in a coordinated manner for the provision of flexibility services to the grid.
This chapter lies in this framework as it proposes an optimization problem where multiple renewable energy communities are coordinated for efficient participation in balancing markets, specifically the Demand Response (DR).

4.1 REC external operations: actors and objectives

This chapter examines the problem of optimal management of a REC from the higher level of external operations: the participation of multiple RECs in the balancing market, with a focus on DR. To increase the flexibility capacity and the effectiveness of the service, several RECs coordinated by an aggregator are managed to track the reference power target coming from the system operator. Also in this case, it is necessary to define the actors operating at this level to properly define the problem settings:

- the energy community participants (ECPs)
- the energy community manager (ECM)
- the energy community aggregator (ECA)

Energy community participants and energy community manager from each REC must be considered at this level. The main features of these two actors have already been analyzed in detail in Chapter 2 and Chapter 3. Recalling briefly their objectives, the participants aim at minimizing

their own costs, while the ECM's goal is to maximize the revenue generated by energy sharing. However, here ECPs also act as flexibility providers since the operational management of multiple energy communities operating in the flexibility energy market is investigated.
The main novelty here lies in the introduction of a new figure, the energy community aggregator, who coordinates multiple RECs for an effective provision of ancillary services. The aggregator serves as intermediary between the DSO and the flexibility providers. The need for an aggregator depends on the number and the capacity of flexibility providers: preserving power quality could be easier and the benefit on the network could be higher by aggregating more end-users, as the available flexibility increases. For instance, in LV networks, which typically comprise small consumers and prosumers with limited flexible energy resources, the aggregator has a critical role as it aggregates flexibility from multiple small sources and negotiates optimal terms and prices in the market (Section 2.3). As regards objectives, the aggregators focuses on tracking the reference DR power value from the DSO. In the previous chapter, which considered a single REC, the ECM was directly responsible for ensuring a proper service provision whereas here this task is assigned to the aggregator who coordinates several RECs. This has a positive effect as expanding the number of involved users increases flexibility and therefore the benefits to the grid.
This specific problem is addressed in this chapter, where the key idea is to aggregate and manage the multiple RECs to cooperatively participate in the balancing market, with a focus on DR, and provide DR by 'sharing' the required power delivery. Also in this case, to encode the presence of different actors, a bi-level architecture is formalized: the low-level models the involved RECs, and both ECPs and ECM goals are considered. At the high-level, the ECA must track the reference DR power value from the DSO. The main assumption here is that the ECA has already participated and won the auction; therefore, the contracted quantity is known as well as the extent of the service provision (deviation from the working point): the upward/downward modulation of active power exchanged with the grid required by the DSO is an input parameter of the problem formulated in this chapter.
Summarizing, the main contributions of this chapter are:

- A novel entity, i.e. the ECA, is introduced which combines and coordinates multiple ECs for an efficient participation in the balancing market, with a focus on DR.
- A bilevel optimization architecture is formalized: EC decision problems are modelled at low level and then transformed using KKT conditions, while the high level considers the ECA tracking problem.

4.2 Decision problem definition

In the following, the proposed optimization models of the two levels are formalized. At the high-level, the ECA aims at following the input target given by the DSO by coordinating the consid-

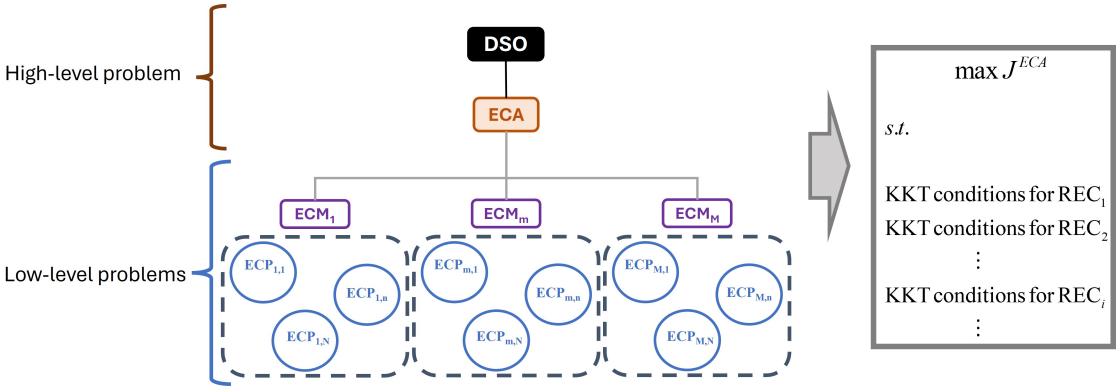

Figure 4.1: Overall architecture

ered RECs. The low-level models each REC considering both ECM and ECPs: each ECM aims at maximizing the incentive related to energy sharing by coordinating all participants, who want to minimize their own costs. To solve the problem, each low-level optimization problem is converted into constraints for the high-level thanks to KKT conditions. A schematic representation of the proposed approach is presented in Figure 4.1.

Before entering in the detail of the the problem formulation, in Table 4.1 all problem variables and data are reported. Three main sets are considered: S^T is the set of time instants, S^M is set of renewable energy communities and S_m^N is the set of energy community participants, for each REC. Therefore, in the formalization that follows, subscript $(\cdot)_{m,n,t}$ refers to quantities in time instant t for ECP n of REC m. Moreover, upper and lower bounds are not explicitly defined as they are well recognizable from notation: they are characterized by an upper bar ($\bar{\cdot}$) and lower bar ($\underline{\cdot}$), respectively.

Table 4.1: Nomenclature

Symbol	Unit	Description
Sets		
$S^T = \{1, \dots, T\}$		Set of time instants
$S^{DR} \subseteq S^T$		Set of time instants where the DSO requires DR services
$S^M = \{1, \dots, M\}$		Set of renewable energy communities
$S_m^N = \{1, \dots, N_m\}$		Set of energy REC participants for each REC m
Variables		
$e_{m,t}^{sh}$	[kWh]	Shared energy for the $m-th$ REC
$\beta_{m,t}$	[kW]	Auxiliary variable to reformulate the ECM objective function for REC m
$p_{m,t}^{EC,G}$	[kW]	Net grid power exchange of REC m
$p_{m,t}^{EC,G,in}$	[kW]	Grid power withdrawal of REC m

Symbol	Unit	Description
$p_{m,t}^{EC,G,out}$	[kW]	Grid power injection of REC m
$p_{m,n,t}^{G,in}$	[kW]	Power absorbed for the grid by ECP n of REC m
$p_{m,n,t}^{G,out}$	[kW]	Power injected into the grid by ECP n of REC m
$p_{m,n,t}^{S,ch}$	[kW]	Charging power of the ESS of ECP n of REC m
$p_{m,n,t}^{S,dch}$	[kW]	Discharging power of the ESS of ECP n of REC m
$x_{m,n,t}^{S}$	[/]	State of charge of the ESS of ECP n of REC m
$p_{m,n,t}^{L,flex}$	[kW]	Flexible load power consumption of ECP n of REC m
$p_{m,n,t}^{EV}$	[kW]	Charging power of the EV of ECP n of REC m
$x_{m,n,t}^{EV}$	[/]	State of charge of the EV of ECP n of REC m
Parameters		
P_{t}^{DR}	[kW]	Demand Response set point given by the DSO
C^{inc}	[€/kWh]	Unitary economic incentive on shared energy
$C_{m,n,t}^{buy}$	[€/kWh]	Grid cost for purchasing energy to the grid
$C_{m,n,t}^{sell}$	[€/kWh]	Grid cost for selling energy to the grid
Δ	[h]	Time step
$P_{m,n,t}^{PV}$	[kW]	Power production from PV of ECP n of REC m
$P_{m,n,t}^{L,fix}$	[kW]	Fixed load power consumption of ECP n of REC m
$\overline{P}_{m,n}^{G}$	[kW]	Maximum power exchange (import/export) with the grid
$CAP_{m,n}^{S}$	[kWh]	Energy capacity of the storage system
$\Gamma_{m,n}^{S,ch}$	[/]	Charging efficiency of the storage system
$\Gamma_{m,n}^{S,dch}$	[/]	Discharging efficiency of the storage system
$\overline{P}_{m,n}^{S}$	[kW]	Maximum exchangeable power with the ESS
$\underline{X}_{m,n}^{S}, \overline{X}_{m,n}^{S}$	[/]	Minimum/Maximum ESS state of charge
$E_{m,n}^{L,flex}$	[kWh]	Total energy required by the flexible load
$\overline{P}_{m,n}^{L,flex}$	[kW]	Maximum power deliverable to the flexible load
$CAP_{m,n}^{EV}$	[kWh]	Battery capacity of the EV
$\Gamma_{m,n}^{EV}$	[/]	Charging efficiency of the EV
$\overline{P}_{m,n}^{EV}$	[kW]	Maximum EV charging power
$\underline{X}_{m,n}^{EV}, \overline{X}_{m,n}^{EV}$	[/]	Minimum/Maximum EV state of charge
$X_{m,n}^{EV*}$	[/]	Desired final SoC of the EV
T_{i}^{EV*}	[h]	Time instant when the desired final EV SoC must be reached

4.2.1 High-level: ECA

The high-level problem encodes an ECA operating in the balancing market, whose primary goal is to provide services to the distribution grid in terms of power quality and DR. The community aggregator participates in the balancing market auction; after the balancing market is cleared, if it is a successful provider, the ECA obtains a certain flexibility (*contracted capacity*); depending on this contracted capacity and on grid conditions (network constraints under normal operating conditions or reconfigurations due to faults and scheduled maintenance), the DSO requires a certain reference DR power value, i.e. the target to be tracked. The target is given by a set point power (P_t^{DR}), defined in a specific time interval within the optimization horizon ($S^{DR} \subseteq S^T$). This behavior is modeled as a quadratic tracking objective function as

$$J^{ECA} = \sum_{t \in S^{DR}} \left(P_t^{DR} - \sum_{m \in S^M} p_{m,t}^{EC,G} \right)^2 \tag{4.1}$$

where $p_{m,t}^{EC,G}$ is net grid power exchange of REC m in each time interval t, calculated as the difference between withdrawn and injected powers

$$p_{m,t}^{EC,G} = p_{m,t}^{EC,G,in} - p_{m,t}^{EC,G,out} \qquad m \in S^M, t \in S^T \tag{4.2}$$

4.2.2 Low-level: RECs

The low-level problems model each REC, considering both manager and participants: therefore, the resulting objective function for each community incorporates both the ECM and ECP goals. The ECM aims at maximizing the economic benefits related to incentivized shared energy, while ECPs pursue their own energy cost minimization.
As regards the ECM, recalling equation (2.1), shared energy for each REC m is defined as the minimum between injected and withdrawn energy

$$e_{m,t}^{sh} = \Delta \min \left(p_{m,t}^{EC,G,in}, p_{m,t}^{EC,G,out} \right) \qquad m \in S^M, t \in S^T \tag{4.3}$$

The net grid withdrawn and injected power of each REC m is given by the contribution of all N_m participants of that REC

$$p_{m,t}^{EC,G,in} = \sum_{n \in S_m^N} p_{m,n,t}^{G,in} \qquad m \in S^M, t \in S^T \tag{4.4}$$

$$p_{m,t}^{EC,G,out} = \sum_{n \in S_m^N} p_{m,n,t}^{G,out} \qquad m \in S^M, t \in S^T \tag{4.5}$$

where $p^{G,in}_{m,n,t}$ and $p^{G,out}_{m,n,t}$ are withdrawn and injected powers by each participant n inside REC m, respectively. Since the aim of the ECM is to maximize shared energy defined in (4.3), the resulting problem would have a $max(min(\cdot))$ formulation; to avoid it, an additional variable $\beta_{m,t}$ is introduced [99] to express ECM objective function such as

$$J^{ECM}_m = -\Delta C^{inc} \sum_{t \in S^T} \beta_{m,t} \qquad m \in S^M \tag{4.6}$$

$s.t.$

$$0 \leq \beta_{m,t} \leq \sum_{n \in S^N_m} p^{G,in}_{m,n,t} \qquad m \in S^M, t \in S^T \tag{4.7}$$

$$\beta_{m,t} \leq \sum_{n \in S^N_m} p^{G,out}_{m,n,t} \qquad m \in S^M, t \in S^T \tag{4.8}$$

where Δ is the length of each time interval and C^{inc} is the fixed economic incentive on shared energy, according to the preliminary phase of the Italian legislation.
Regarding ECPs, their goal is to minimize their own costs. So, the objective function of each ECP n in community m is designed as

$$J^{ECP}_{m,n} = \Delta \sum_{t \in S^T} \left(C^{buy}_{m,n,t} p^{G,in}_{m,n,t} - C^{sell}_{m,n,t} p^{G,out}_{m,n,t} \right) \qquad m \in S^M, n \in S^N_m \tag{4.9}$$

where C^{buy} and C^{sell} are grid costs for purchasing and selling energy, respectively. Real-case scenarios consider $C^{buy}_t > C^{sell}_t \quad \forall t \in S^T$, thus limiting each user to not buy and sell energy simultaneously.
Since at this level, RECs are modeled in their entirety considering all actors, a unique objective function is formalized including ECM and ECPs objectives resulting in a multi-objective optimization problem

$$J^{EC}_m = J^{ECM}_m + \sum_{n \in S^N_m} J^{ECP}_{m,n} \qquad m \in S^M \tag{4.10}$$

Of course, all ECPs must respected technical and physical constraints of the technologies they have. Therefore, the following equations mus be included as constraints for the low-level problems. All technologies are considered when modeling ECP constraints; then, data are set such that for each ECP only the suitable devices are actually implemented. The constraints of the low-level problems are:

$$p^{G,in}_{m,n,t} + P^{PV}_{m,n,t} + p^{S,dch}_{m,n,t} = p^{G,out}_{m,n,t} + P^{L,fix}_{m,n,t} + p^{L,flex}_{m,n,t} + p^{S,ch}_{m,n,t} + p^{EV}_{m,n,t} \quad m \in S^M, n \in S^N_m, t \in S^T \tag{4.11}$$

$$0 \leq p^{G,out}_{m,n,t} \leq \overline{P}^G_{m,n} \qquad m \in S^M, n \in S^N_m, t \in S^T \tag{4.12}$$

$$0 \leq p^{G,in}_{m,n,t} \leq \overline{P}^G_{m,n} \qquad m \in S^M, n \in S^N_m, t \in S^T \tag{4.13}$$

$$x^S_{m,n,t} = x^S_{m,n,t-1} + \frac{\Delta}{CAP^S_{m,n}} \left(\Gamma^{S,ch}_{m,n} p^{S,ch}_{m,n,t} - \frac{1}{\Gamma^{S,dch}_{m,n}} p^{S,dch}_{m,n,t} \right) \quad m \in S^M, n \in S^N_m, t \in S^T \tag{4.14}$$

$$0 \leq p^{S,ch}_{m,n,t} \leq \overline{P}^S_{m,n} \qquad m \in S^M, n \in S^N_m, t \in S^T \tag{4.15}$$

$$0 \leq p^{S,dch}_{m,n,t} \leq \overline{P}^S_{m,n} \qquad m \in S^M, n \in S^N_m, t \in S^T \tag{4.16}$$

$$\underline{X}^S_{m,n} \leq x^S_{m,n,t} \leq \overline{X}^S_{m,n} \qquad m \in S^M, n \in S^N_m, t \in S^T \tag{4.17}$$

$$\sum_{t \in S^T} p^{L,flex}_{m,n,t} \Delta \geq E^{L,flex}_{m,n} \qquad m \in S^M, n \in S^N_m \tag{4.18}$$

$$0 \leq p^{L,flex}_{m,n,t} \leq \overline{P}^{L,flex}_{m,n} \qquad m \in S^M, n \in S^N_m, t \in S^T \tag{4.19}$$

$$x^{EV}_{m,n,t} = x^{EV}_{m,n,t-1} + \frac{\Delta}{CAP^{EV}_{m,n}} \Gamma^{EV}_{m,n} p^{EV}_{m,n,t} \qquad m \in S^M, n \in S^N_m, t \in S^T \tag{4.20}$$

$$0 \leq p^{EV}_{m,n,t} \leq \overline{P}^{EV}_{m,n} \qquad m \in S^M, n \in S^N_m, t \in S^T \tag{4.21}$$

$$\underline{X}^{EV}_{m,n} \leq x^{EV}_{m,n,t} \leq \overline{X}^{EV}_{m,n} \qquad m \in S^M, n \in S^N_m, t \in S^T \tag{4.22}$$

$$x^{EV}_{m,n,t} \geq X^{EV*}_{m,n} \qquad m \in S^M, n \in S^N_m, t = T^{EV*}_{m,n} \tag{4.23}$$

Constraint (4.11) is the power balance for each user, where $P^{PV}_{m,n,t}$ is power from photovoltaic plant, $p^{S,ch}_{m,n,t}$ and $p^{S,ch}_{m,n,t}$ are the power flows relevant to charging and discharging the storage, $P^{L,fix}_{m,n,t}$ is the fixed power load which cannot be controlled, $p^{L,flex}_{m,n,t}$ is the flexible power load portion, i.e. the load that can be shifted along the day, and $p^{EV}_{m,n,t}$ is the charging power of the electric vehicle. In constraints (4.12) and (4.13) the two positive terms defining the power exchange with the main grid are upper bounded by the maximum exchangeable power according to each ECP's contract. The constraints relevant to the energy storage system are (4.14)-(4.17). (4.14) is the ESS dynamic equation where $x^S_{m,n,t}$ is the ESS state of charge, $CAP^S_{m,n}$ its capacity, $\Gamma^{S,ch}_{m,n}$ and $\Gamma^{S,dch}_{m,n}$ its charging and discharging efficiencies. Then, constraints (4.15)-(4.17) represent upper and lower bounds of ESS power flows and states of charge. Equations (4.18) and (4.19) operate the deferrable loads. Equation (4.18) imposes that the energy required by this kind of load is delivered over the entire optimization horizon. Please note that using the greater equal is preferred over the equal to alleviate the problem; this choice is further justified if one considers that the buying price from the network is always greater than the overall benefit (selling price + EC incentive) thus the solver for sure tends to satisfy $E^{L,flex}_{m,n}$ as much as enough without exceeding it. Then, the power devoted to feed the flexible loads is bounded in (4.19). The constraints relevant to electric vehicles are (4.20)-(4.23). (4.20) is the EV dynamic equation, where $x^{EV}_{m,n,t}$ is the EV state of charge, $CAP^{EV}_{m,n}$ its capacity and $\Gamma^{EV}_{m,n}$ its charging efficiency. For EVs, only the charging mode is considered to have all energy resource from RES, as imposed by the legislation. Constraints (4.21) and (4.22) represent the upper and lower bounds of EV power flows and states of charge. Finally, constraint (4.23) ensures that the desired value for the EV state of charge is reached (and possibly exceeded) at the desired time instant $T^{EV*}_{m,n}$. As already discussed, among

the technologies allowed in RECs few of them have some limitations related to shared energy calculation, which must be totally from renewable. Nevertheless, the condition for ESS energy to count for shared energy calculation is satisfied because the energy buying price is greater than the benefits (energy selling price and EC incentive); as regards EVs, they are operated only in charging mode.

4.3 Overall optimization problem

To model a multi-agent framework, a multi-level optimization approach (see Section 3.2.2.1) is adopted. In this section, the low-level problems are first reformulated in their canonical form and then expressed through the corresponding KKT conditions.

4.3.1 Low-level problem reformulation

In order to derive KKT conditions for each low-level optimization problem (4.6)-(4.23), it is necessary to express it in canonical form. Since each low-level problem is formalized in the same way according to the model just described, KKT conditions are the same for each REC. Therefore, index m related to each energy community is neglected in the following.
First, by substituting the power balance (4.11) in (4.9) and rewriting $p_{n,t}^{G,in}$ in terms of remaining decision control variables, ECP objective function can be rearranged as

$$J_n^{ECP} = \Delta \sum_{t \in T} \left[C_{n,t}^{buy} \left(p_{n,t}^{G,out} + p_{n,t}^{L,flex} + p_{n,t}^{S,ch} + p_{n,t}^{EV} - p_{n,t}^{S,dch} + P_{n,t}^{L,fix} - P_{n,t}^{PV} \right) + -\Delta C_{n,t}^{sell} p_{n,t}^{G,out} \right] \quad n \in S^N \tag{4.24}$$

Thus, neglecting constant terms related to $P_{n,t}^{L,fix}$ and $P_{n,t}^{PV}$, REC objective function can be written in matrix form as

$$J^{EC} = \Delta \mathbf{\Gamma u} \tag{4.25}$$

where $\mathbf{\Gamma}$ is REC the cost row-vector, and $\mathbf{u}$ is the control variable column-vector. Both terms originate combining each ECP components ($\mathbf{\Gamma_n}$, $\mathbf{u_n}$), along with the term associated with ECM ($-\mathbf{C^{inc}1^{1xT}}$) as follows

$$\mathbf{\Gamma_n} = \left[(\mathbf{C_n^{buy}} - \mathbf{C_n^{sell}}) \quad \mathbf{C_n^{buy}} \quad \mathbf{C_n^{buy}} \quad -\mathbf{C_n^{buy}} \quad \mathbf{C_n^{buy}} \right] \quad n \in S^N \tag{4.26}$$

$$\mathbf{\Gamma} = \left[\mathbf{\Gamma_1} \cdots \mathbf{\Gamma_n} \cdots \quad \mathbf{\Gamma_N} \quad -\mathbf{C^{inc}1^{1xT}} \right] \tag{4.27}$$

$$\mathbf{u_n} = \begin{bmatrix} \mathbf{p_n^{out}} \\ \mathbf{p_n^{flex}} \\ \mathbf{p_n^{S,ch}} \\ \mathbf{p_n^{S,dch}} \\ \mathbf{p_n^{EV}} \end{bmatrix} n \in S^N, \qquad \mathbf{u} = \begin{bmatrix} \mathbf{u}_1 \\ \vdots \\ \mathbf{u}_n \\ \vdots \\ \mathbf{u}_N \\ \boldsymbol{\beta} \end{bmatrix} \tag{4.28}$$

where $\mathbf{1^{1xT}}$ is row-vector of ones with length T.
Then, ESS and EV dynamic state equations in (4.14) and (4.20) are converted to static forms as follows

$$\mathbf{x_n^S} = \begin{bmatrix} \mathbf{0} & \mathbf{0} & \mathbf{K_n^{S,ch}} & \mathbf{K_n^{S,dch}} & \mathbf{0} \end{bmatrix} \mathbf{u_n} + X_{n,0}^S \quad n \in S^N \tag{4.29}$$

$$\mathbf{x_n^{EV}} = \begin{bmatrix} \mathbf{0} & \mathbf{0} & \mathbf{0} & \mathbf{0} & \mathbf{K_n^{EV}} \end{bmatrix} \mathbf{u_n} + X_{n,0}^{EV} \quad n \in S^N \tag{4.30}$$

where, for each ECP, $\mathbf{K_n^*}$ are TxT upper-triangular matrices defined as

$$\mathbf{K_n^{S,ch}} = \begin{cases} k_{i,j} = 0 & i < j \\ k_{i,j} = \frac{\Gamma_n^{S,ch}\Delta}{CAP_n^S} & i \geq j \end{cases} \quad n \in S^N \tag{4.31}$$

$$\mathbf{K_n^{S,dch}} = \begin{cases} k_{i,j} = 0 & i < j \\ k_{i,j} = -\frac{\Delta}{\Gamma_n^{S,dch} CAP_n^S} & i \geq j \end{cases} \quad n \in S^N \tag{4.32}$$

$$\mathbf{K_n^{EV}} = \begin{cases} k_{i,j} = 0 & i < j \\ k_{i,j} = \frac{\Gamma_n^{EV}\Delta}{CAP_n^{EV}} & i \geq j \end{cases} \quad n \in S^N \tag{4.33}$$

Finally, making appropriate substitutions and some algebraic manipulations, all inequality constraints can be written in matrix form such as

$$\mathbf{\Omega u} + \mathbf{\Psi} \leq \mathbf{0} \tag{4.34}$$

where $\mathbf{\Omega}$ and $\mathbf{\Psi}$ are matrices composed by N ECP-related matrices ($\mathbf{\Omega_n}$ and $\mathbf{\Psi_n}$) and the ECM-related ones ($\mathbf{\Omega_n^{\beta}}$, $\mathbf{\Omega^{\beta}}$, and $\mathbf{\Psi^{\beta}}$)

$$\mathbf{\Omega_n} = \begin{bmatrix} -\mathbf{I} & \mathbf{0} & \mathbf{0} & \mathbf{0} & \mathbf{0} \\ \mathbf{I} & \mathbf{0} & \mathbf{0} & \mathbf{0} & \mathbf{0} \\ \mathbf{0} & -\mathbf{\Delta 1^{1xT}} & \mathbf{0} & \mathbf{0} & \mathbf{0} \\ \mathbf{0} & -\mathbf{I} & \mathbf{0} & \mathbf{0} & \mathbf{0} \\ \mathbf{0} & \mathbf{I} & \mathbf{0} & \mathbf{0} & \mathbf{0} \\ \mathbf{0} & \mathbf{0} & -\mathbf{I} & \mathbf{0} & \mathbf{0} \\ \mathbf{0} & \mathbf{0} & \mathbf{I} & \mathbf{0} & \mathbf{0} \\ \mathbf{0} & \mathbf{0} & \mathbf{0} & -\mathbf{I} & \mathbf{0} \\ \mathbf{0} & \mathbf{0} & \mathbf{0} & \mathbf{I} & \mathbf{0} \\ \mathbf{0} & \mathbf{0} & -\mathbf{K_n^{S,ch}} & -\mathbf{K_n^{S,dch}} & \mathbf{0} \\ \mathbf{0} & \mathbf{0} & \mathbf{K_n^{S,ch}} & \mathbf{K_n^{S,dch}} & \mathbf{0} \\ \mathbf{0} & \mathbf{0} & \mathbf{0} & \mathbf{0} & -\mathbf{I} \\ \mathbf{0} & \mathbf{0} & \mathbf{0} & \mathbf{0} & \mathbf{I} \\ \mathbf{0} & \mathbf{0} & \mathbf{0} & \mathbf{0} & -\mathbf{K_n^{EV}} \\ \mathbf{0} & \mathbf{0} & \mathbf{0} & \mathbf{0} & \mathbf{K_n^{EV}} \\ \mathbf{0} & \mathbf{0} & \mathbf{0} & \mathbf{0} & \mathbf{K_{n|T^{EV*}}^{EV}} \\ -\mathbf{I} & -\mathbf{I} & -\mathbf{I} & \mathbf{I} & -\mathbf{I} \\ \mathbf{I} & \mathbf{I} & \mathbf{I} & -\mathbf{I} & \mathbf{I} \end{bmatrix}, \quad \mathbf{\Psi_n} = \begin{bmatrix} \mathbf{0} \\ -\overline{\mathbf{P}}_{\mathbf{n}}^{\mathbf{G}} \\ E_n^{L,flex} \\ \mathbf{0} \\ -\overline{\mathbf{P}}_{\mathbf{n}}^{\mathbf{L,flex}} \\ \mathbf{0} \\ -\overline{\mathbf{P}}_{\mathbf{n}}^{\mathbf{S}} \\ \mathbf{0} \\ -\overline{\mathbf{P}}_{\mathbf{n}}^{\mathbf{S}} \\ \underline{\mathbf{X}}_{\mathbf{n}}^{\mathbf{S}} - \mathbf{X}_{\mathbf{n,0}}^{\mathbf{S}} \\ \mathbf{X}_{\mathbf{n,0}}^{\mathbf{S}} - \overline{\mathbf{X}}_{\mathbf{n}}^{\mathbf{S}} \\ \mathbf{0} \\ -\overline{\mathbf{P}}_{\mathbf{n}}^{\mathbf{EV}} \\ \underline{\mathbf{X}}_{\mathbf{n}}^{\mathbf{EV}} - \mathbf{X}_{\mathbf{n,0}}^{\mathbf{EV}} \\ \mathbf{X}_{\mathbf{n,0}}^{\mathbf{EV}} - \overline{\mathbf{X}}_{\mathbf{n}}^{\mathbf{EV}} \\ X_{n,T^{EV*}}^{EV} - X_{n,0}^{EV} \\ \mathbf{P_n^{PV}} - \mathbf{P_n^{L,fix}} \\ -\mathbf{P_n^{PV}} + \mathbf{P_n^{L,fix}} - \overline{\mathbf{P}}_{\mathbf{n}}^{\mathbf{G}} \end{bmatrix} \quad n \in S^N$$

$$\mathbf{\Omega_n^{\beta}} = \begin{bmatrix} \mathbf{0} & \mathbf{0} & \mathbf{0} & \mathbf{0} & \mathbf{0} \\ -\mathbf{I} & \mathbf{0} & \mathbf{0} & \mathbf{0} & \mathbf{0} \\ -\mathbf{I} & -\mathbf{I} & -\mathbf{I} & \mathbf{I} & -\mathbf{I} \end{bmatrix} n \in S^N, \quad \mathbf{\Omega^{\beta}} = \begin{bmatrix} -\mathbf{I} \\ \mathbf{I} \\ \mathbf{I} \end{bmatrix}, \quad \mathbf{\Psi^{\beta}} = \begin{bmatrix} \mathbf{0} \\ \mathbf{0} \\ (\mathbf{P^{PV}} - \mathbf{P^{L,fix}})\mathbf{1^{N \times 1}} \end{bmatrix}$$

$$\mathbf{\Omega} = \begin{bmatrix} \mathbf{\Omega_1} & \mathbf{0} & & \cdots & & \mathbf{0} \\ \mathbf{0} & \ddots & & & & \\ & & \mathbf{\Omega_n} & & & \vdots \\ \vdots & & & \ddots & & \\ \mathbf{0} & & \cdots & \mathbf{0} & \mathbf{\Omega_N} & \mathbf{0} \\ \mathbf{\Omega_1^{\beta}} & \cdots & \mathbf{\Omega_n^{\beta}} & \cdots & \mathbf{\Omega_N^{\beta}} & \mathbf{\Omega^{\beta}} \end{bmatrix}, \quad \mathbf{\Psi} = \begin{bmatrix} \mathbf{\Psi_1} \\ \vdots \\ \mathbf{\Psi_n} \\ \vdots \\ \mathbf{\Psi_N} \\ \mathbf{\Psi^{\beta}} \end{bmatrix}$$

where $\boldsymbol{I}$ and $\mathbf{0}$ are the identity and zeros matrices, respectively.

4.3.2 Deriving KKT conditions

At this point, each low-level optimization problem is formulated as an inequality-constrained convex optimization problem, which leads to a compact formulation of KKT conditions. It is

appropriate to recall that, for a convex optimization problem with a given solution as in this case, first-order KKT conditions are sufficient to ensure global optimality for the low-level problems [108]. Given the problem just defined, KKT conditions of each low-level decision problem can be easily derived as

$$\Delta\boldsymbol{\Gamma} + \boldsymbol{\mu}^{\mathbf{T}}\boldsymbol{\Omega} = \mathbf{0} \tag{4.35}$$

$$\boldsymbol{\mu}^{\mathbf{T}}(\boldsymbol{\Omega}\boldsymbol{u} + \boldsymbol{\Psi}) = \mathbf{0} \tag{4.36}$$

$$\boldsymbol{\mu} \geq \mathbf{0} \tag{4.37}$$

where $\boldsymbol{\mu}$ is the vector of the Lagrange multipliers. Of course, also (4.34) must be considered among KKT conditions. Among KKT conditions, (4.34) encodes primal feasibility, (4.35) represents stationarity and (4.36)-(4.37) denote complementarity. Condition (4.36) makes the overall problem a non-linear programming problem (NLP); however, replacing equation (4.35) in (4.36) allows to get the following linear expression:

$$\Delta\boldsymbol{\Gamma}\boldsymbol{u} + \boldsymbol{\mu}^{\mathbf{T}}\boldsymbol{\Psi} = \mathbf{0} \tag{4.38}$$

The overall optimization problem is finally formulated by the ECA objective function in (4.1), subjected to (4.34)-(4.35), (4.37)-(4.38).

4.4 Application to a Case Study

In this section, the proposed methodology is tested on a case study and the main results are discussed. Four scenarios are compared: the first two scenarios consider all modeled technologies; Scenario A analyses the case where RECs are coordinated by an ECA, while in Scenario B the coordinating role of the ECA is neglected. Then, in the last two scenarios ESSs are disregarded to assess how the system flexibility changes; also in this case, the aggregator action is considered (Scenario C) and neglected (Scenario D). Finally, in the last part of this section, a scalability analysis is presented to prove the suitability of this approach for larger scenarios, and a sensitivity analysis on the DR reference power value is described.

4.4.1 Problem Data

Here, the main data of the optimization problem are presented. The proposed methodology is tested on a case study characterized by three RECs with 5, 3 and 8 ECPs, respectively. Table 4.2 reports the general data relevant to the optimization problem, while the data relevant to all ECPs are shown in Table 4.3, where only data ranges are reported for sake of brevity. Electrical load data have been collected from Italian users' standard profiles [109], while PV production curves have been normalized from historical real-data of Savona Campus facility [110]. A one-hour time

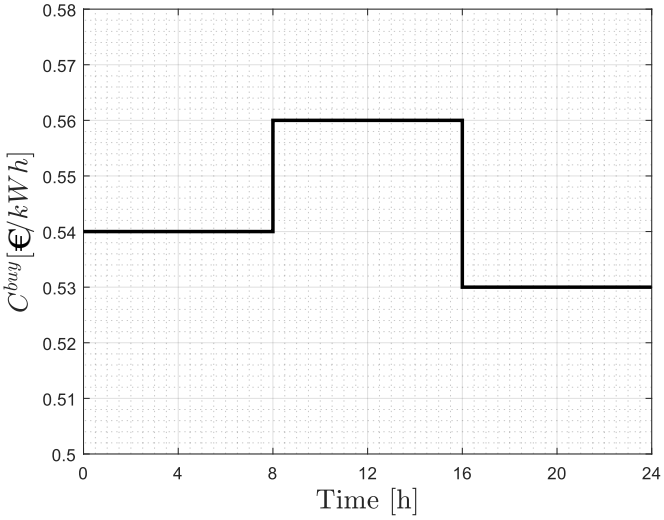

Figure 4.2: Energy buying price

step is considered as generally required by regulation on shared energy. Then, the buying price from the main grid for each ECP (C_t^{buy}) is considered to be time-variant (Figure 4.2) following the typical Italian multi-rate tariff time-slots (F1, F2, F3); price values are averaged along year 2022.

4.4.2 Optimization results

The proposed methodology is tested on the case study just described and a detailed description of the results is provided. Thanks to the linearization in (4.38), the resulting optimization problem is a LP, and the solution is obtained via GUROBI solver in MATLAB on an Intel Core i7-1370P 1.90GHz 32GB RAM processor in 0.2[s] , which makes it suitable for online operations.

Table 4.2: Problem data

T	Δ[h]	C^{inc}[€/kWh]	C^{sell}[€/kWh]	$\overline{P}^{G}$[kW]	$\overline{P}^{L,flex}$[kW]	$\underline{X}^{S}$[/]	$\overline{X}^{S}$[/]
24	1	0.11	0.08	30	2	0.2	1
X_0^S[/]	$\Gamma^{S,ch}$[/]	$\Gamma^{S,dch}$ [/]	$\overline{P}^{EV}$[kW]	CAP^{EV}[kWh]	$\underline{X}^{EV}$[/]	$\overline{X}^{EV}$[/]	Γ^{EV}[/]
0.2	0.95	0.95	3	10	0.1	0.9	0.95

Table 4.3: ECP data

Parameter	Value range	Parameter	Value range	Parameter	Value range
P^{PV}	$0 \div 15$[kW]	$P^{L,fix}$	$0.3 \div 2.3$[kW]	$E^{L,flex}$	$3 \div 20$[kWh]
CAP^{S}	$1 \div 30$[kWh]	$\overline{P}^{S,ch}$	$0 \div 10$[kW]	$\overline{P}^{S,dch}$	$0 \div 10$[kW]
X_0^{EV}	$0.2 \div 0.5$[/]	X^{EV*}	$0.2 \div 0.9$[/]	T^{EV*}	$1 \div 24$[h]

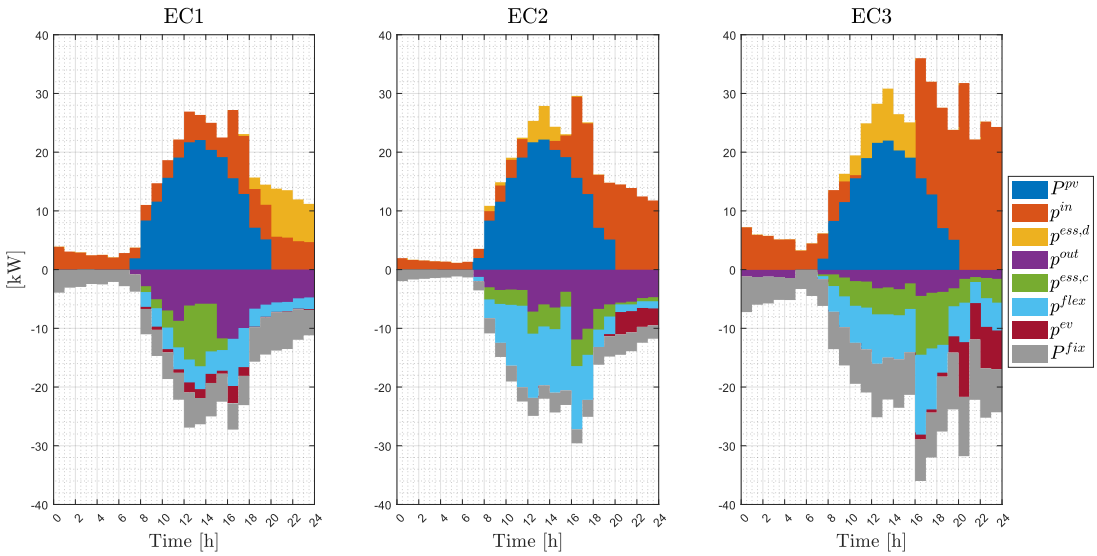

Figure 4.3: Power balance for each REC (Scenario A)

4.4.2.1 Scenario A and B

Scenario A and B investigate how the the considered system behaves when all considered technologies are implemented, including ESSs. Scenario A integrates also the participation to DR services with the ECA coordination, while Scenario B neglects this possibility.
Figure 4.3 shows the power balance for each energy community in Scenario A, summing all power flows for all ECPs. All simulated RECs have similar configurations, with homogeneous application regarding implemented technologies, i.e. PV, flexible load, ESS and EV. The third REC, $EC3$ in the figure, counts more members resulting in slightly-greater power values, especially in the second-half of the optimization horizon. Moreover, it is possible to notice a strong correlation between purchasing cost and withdrawn power, since the energy purchase is concentrated when buying cost is minimum.

In Table 4.4, total costs for aggregator, managers and participants are reported. A null cost for the ECA indicates a perfect tracking of the power target imposed by the DSO for the DR program. Due to the problem structure, based on the transformation of low-level into constraints for the high-level thanks to KKT conditions, the low-level problems' optimality constraints the

Table 4.4: Optimal objective function values - Scenario A

ECA [kW^2]	ECMs [€]	ECPs [€]
0.00	-24.11	154.8

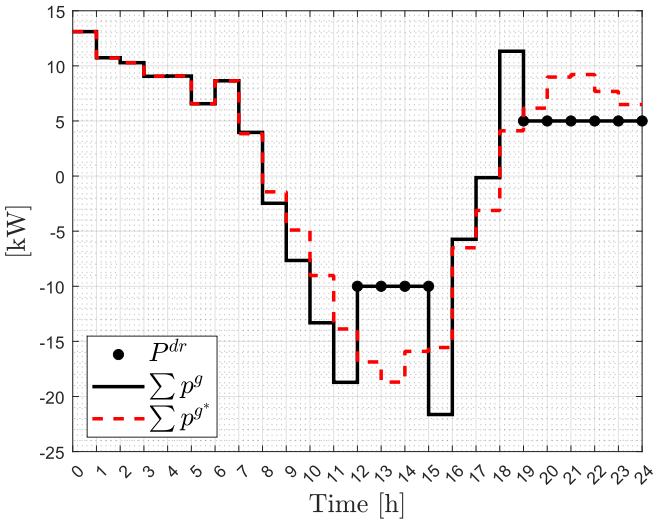

Figure 4.4: Overall grid power exchange (Scenarios A and B)

high-level solution: KKT conditions fix the low-level solution at the optimal cost, while the high-level solution is given by the optimal option among the equivalent low-level solutions. Therefore, ECMs and ECPs costs are not affected by the DR program. A noteworthy benefit of participating in an REC is the overall cost reduction due to ECM profits, which is amounts to 15.5%.

In the following figures, two curves are represented for each optimal control variable: the continuous one corresponds to the optimization results including the participation in DR programs (Scenario A), while the dashed curve corresponds to the case excluding the participation in DR programs (Scenario B). Figure 4.4 shows the overall power exchange with the grid, given by the aggregation of all ECP profiles. The required DR power, P_t^{DR} in equation (4.1), is selected to remain relatively close to the optimal power values observed in absence of DR program. This figure allows to appreciate that during the time window S^{DR} (12:00-15:00 and 19:00-24:00), the overall power exchange in Scenario A aligns perfectly with the target values and, as a consequence, it adjusts during the remaining hours of the day. Figure 4.5 depicts the overall shared energy as sum of all β_m values over all RECs. Since shared energy directly depends on the power exchange with the grid, its value obviously changes whether DR is considered or not. Nevertheless, the area subtended by the two curves remains the same (as well as the incentive) due to low-level KKT conditions, which constraint the ECMs to meet the optimal working point for ECPs in Table 4.4. Finally, Figure 4.6 shows the overall power flows related to each technology, as sum over all ECPs. As a direct consequence of the power balance, all control variables are af-

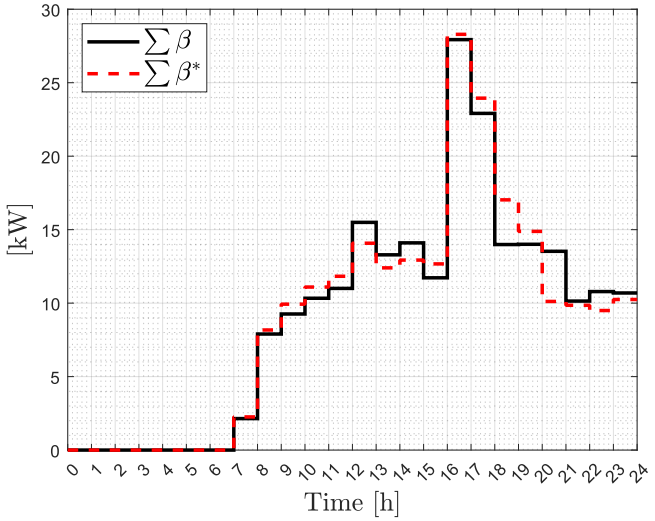

Figure 4.5: Overall shared energy (Scenarios A and B)

fected by the DR participation and are adjusted to meet the request for flexibility from high-level problem. In particular, ESS powers ($p^{S,*}$) experience the greatest change within the optimization horizon because the ESS, being an energy storage device, is the main source of flexibility.

4.4.2.2 Scenario C and D

These last two scenarios are devised to evaluate the technical and economic impact of the ESS technology and, most of all, to assess its importance on the flexibility of the considered system; therefore, an analysis is performed by removing the ESSs. Also in this case, Scenario C integrates the ECA tracking problem, while Scenario D neglects DR participation. The most interesting result concerns the ECA objective in Scenario C (Table 4.5): the non-null value of the high-level objective function proves that removing the ESSs leads to reduced flexibility potential and a consequent noncompliance in tracking the reference DR power value given by the DSO. Obviously, the objectives of ECMs and ECPs change accordingly, showing a minor cost increase: +2.7% and +8.6% respectively. Figure 4.7 reports the aggregated power flows for the remaining technologies, i.e. EVs and deferrable loads. Also in this case, the continuous curve corresponds to the optimization results including the DR power tracking (Scenario C), while the dashed one corresponds to the case excluding the participation in DR programs (Scenario D). It is visible that, when the ESS is neglected, the technology that undergoes the most significant variation are the flexible loads ($p^{L,flex}$).

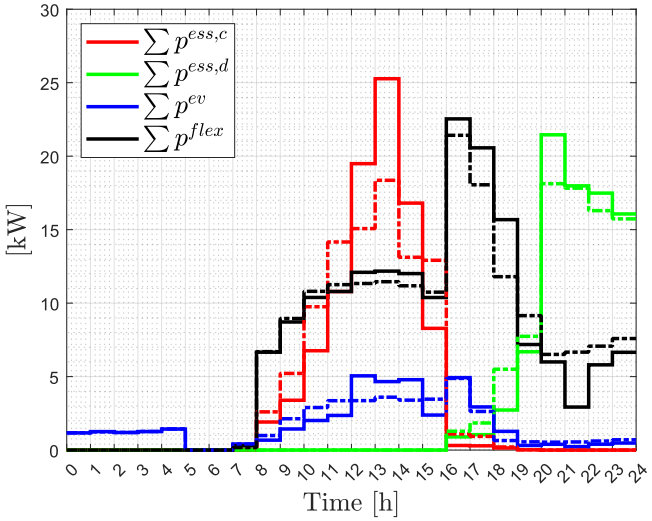

Figure 4.6: Overall control power flows, with and without DR (Scenarios A and B)

Table 4.5: Optimal objective function values - Scenario C

ECA [kW^2]	ECMs [€]	ECPs [€]
7.52	−23.46	168.1

4.4.3 Scalability and Sensitivity analysis

To assess the scalability of the proposed approach, instances of increasing size are tested. In practical implementations the perimeter defined by the primary substation may encompass a geographically extended and heterogeneous area, potentially including a large number of users and energy assets. In principle, a single large REC spanning the entire primary substation area could represent an ideal configuration from the perspective of maximizing shared energy; however, such a solution is often unrealistic in practice due to organizational, social, and administrative barriers. Therefore, having many small RECs coordinated by an aggregator is a more realistic scenario. Table 4.6 reports the runtime results for instances of increasing size. For each instance, the number of RECs (M) and the number of participants for each REC (N_m) are specified; please note that for some RECs the ECP number is significant, reaching up to 18 members. The results prove that the proposed approach scales reasonably; indeed, it performs well even in the case of the largest instance, whose runtime is compatible with the one-hour discretization step typical of REC applications.
Table 4.6 also shows the value of the ECA objective. The focus of this analysis is scalability in terms of runtime; therefore, the DSO reference power value is kept the same as in the base instance (3 RECs). This is the reason why objective J^{ECA} increases: as the number of RECs and, consequently, the number of involved users increase, the total power exchanged with the

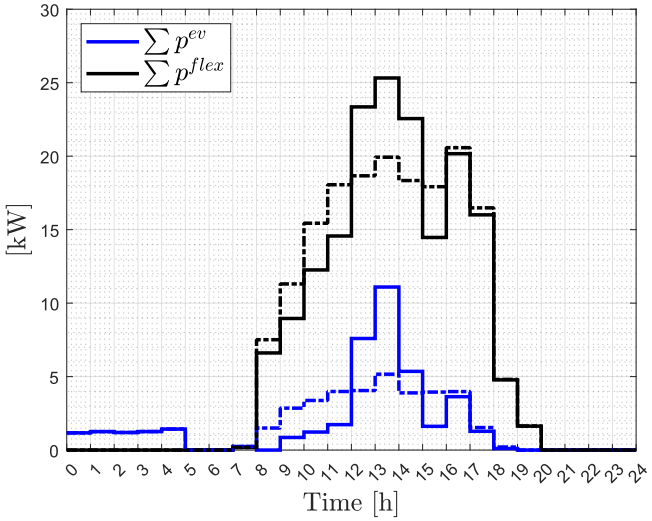

Figure 4.7: Overall control power flows (Scenarios C and D)

Table 4.6: Scalability analysis on runtime

M	N_m	Runtime[s]	$J^{ECA}[kW^2]$
3	[3,5,8]	0.197471	0
4	[3,5,8,6]	0.263216	0
5	[3,5,8,6,17]	0.504469	1.12E+03
8	[3,5,8,6,17,4,5,7]	0.645039	1.12E+03
15	[3,5,8,6,17,4,5,7,5,14,9,6,8,5,13]	1.528983	8.74E+03
20	[3,5,8,6,17,4,5,7,5,14,9,6,8,5,13,4,15,7,5,4]	2.175814	1.39E+04
30	[3,5,8,6,17,4,5,7,5,14,9,6,8,5,13,4,15,7,5,4,8,16,9,9,6,18,9,6,8,5]	4.510472	5.36E+04

grid increases until it reaches a configuration that is no longer compatible with the selected P^{DR}. Indeed, the DSO reference power value depends on the contracted capacity that the ECA wins in the market clearing and, consequently, on the considered configuration. In this regard, a sensitivity analysis is performed on the flexibility that the base instance is able to offer on the DR market (Table 4.7). The DSO reference power value is modified: the time instants where the DSO requires DR services are kept the same, while the set point power value is modified. The results show that by modifying P^{DR}, the value of J^{ECA} increases, indicating that the system is no longer able to track the target. To visually appreciate this, Figure 4.8 shows the overall grid power exchange for the two cases resulting in the highest J^{ECA} values. This demonstrates that submitting on the balancing market a bid that is consistent with the configuration is essential to offer an effective service provision.

Table 4.7: Sensitivity analysis on P^{DR}

P^{DR} [12:00-15:00][kW]	P^{DR} [19:00-24:00][kW]	$J^{ECA}[kW^2]$	Graph
-10	5	-4.44E-11	Figure 4.4
0	5	1.42E+02	Figure 4.8 *(a)*
-5	5	10.5017	
-15	5	-1.26E-11	
-20	5	-1.40E-11	
-25	5	0.7706	
-30	5	86.3915	
-10	15	1.88E+02	Figure 4.8 *(b)*
-10	10	6.4156	
-10	0	33.1385	

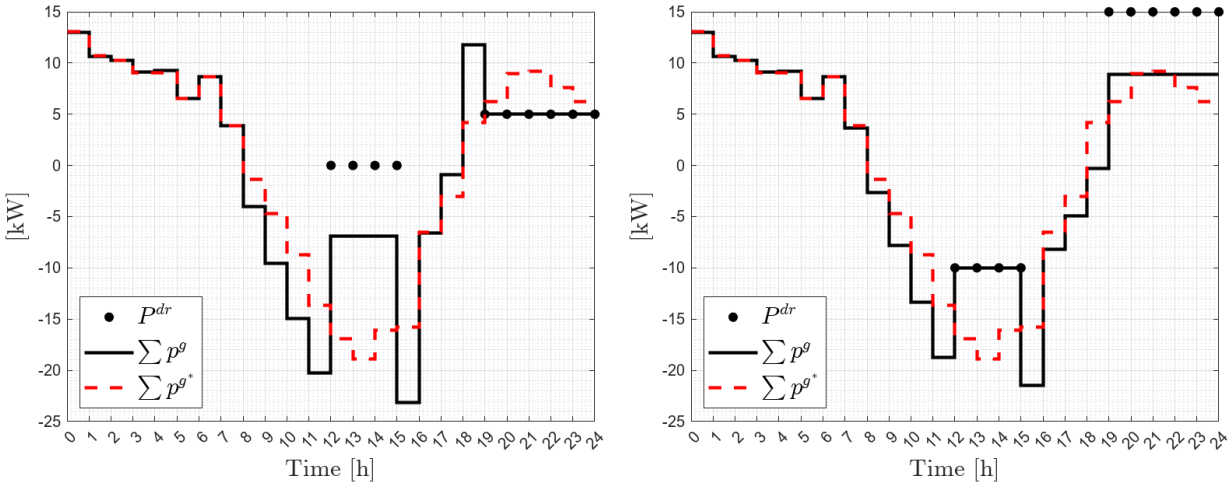

(a) (b)

Figure 4.8: Overall grid power exchange (Sensitivity Analysis on P^{DR})

Chapter 5

Real-time energy management in smart parking lots

From this chapter on, the focus is on entities that can form or join a REC. While RECs are often associated with domestic users such as individual households or residential condominiums, the current regulatory framework also allows the participation of more complex and structured entities and aggregated energy systems: RECs can naturally extend beyond purely domestic settings to include infrastructures characterized by high power demand, flexible operation, and advanced energy management capacity. The following chapters examine the problem of optimal management of a REC at a microscopic level, focusing on individual participants or on configurations that could potentially form an REC: the analyzed entities have a huge potential as RECs or REC participants but their potential as RECs (or participants) can be further enhanced if these entities are properly managed and controlled at the grassroots level. Therefore, once usual EMSs are efficient, they could be integrated with community-level constraints, regulation-aware equations, and energy sharing maximization objectives to encourage sustainable cooperation among prosumers and increase collective efficiency and sustainability. As potential EPCs, smart parking lots and multi-vector energy hubs are investigated (Section 2.2.3) since they represent two particularly relevant and emerging applications. In particular, these entities are explicitly addressed in the following chapters of this thesis, where the focus deliberately remains on the individual ECP and therefore the described optimal management problems concern a SPL and a multi-vector energy hubs without placing them within the REC context.

In particular, this chapter is dedicated to the optimal management of a Smart Parking Lot (SPL). Because of the massive electrification of the transport system, these entities represent a significant and concentrated load on the grid [111]. The impact of this aggregated load can be alleviated by the smart charging strategies [29], briefly mentioned in the introduction, especially when combined with demand response strategies and grid services. In addition to that, the load represented by smart PLs can be integrated with RES and satisfied locally, in line with the key purpose of renewable energy communities: increasing local consumption through the concept of shared energy. Therefore, smart charging strategies could be enhanced with the integration of regulatory concepts such as shared energy and with constraints modeling the regulation on the matter. In most cases, smart parking lots have a single connection point to the public electricity grid (PCC – Point of Common Coupling); therefore, in the context of RECs, the parking lot operator can also assume the role of ECP, acting mainly as consumer.
This chapter addresses the optimal management problem of a smart PL equipped with multiple EV charging stations; the model representing the system is characterized by its comprehensive consideration of charging rates, EV timetabling constraints, multiphase grid interactions, and DR constraints. The solution method relies on an extended version of the Newton-based Bregman Alternating Direction Method of Multipliers which accelerates convergence.

Smart charging strategies and grid service provision are a complex research topic, which many papers have dealt with. As an example, in [112] a SPL integrated within a virtual multi-energy hub is managed to maximize profit via a goal-oriented heuristic dynamic programming tool. The IoT platform designed in [113] optimally manages the charging of an EV fleet in a grid-connected SPL with a dedicated solar PV plant coupled with an ESS. In the case of smart park-

ing lots for EVs, the factors to consider increase: different EVs must be properly coordinated, grid services must be complied with to provide adequate service to the DSO, and owners' requirements must be respected to provide adequate service to customers. However, research in this field usually focuses only one of these aspects at a time. In [114], [115] DR strategies are integrated into the optimal management optimization strategies for PLs. Authors in [114] optimize self-consumption and price-based DR via a MILP multi-objective optimization problem that minimizes the electricity cost and the battery degradation of employees' EV batteries parked in a company SPL. In [115], a linear programming approach is adopted to solve a real-time optimization-based energy management model for an EV parking lot. A DR program is integrated into the EMS to achieve peak load limitation and therefore provide operational flexibility to the system operator. Users' behavior and preferences, which improve service quality and fairness, are considered in [116–120]. Stochastic random behaviors of vehicle owners are accounted for in [116], where an optimal energy management strategy for charging and discharging EVs in intelligent PLs is presented, with the aim of maximizing profits for both the SPL and EV owners, while improving energy efficiency and load balancing. The model also integrates penalties and incentives to encourage compliance and ensure fairness. In [117], a smart real-time energy management strategy is proposed to maximize the penetration level of EVs in an intelligent SPL. EVs are classified considering the coupling relationship among their travel information, battery status and other characteristics, and a charging/discharging priority evaluation model is established based on fuzzy control theory. In [118], a bi-objective optimization model for EV charging scheduling at a workplace charging stations is presented and one of the two objectives, in addition to cost minimization, is minimizing the deviation from the desired State-Of-Charge (SOC). Authors also address the concept of fairness: besides minimizing the sum of deviations, another approach minimizes the worst deviation, a fairness criterion based on a min-max approach. Authors in [119] develop an energy management system for the optimal EV charging process in a community SPL in three stages to consider day-ahead and real-time scheduling, as well as owners' preferences. To compensate for the changes in car charging demand due to the unpredictable car behavior, authors in [120] integrate the day-ahead market with the participation in the balance market. Few papers consider all these aspects together, also because integrating grid services provision, user-aware strategies and a detailed grid modeling makes the model more accurate and reliable, but solving the resulting optimization problems efficiently (especially in large-scale or real-time scenarios) requires computationally effective models and algorithms. To address these challenges, recent research has focused on enhancing the performance and scalability of power management strategies in intelligent PLs through advanced optimization frameworks. The optimal charging scheduling method proposed in [121] balances the interests of both the DSO and the EV parking lot operator: the DSO aims to maximize the load factor, while the EV operator seeks to minimize charging costs. The solution, is achieved in 0.891 s for 120 EVs using an optimization-based coordination method. Authors in [122] propose a real-time charging scheduling scheme that coordinates a central operator and individual chargers to achieve the optimal EV charging schedule. The central operator estimates the optimal aggregate charging energy at a coarse time granularity over a long time horizon and generates charging energy ref-

Table 5.1: Comparison with state of the art works methods and their features

	II order method	**Battery model**	**Phases**	**Desired SOC**		**DR policies**
				Tracking	**Constraint**	
[112]	-	Linear	-	-	✓	✓
[113]	-	Linear	-	-	✓	-
[119]	-	Linear	-	-	✓	-
[120]	-	Linear	-	-	✓	-
[114]	-	Linear	-	-	✓	-
[115]	-	Linear	-	-	✓	✓
[116]	-	Linear	-	✓	-	-
[117]	-	Linear	-	-	✓	-
[118]	-	Linear	-	✓	✓	-
[121]	-	Linear	-	-	✓	-
[122]	-	Linear	-	-	✓	-
[123]	-	Linear	-	-	✓	-
[124]	-	Piece-wise linear	✓	✓	-	✓
This work	✓	Piece-wise linear	✓	✓	-	✓

erences for individual chargers. Each charger then determines the actual charging power at a fine time granularity based on the charging energy reference and stochastic departure scenarios. The maximum solving time is 1.4s for a case with 200 EVs, but unified EV chargers are tested. To preserve privacy and reduce the computational burden, [123] introduces a two-stage scheme: in the first stage, the aggregate EV power flexibility region inside each charging station is derived by solving an optimization problem, and it is proven that any trajectory within this region corresponds to at least one feasible EV dispatch strategy. In the second stage, a coordination mechanism is proposed to achieve a socially optimal solution. The proposed mechanism is not sensitive to the number of charging stations, as the calculations of charging stations can be run in parallel. Still, for 20 EVs the computational time of the two stages is 7s and 150s, respectively. These papers propose solution methods that perform well from a computational point of view, but the model is not accurate: as an example, grid service provision, phases, and a non-linear battery model are not considered. Table 5.1 summarizes the literature review conducted above and highlights the features offered by the proposed study; specifically, it is evident that none of the analyzed papers, except for [124], considers these aspects at the same time. However, with DR strategies the system flexibility is at disposal of the grid, considering phases and their balancing (objective J_4) is fundamental to preserve system stability, and a non-linear battery model allows for a more precise and realistic SOC estimation. As regards the solution method, none of the analyzed papers considers a II-order method.

The work proposed in this chapter is able to address both challenges: the SPL is modeled in an accurate way and the designed optimization algorithm achieves convergence in a runtime that allows real-time operations and eventually the integration of additional features such as the

ones specific to RECs. Indeed, the considered SPL is equipped with EV charging stations and is modeled considering DR constraints to provide some flexibility services to the grid, multiphase grid interactions in order to present a real interaction of a large-size SPL with the main grid, and the main characteristics peculiar to EVs, such as timetabling constraints and a piece-wise linear model for the batteries. The main novelty here lies in the solution method, which relies on the Newton-based Bregman Alternating Direction Method of Multipliers (Nwt-BADMM) algorithm; indeed, it is extended by integrating a second-order Newton step for the dual update, facilitating accelerated convergence without imposing strict convexity or Hessian invertibility constraints.
Summarizing, the main contributions of this chapter are:

- With respect to the paper [125], the condition of invertibility of the hessian is extended to the case where both the cost functions can be positive semi-definite.
- The introduction of a piece-wise linear model for the EV batteries that can represent the actual dependence of the charging rate on the state of charge.
- Considering phases to present a real interaction

5.1 Decision problem definition

This section describes the optimization problem for the power management of a smart parking lot. In particular, the parking lot operator pursues the real-time optimal energy management of the SPL depicted in Figure 5.1 with the final goal of satisfying the energy demand of each EV, while minimizing grid costs. At the same time, the flexible load represented by several EVs parked for long time periods is made available to the DSO for ancillary services provision to the grid.

Before starting to define the overall problem, Table 5.2 reports problem variables and parameters. Since a multi-phase system is considered, charging stations are classified into single (S^{CS1}) and three (S^{CS3}) phase CSs, depending on the connection to the grid: in fact, once the cables are laid, the phase to which each CS is connected is fixed. For brevity, we define the set of all charging stations, each with a certain number of sockets. Therefore, four main sets are considered: S^{CS} is set of all charging stations, S_i^S is the set of sockets for each CS, S^P is the set of phases, and S^T is the set of time instants. Each vehicle is uniquely identified by the column and the socket to which it is connected: hence, each EV is uniquely defined by the combination of CS i and socket j. Therefore, in the formalization that follows, subscript $(\cdot)_{i,j,p,t}$ refers to vehicle (i, j), and quantities in time instant t for phase p. Moreover, upper and lower bounds are not explicitly defined as they are well recognizable from notation: they are characterized by an upper bar ($\bar{\cdot}$) and lower bar ($\underline{\cdot}$), respectively.

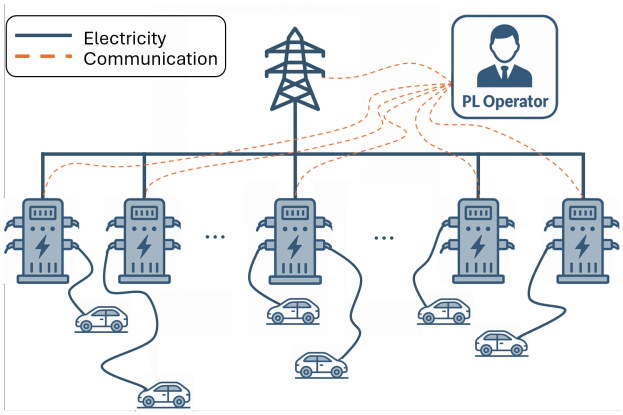

Figure 5.1: Graphic representation of the considered system

Table 5.2: Nomenclature

Symbol	Unit	Description
Sets		
$S^T = \{1, \dots, T\}$		Set of time instants
$S^{DR} \subseteq S^T$		Set of time instants where the DSO requires DR services
S^{CS1}		Set of single-phase charging stations
S^{CS3}		Set of three-phase charging stations
$S^{CS} = S^{CS1} \cup S^{CS3} = \{1, \dots, I\}$		Set of all charging stations
$S_i^S = \{1, \dots, J_i\}$		Set of sockets for each charging station, $i \in S^{CS}$
$S^P = \{a, b, c\}$		Set of phases
Variables		
$p_{p,t}^G$	[kW]	Power exchange with the grid on phase p and time t
$p_{i,j,p,t}^{EV}$	[kW]	Charging power at time t of EV (i, j)
$x_{i,j,t}^{EV}$	[/]	State of charge of EV (i, j)
Parameters		
Δ	[h]	Duration of each time step
α_k	[/]	Weights in the multi-objective function
C_t^{buy}	[€/kWh]	Electricity purchase price at time t
P_t^{DR}	[kW]	Demand response reference power at time t
$P_{p,t}^{RES}$	[kW]	Renewable generation at phase p and time t
$P_{p,t}^L$	[kW]	Load demand at phase p and time t
$\underline{P}_p^G, \overline{P}_p^G$	[kW]	Lower/Upper grid power limits
$CAP_{i,j}^{EV}$	[kWh]	Battery capacity of the EV (i, j)
$\Gamma_{i,j}^{EV}$	[/]	Charging efficiency of EV (i, j)

Symbol	Unit	Description
$\overline{P}_{i,j}^{EV}$	[kW]	Maximum charging power of EV (i,j)
$\underline{X}_{i,j,t}^{EV}, \overline{X}_{i,j,t}^{EV}$	[/]	Minimum/Maximum EV SoC
$T_{i,j}^{rl}$	[h]	Arrival time of EV (i,j)
$T_{i,j}^{dl}$	[h]	Departure time of EV (i,j)
X_0^{EV}	[/]	Initial Soc of EV (i,j)
$X_{i,j}^{EV*}$	[/]	Desired SoC of EV (i,j) to be reached at the deadline
$\overline{P}_{i,p}^{CS}$	[kW]	Maximum power deliverable by CS i on phase p
$H_{i,j,p}^{P}$	[/]	Matrix denoting at which phase each CS is connected
$a_{i,j}^{EV}$, $c_{i,j}^{EV}$, $d_{i,j}^{EV}$	[/]	Parameters of the piecewise-linear charging curve

The proposed formulation takes into account a multiobjective formulation with four terms. In particular, it is possible to write the objective function as follows

$$\min f(x) = \alpha_1 J^1 + \alpha_2 J^2 + \alpha_3 J^3 + \alpha_4 J^4 \tag{5.1}$$

where

$$J^1 = \sum_{i \in S^{CS}} \sum_{j \in S_i^S} \left[\left(x_{i,j,T_{i,j}^{dl}}^{EV} - X_{i,j}^{EV*} \right)^2 \right] \tag{5.2}$$

$$J^2 = \sum_{t \in S^T} \left\{ \left[\left(\sum_{p \in S^P} p_{p,t}^G \right) - P_t^{DR} \right]^2 \right\} \tag{5.3}$$

$$J^3 = \sum_{t \in S^T} \left\{ C_t^{buy} \sum_{p \in S^P} \left(p_{p,t}^G \, \Delta \right) \right\} \tag{5.4}$$

$$J^4 = \sum_{t \in S^T} \left\{ \left(p_{a,t}^G - p_{b,t}^G \right)^2 + \left(p_{b,t}^G - p_{c,t}^G \right)^2 \right\} \tag{5.5}$$

In particular, J_1 in (5.2) is used to minimize the difference between the state of charge when t corresponds to the deadline ($T_{i,j}^{dl}$) and the desired one $X_{i,j}^{EV*}$. Equation (5.3) applies DR policies and tracks the reference power value P_t^{DR} given by the DSO in a specific subset $S^{DR} \subseteq S^T$. In J_3, introduced in (5.4), the cost of the power purchased from the grid in each time interval is minimized. The last term of the objective function, presented in (5.5), is used to balance the power purchased from the grid between phases.
The objective function in (5.1) is subject to the following constraints

$$p_{p,t}^G + P_{p,t}^{RES} = \sum_{i \in S^{CS}} \sum_{j \in S_i^S} p_{i,j,p,t}^{EV} + P_{p,t}^L \qquad t \in S^T, p \in S^P \tag{5.6}$$

$$\underline{P}_p^G \leq p_{p,t}^G \leq \overline{P}_p^G \qquad t \in S^T, p \in S^P \tag{5.7}$$

$$x_{i,j,t+1}^{EV} = x_{i,j,t}^{EV} + \frac{\Delta}{CAP_{i,j}^{EV}} \left(\Gamma_{i,j}^{EV} \cdot \sum_{p=1}^{3} p_{i,j,p,t}^{EV} \right) \qquad t \in S^T, i \in S^{CS}, j \in S_i^S \tag{5.8}$$

$$p_{i,j,1,t}^{EV} = p_{i,j,2,t}^{EV} = p_{i,j,3,t}^{EV} \qquad t \in S^T, i \in S^{CS3}, j \in S_i^S \tag{5.9}$$

$$p_{i,j,p,t}^{EV} = 0 \quad \left(t < T_{i,j}^{rl}\right) \vee \left(t > T_{i,j}^{dl}\right), p \in S^P, i \in S^{CS}, j \in S_i^S \tag{5.10}$$

$$0 \leq p_{i,j,p,t}^{EV} \qquad t \in S^T, p \in S^P, i \in S^{CS}, j \in S_i^S \tag{5.11}$$

$$p_{i,j,p,t}^{EV} \leq \begin{cases} \overline{P}_{i,j}^{EV} H_{i,j,p}^P, & \text{if } x_{i,j,t}^{EV} \leq a_{i,j}^{EV} \\ \left(c_{i,j}^{EV} \cdot x_{i,j,t}^{EV} + d_{i,j}^{EV}\right) H_{i,j,p}^P, & \text{if } x_{i,j,t}^{EV} > a_{i,j}^{EV} \end{cases} \quad t \in S^T, p \in S^P, i \in S^{CS}, j \in S_i^S \tag{5.12}$$

$$\underline{X}_{i,j,t}^{EV} \leq x_{i,j,t}^{EV} \leq \overline{X}_{i,j,t}^{EV} \qquad t \in S^T, i \in S^{CS}, j \in S_i^S \tag{5.13}$$

$$\sum_{j \in S_i^S} p_{i,j,p,t}^{EV} \leq \overline{P}_{i,p}^{CS} \qquad t \in S^T, p \in S^S, i \in S^{CS} \tag{5.14}$$

Equation (5.6) imposes the power balance on each phase. The left side of the equation counts power generation, given by the power from the grid and the power from renewable sources. The right side is instead relevant to power consumption, which considers the EV charging power and the fixed load power. Upper and lower bounds for the power exchange with the grid are imposed by (5.7). The remaining constraints are relevant to the electric vehicles. Constraint (5.8) is the dynamic equation of each EV (i, j), where $\Gamma_{i,j}^{EV}$ is its charging efficiency and $CAP_{i,j}^{EV}$ its capacity. For three-phase EVs, the charging power has to be balanced between phases as imposed in (5.9). Constraint (5.10) ensures that a vehicle cannot be charged until it arrives at the SPL ($T_{i,j}^{rl}$) and after its departure ($T_{i,j}^{dl}$). Equation (5.11) imposes the EV charging power to be positive, neglecting vehicle-to-grid operations. Constraint (5.12) models a piece-wise linear model for EV batteries; in particular, this model explicitly encodes the dependency of the maximum charging power on the state of charge. In fact, while $x_{i,j,t}^{EV}$ is lower than parameter $a_{i,j}^{EV}$, the power that can be fed to the EV battery is the maximum one; when $a_{i,j}^{EV}$ is exceeded, the upper bound is represented by a linear function of the state of charge with parameters $c_{i,j}^{EV}$ and $d_{i,j}^{EV}$. Note that $H_{i,j,p}^P$ is a matrix mapping the phases to which each CS is connected: therefore, its value is equal to 1 if CS i, and consequently all its sockets, is connected to phase p, 0 otherwise. This results in the charging power being set to zero for phases to which the EV is not connected for single-phase EVs. Then, the state of charge of each EV is bounded in (5.13). Finally, the maximum power that can be delivered by the charging station is defined in (5.14).
Summarizing, the overall optimization problem is given by (5.1) subject to (5.6)-(5.14).

5.2 Optimization algorithm

In this section, the proposed optimization algorithm is described. Before that, the following section recalls the basic mathematical background needed to develop it. Then, the problem formulation in its canonical form is derived and the proposed algorithm is presented.

5.2.1 Mathematical Background

This section is dedicated to briefly recall some basic concepts and definitions that are useful to develop the designed optimization algorithm. Specifically, the Alternating Direction Method of Multipliers algorithm is defined in its standard form and then it is extended thanks to the Bregman Divergence.

MB1. ADMM ADMM considers the problem of minimizing composite objective functions subject to an equality constraint:

$$\min_{\mathbf{u}\in U,\mathbf{z}\in Z} f(\mathbf{u}) + g(\mathbf{z}) \quad \text{s.t. } \mathbf{A}\mathbf{u} + \mathbf{B}\mathbf{z} = \mathbf{c}, \tag{5.15}$$

where f and g are convex functions, $\mathbf{A} \in \mathbb{R}^{m\times n_1}$, $\mathbf{B} \in \mathbb{R}^{m\times n_2}$, $\mathbf{c} \in \mathbb{R}^m$, $\mathbf{u} \in \mathbb{R}^{n_1}$, $\mathbf{z} \in \mathbb{R}^{n_2}$, and U, Z are non-empty closed convex sets. The partial augmented Lagrangian of the problem is:

$$L_\rho(\mathbf{u}, \mathbf{z}, \boldsymbol{\lambda}) = f(\mathbf{u}) + g(\mathbf{z}) + \boldsymbol{\lambda}^T (\mathbf{A}\mathbf{u} + \mathbf{B}\mathbf{z} - \mathbf{c}) + \frac{\rho}{2}\|\mathbf{A}\mathbf{u} + \mathbf{B}\mathbf{z} - \mathbf{c}\|_2^2 \tag{5.16}$$

where $\boldsymbol{\lambda} \in \mathbb{R}^m$ is the dual variable, and $\rho > 0$ is the penalty parameter. ADMM consists of the following updates:

$$\mathbf{u}_{\tau+1} = \arg\min_{\mathbf{u}\in U} L_\rho(\mathbf{u}, \mathbf{z}_\tau, \boldsymbol{\lambda}_\tau) \tag{5.17}$$

$$\mathbf{z}_{\tau+1} = \arg\min_{\mathbf{z}\in Z} L_\rho(\mathbf{u}_{\tau+1}, \mathbf{z}, \boldsymbol{\lambda}_\tau) \tag{5.18}$$

$$\boldsymbol{\lambda}_{\tau+1} = \boldsymbol{\lambda}_\tau + \rho(\mathbf{A}\mathbf{u}_{\tau+1} + \mathbf{B}\mathbf{z}_{\tau+1} - \mathbf{c}). \tag{5.19}$$

MB2. Bregman Divergence Let $\phi : \Omega \to \mathbb{R}$ be a continuously differentiable and strictly convex function. The Bregman divergence D_ϕ induced by ϕ is defined as:

$$D_\phi(h, k) = \phi(h) - \phi(k) - \nabla\phi(k)^T(h - k). \tag{5.20}$$

Note that this represents a measure of distance between two points h and k.

MB3. Generalized BADMM To allow different Bregman divergences for the $\mathbf{u}$ and $\mathbf{z}$ updates, we generalize BADMM as:

$$\mathbf{u}_{\tau+1} = \arg\min_{\mathbf{u}\in U} L_\rho(\mathbf{u}, \mathbf{z}_\tau, \boldsymbol{\lambda}_\tau) + \rho_u D_{\phi_u}(\mathbf{u}, \mathbf{u}_\tau) \tag{5.21}$$

$$\mathbf{z}_{\tau+1} = \arg\min_{\mathbf{z}\in Z} L_\rho(\mathbf{u}_{\tau+1}, \mathbf{z}, \boldsymbol{\lambda}_\tau) + \rho_z D_{\phi_z}(\mathbf{z}, \mathbf{z}_\tau), \tag{5.22}$$

$$\boldsymbol{\lambda}_{\tau+1} = \boldsymbol{\lambda}_\tau + \zeta(\mathbf{A}\mathbf{u}_{\tau+1} + \mathbf{B}\mathbf{z}_{\tau+1} - \mathbf{c}), \tag{5.23}$$

where $\rho_u, \rho_z, \zeta > 0$ are additional parameters and D_{ϕ_u}, D_{ϕ_z} are specific Bregman divergences for the $\mathbf{u}$ and $\mathbf{z}$ updates.

5.2.2 Problem reformulation

In order to apply the designed algorithm, the problem described in the previous section must be reformulated as a quadratic programming (QP) problem. The methodology in [126] can be applied to rewrite the proposed optimization problem as

$$\begin{aligned} min \quad & \mathbf{u}^T\mathbf{Q}\mathbf{u} + \mathbf{q}^T\mathbf{u} \\ & s.t. \\ & \mathbf{A}\mathbf{u} - \mathbf{b} = 0 \\ & \mathbf{C}\mathbf{u} - \mathbf{d} \leq 0 \end{aligned} \tag{5.24}$$

where $\mathbf{u}$ is the vector of decision variables defined as

$$\mathbf{u} = col\{p^{EV}_{i,j,p,t}, i \in S^{CS}, j \in S^S_i, p \in S^P, t \in S^T\} \tag{5.25}$$

and matrices $\mathbf{Q}$ and $\mathbf{q}$ are appropriately constructed from the optimization problem described in Section 5.1.

To achieve the formulation in (5.24), the state equation (5.8) for each vehicle (i, j) must be reformulated in static form as a function of the initial state of charge (X^{EV}_0) and of decision variable $\mathbf{u}$.

$$\mathbf{x} = \mathbf{T} \cdot X^{EV}_0 + \mathbf{S} \cdot \mathbf{u} \tag{5.26}$$

where $\mathbf{x} = col\{x^{EV}_{i,j,t}, i \in S^{CS}, j \in S^S_i, t \in S^T\}$ is the vector of state variables, $\mathbf{S} = diag\{\mathbf{S}_{i,j}, i \in S^{CS}, j \in S^S_i\}$ and $\mathbf{T} = col\{\mathbf{T}_{i,j}, j \in S^S_i\}$ with

$$\mathbf{S}_{i,j} = \begin{bmatrix} \frac{\Gamma_{i,j}}{CAP_{i,j}}\Delta & 0 & \cdots & 0 \\ \frac{\Gamma_{i,j}}{CAP_{i,j}}\Delta & \frac{\Gamma_{i,j}}{CAP_{i,j}}\Delta & \cdots & 0 \\ \cdots & \ddots & \ddots & \vdots \\ \frac{\Gamma_{i,j}}{CAP_{i,j}}\Delta & \frac{\Gamma_{i,j}}{CAP_{i,j}}\Delta & \cdots & \frac{\Gamma_{i,j}}{CAP_{i,j}}\Delta \end{bmatrix} \quad \mathbf{T}_{i,j} = \mathbf{1} \tag{5.27}$$

Then, by introducing a slack variable $\mathbf{s}$, it is possible to write the optimization problem only with equality and positivity constraints [127]. Moreover, to obtain a suitable problem formulation for the application of our algorithm, the approach presented in [128] has been adopted.

5.2.3 Nwt-BADMM algorithm

To define a new BADMM-based algorithm that employs a Newton step for the dual update, it is necessary to consider the dual function in (5.28).

$$d(\boldsymbol{\lambda}) = \min_{\mathbf{u},\mathbf{z}} L_\rho^D(\mathbf{u}, \mathbf{z}, \boldsymbol{\lambda}) \tag{5.28}$$

with

$$L_\rho^D(\mathbf{u}, \mathbf{z}, \boldsymbol{\lambda}) = L_\rho(\mathbf{u}, \mathbf{z}, \boldsymbol{\lambda}) + \rho_u D_{\phi_u}(\mathbf{u}, \mathbf{u}') + \rho_z D_{\phi_z}(\mathbf{z}, \mathbf{z}') \tag{5.29}$$

As a first step, we impose the first-order conditions for (5.29) with respect to the primal variables $\mathbf{u}, \mathbf{z}$.

$$\nabla_u \left[L_\rho^D(\mathbf{u}, \mathbf{z}, \boldsymbol{\lambda})\right] = \nabla_u f(\mathbf{u}) + \mathbf{A}^T\boldsymbol{\lambda} + \rho\mathbf{A}^T(\mathbf{A}\mathbf{u} + \mathbf{B}\mathbf{z} - \mathbf{c}) + \rho_u\nabla_u\phi_u(\mathbf{u}) - \rho_u\nabla_u\phi_u(\mathbf{u}') = 0 \tag{5.30}$$

$$\nabla_z \left[L_\rho^D(\mathbf{u}, \mathbf{z}, \boldsymbol{\lambda})\right] = \nabla_z g(\mathbf{z}) + \mathbf{B}^T\boldsymbol{\lambda} + \rho\mathbf{B}^T(\mathbf{A}\mathbf{u} + \mathbf{B}\mathbf{z} - \mathbf{c}) + \rho_z\nabla_u\phi_z(\mathbf{z}) - \rho_z\nabla_z\phi_z(\mathbf{z}') = 0 \tag{5.31}$$

Conditions (5.30) and (5.31) are implicit nonlinear systems of equations:

$$F(\mathbf{u}, \mathbf{z}, \boldsymbol{\lambda}) = \begin{bmatrix} \nabla_u L_\rho^D(\mathbf{u}, \mathbf{z}, \boldsymbol{\lambda}) \\ \nabla_z L_\rho^D(\mathbf{u}, \mathbf{z}, \boldsymbol{\lambda}) \end{bmatrix} = 0 \tag{5.32}$$

whose solution is a couple $\mathbf{u}(\boldsymbol{\lambda})$ and $\mathbf{z}(\boldsymbol{\lambda})$ of functions of $\boldsymbol{\lambda}$, with $\boldsymbol{\lambda}$ as a parameter. Thanks to the implicit function theorem [129], these functions are continuous and differentiable if the Jacobian matrix of $F(\mathbf{u}, \mathbf{z})$ with respect to $\mathbf{u}$ and $\mathbf{z}$ is invertible at least in a neighborhood of the optimal values $\mathbf{u}^*, \mathbf{z}^*$. Such a matrix is

$$\mathbf{J}_{u,z}(F(\mathbf{u}, \mathbf{z})) = \begin{bmatrix} a_{11} & a_{12} \\ a_{21} & a_{22} \end{bmatrix} \tag{5.33}$$

with

$$a_{11} = \nabla_{uu}^2 f(\mathbf{u}) + \rho\mathbf{A}^T\mathbf{A} + \rho_u\nabla_{uu}^2\phi_u(\mathbf{u}) \tag{5.34}$$

$$a_{12} = \rho\mathbf{A}^T\mathbf{B} \tag{5.35}$$

$$a_{21} = \rho\mathbf{B}^T\mathbf{A} \tag{5.36}$$

$$a_{22} = \nabla_{zz}^2 g(\mathbf{z}) + \rho\mathbf{B}^T\mathbf{B} + \rho_z\nabla_{zz}^2\phi_z(\mathbf{z}) \tag{5.37}$$

Theorem 5.1. *Matrix in* (5.33) *is positive definite, thus it is invertible.*

Proof. A $q \times q$ symmetric matrix M is said to be positive definite if

$$\boldsymbol{\nu}^T \mathbf{M} \boldsymbol{\nu} > 0 \;\; \boldsymbol{\nu} \in \mathbb{R}^q \backslash \{0\} \tag{5.38}$$

By applying definition (5.38) to (5.33) we have $\boldsymbol{\nu}_1, \boldsymbol{\nu}_2 \in \mathbb{R}^q \backslash \{0\}$

$$\begin{bmatrix} \boldsymbol{\nu}_1 & \boldsymbol{\nu}_2 \end{bmatrix} \mathbf{J}_{u,z} \left(F \left(\mathbf{u}, \mathbf{z} \right) \right) \begin{bmatrix} \boldsymbol{\nu}_1 \\ \boldsymbol{\nu}_2 \end{bmatrix} > 0 \tag{5.39}$$

$$\begin{aligned} \boldsymbol{\nu}_1{}^T \nabla^2_{uu} f \left(\mathbf{u} \right) \boldsymbol{\nu}_1 + \rho \boldsymbol{\nu}_1{}^T \mathbf{A}^T \mathbf{A} \boldsymbol{\nu}_1 + \rho_u \boldsymbol{\nu}_1{}^T \nabla^2_{uu} \phi_u(\mathbf{u}) \boldsymbol{\nu}_1 + \rho \boldsymbol{\nu}_1{}^T \mathbf{A}^T \mathbf{B} \boldsymbol{\nu}_2 + \rho \boldsymbol{\nu}_2{}^T \mathbf{B}^T \mathbf{A} \boldsymbol{\nu}_1 \\ + \boldsymbol{\nu}_2{}^T \nabla^2_{zz} g \left(\mathbf{z} \right) \boldsymbol{\nu}_2 + \rho \boldsymbol{\nu}_2{}^T \mathbf{B}^T \mathbf{B} \boldsymbol{\nu}_2 + \rho_z \boldsymbol{\nu}_2{}^T \nabla^2_{zz} \phi_z(\mathbf{z}) \boldsymbol{\nu}_2 > 0 \end{aligned} \tag{5.40}$$

By collecting (5.40) we have

$$\boldsymbol{\nu}_1{}^T \nabla^2_{uu} f \left(\mathbf{u} \right) \boldsymbol{\nu}_1 + \boldsymbol{\nu}_2{}^T \nabla^2_{zz} g \left(\mathbf{z} \right) \boldsymbol{\nu}_2 + \rho \left\| \mathbf{A} \boldsymbol{\nu}_1 + \mathbf{B} \boldsymbol{\nu}_2 \right\|_2^2 + \rho_u \boldsymbol{\nu}_1{}^T \nabla^2_{uu} \phi_u(\mathbf{u}) \boldsymbol{\nu}_1 + \rho_z \boldsymbol{\nu}_2{}^T \nabla^2_{zz} \phi_z(\mathbf{z}) \boldsymbol{\nu}_2 > 0 \tag{5.41}$$

That is positive definite since by definition ϕ is strictly convex. This completes the proof. □

It is relevant to highlight that there are no binding conditions about the properties of the objective functions of the original optimization problem, widening the applicability of the proposed algorithm.
Thanks to the previous statements, the solution associated with the first-order conditions of the augmented Lagrangian generates a couple $\mathbf{u}(\boldsymbol{\lambda})$ and $\mathbf{z}(\boldsymbol{\lambda})$ that are continuous and differentiable functions of $\boldsymbol{\lambda}$. Thus, it is possible to define the gradient of the dual function in (5.28) as

$$\nabla_\lambda d \left(\boldsymbol{\lambda} \right) = \mathbf{A} \mathbf{u} \left(\boldsymbol{\lambda} \right) + \mathbf{B} \mathbf{z} \left(\boldsymbol{\lambda} \right) - \mathbf{c} + \left(\mathbf{J}_\lambda \left(\mathbf{u} \left(\boldsymbol{\lambda} \right) \right) \right)^T \nabla_u \left[L^D_\rho (\mathbf{u}(\boldsymbol{\lambda}), \mathbf{z}(\boldsymbol{\lambda}), \boldsymbol{\lambda}) \right] + \left(\mathbf{J}_\lambda \left(\mathbf{z} \left(\boldsymbol{\lambda} \right) \right) \right)^T \nabla_z \left[L^D_\rho (\mathbf{u} \left(\boldsymbol{\lambda} \right), \mathbf{z} \left(\boldsymbol{\lambda} \right), \boldsymbol{\lambda}) \right] \tag{5.42}$$

By considering (5.30) and (5.31), we have that

$$\nabla_u \left[L^D_\rho (\mathbf{u} \left(\boldsymbol{\lambda} \right), \mathbf{z} \left(\boldsymbol{\lambda} \right), \boldsymbol{\lambda}) \right] = 0 \tag{5.43}$$

$$\nabla_z \left[L^D_\rho (\mathbf{u} \left(\boldsymbol{\lambda} \right), \mathbf{z} \left(\boldsymbol{\lambda} \right), \boldsymbol{\lambda}) \right] = 0 \tag{5.44}$$

Collecting from (5.42) and thanks to (5.43) and (5.44), we have

$$\nabla_\lambda d \left(\boldsymbol{\lambda} \right) = \mathbf{A} \mathbf{u} \left(\boldsymbol{\lambda} \right) + \mathbf{B} \mathbf{z} \left(\boldsymbol{\lambda} \right) - \mathbf{c} \tag{5.45}$$

Thus, we compute the Hessian $\nabla^2_{\lambda\lambda} d \left(\boldsymbol{\lambda} \right)$

$$\nabla^2_{\lambda\lambda} d \left(\boldsymbol{\lambda} \right) = \mathbf{A} \mathbf{J}_\lambda \mathbf{u} \left(\boldsymbol{\lambda} \right) + \mathbf{B} \mathbf{J}_\lambda \mathbf{z} \left(\boldsymbol{\lambda} \right) \tag{5.46}$$

To obtain $\mathbf{J}_\lambda \left(\mathbf{u} \left(\boldsymbol{\lambda} \right) \right)$ and $\mathbf{J}_\lambda \left(\mathbf{z} \left(\boldsymbol{\lambda} \right) \right)$, we differentiate (5.43) and (5.44) with respect to $\boldsymbol{\lambda}$

$$\left[\nabla^2_{uu} f \left(\mathbf{u} \left(\boldsymbol{\lambda} \right) \right) + \rho \mathbf{A}^T \mathbf{A} + \rho_u \nabla^2_{uu} \phi_u(\mathbf{u}(\boldsymbol{\lambda})) \right] \mathbf{J}_\lambda \left(\mathbf{u} \left(\boldsymbol{\lambda} \right) \right) + \left(\rho \mathbf{A}^T \mathbf{B} \right) \mathbf{J}_\lambda \left(\mathbf{z} \left(\boldsymbol{\lambda} \right) \right) + \mathbf{A}^T = 0 \tag{5.47}$$

$$\left[\nabla^2_{zz} g\left(\mathbf{z}\left(\boldsymbol{\lambda}\right)\right) + \rho \mathbf{B}^T\mathbf{B} + \rho_z \nabla^2_{zz}\phi_z(\mathbf{z}(\boldsymbol{\lambda}))\right] \mathbf{J}_\lambda\left(\mathbf{z}\left(\boldsymbol{\lambda}\right)\right) + \left(\rho \mathbf{B}^T\mathbf{A}\right) \mathbf{J}_\lambda\left(\mathbf{u}\left(\boldsymbol{\lambda}\right)\right) + \mathbf{B}^T = 0 \quad (5.48)$$

Collecting (5.47) and (5.48) in matrix form, we have

$$\mathbf{J}\left(F\left(\mathbf{u}(\boldsymbol{\lambda}), \mathbf{z}(\boldsymbol{\lambda}), \boldsymbol{\lambda}\right)\right) \begin{bmatrix} \mathbf{J}_\lambda\left(\mathbf{u}\left(\boldsymbol{\lambda}\right)\right) \\ \mathbf{J}_\lambda\left(\mathbf{z}\left(\boldsymbol{\lambda}\right)\right) \end{bmatrix} = - \begin{bmatrix} \mathbf{A}^T \\ \mathbf{B}^T \end{bmatrix} \quad (5.49)$$

with $F\left(\mathbf{u}(\boldsymbol{\lambda}), \mathbf{z}(\boldsymbol{\lambda}), \boldsymbol{\lambda}\right) = \begin{bmatrix} (5.43) \\ (5.44) \end{bmatrix}$. Finally, we have the final form of the Hessian matrix as follows

$$\nabla^2_{\lambda\lambda} d\left(\boldsymbol{\lambda}\right) = - \begin{bmatrix} \mathbf{A} & \mathbf{B} \end{bmatrix} \mathbf{J}\left(F\left(\mathbf{u}(\boldsymbol{\lambda}), \mathbf{z}(\boldsymbol{\lambda}), \boldsymbol{\lambda}\right)\right)^{-1} \begin{bmatrix} \mathbf{A}^T \\ \mathbf{B}^T \end{bmatrix} \quad (5.50)$$

Based on the previous discussion, it is possible to define the Nwt-BADMM algorithm. The updates for $\mathbf{u}$ and $\mathbf{z}$ are the same as in (5.21) and (5.22); what changes is the $\boldsymbol{\lambda}$ update, which is improved as

$$\boldsymbol{\lambda}_{\tau+1} = \boldsymbol{\lambda}_\tau + \mathbf{M}\left(\mathbf{u}_{\tau+1}, \mathbf{z}_{\tau+1}, \boldsymbol{\lambda}_\tau\right)^{-1} \left(\mathbf{A}\mathbf{u}_{\tau+1} + \mathbf{B}\mathbf{z}_{\tau+1} - \mathbf{c}\right) \quad (5.51)$$

with

$$\mathbf{M}\left(\mathbf{u}_{\tau+1}, \mathbf{z}_{\tau+1}, \boldsymbol{\lambda}_\tau\right) = \begin{bmatrix} \mathbf{A} & \mathbf{B} \end{bmatrix} \mathbf{J}\left(F\left(\mathbf{u}_{\tau+1}, \mathbf{z}_{\tau+1}, \boldsymbol{\lambda}_\tau\right)\right)^{-1} \begin{bmatrix} \mathbf{A}^T \\ \mathbf{B}^T \end{bmatrix} \quad (5.52)$$

The following theorem addresses the invertibility of the matrix (5.52).

Theorem 5.2. *If* $\mathbf{J}\left(F\left(\mathbf{u}_{\tau+1}, \mathbf{z}_{\tau+1}, \boldsymbol{\lambda}_\tau\right)\right)$ *is invertible, then* $\mathbf{M}\left(\mathbf{u}_{\tau+1}, \mathbf{z}_{\tau+1}, \boldsymbol{\lambda}_\tau\right)$ *is also invertible.*

Proof. The above result is automatically proven by the LICQ assumption on problem (5.15), which implies that there does not exist any nonzero vector $\boldsymbol{\nu}$ such that $\boldsymbol{\nu}^T \begin{bmatrix} \mathbf{A} & \mathbf{B} \end{bmatrix} = 0$. Then, setting $\mathbf{z} = \boldsymbol{\nu}^T \begin{bmatrix} \mathbf{A} & \mathbf{B} \end{bmatrix}$, the quadratic form associated with (5.52) is the same as for (5.33). Thus, matrices (5.33) and (5.52) share the same properties regarding invertibility. This completes the proof. □

5.3 Application to a case study

In this section, the proposed approach is tested on a case study and the main results are discussed. First, a base scenario with few EVs is conducted to better visualize the results. Then, a scalability analysis is performed on a larger instance to assess how the proposed algorithm performs on larger problems. Finally, a multi-objective analysis is conducted to explore the trade-offs among the different performance indicators and to assess how conflicting objectives interact and compete. All results presented in the following have been retrieved using an AMD Ryzen 7 5800H 3.2 GHz with 16GB RAM.

Table 5.3: EV data - Base Scenario

EV	$Phase$	CS	Socket	$\overline{P}^{CS}$ [kW]	X_0^{EV} [/]	X^{EV*} [/]	CAP^{EV} [kWh]	$\overline{P}^{EV}$ [kW]	c^{EV} [kW]	d^{EV} [kW]	t^{rt} [h]	t^{dl} [h]
1	A	1	1	60.75	0.40	0.8	52	50	-250	250	12.0	14.0
2	A	1	2	60.75	0.50	0.9	42	85	-425	425	8.0	11.0
3	B	2	1	56.25	0.30	0.8	50	75	-375	375	3.0	6.0
4	B	2	2	56.25	0.45	0.9	40	50	-250	250	5.0	7.0
5	C	3	1	49.5	0.35	0.8	40	50	-250	250	11.0	12.0
6	C	3	2	49.5	0.40	0.9	55	60	-300	300	2.0	5.0
7	tri	1 - tri	1	67.5	0.40	0.8	60	100	-500	500	144.0	192.0
8	tri	1 - tri	2	67.5	0.50	0.9	40	50	-250	250	96.0	132.0

5.3.1 Problem data

Here, the main data of the optimization problem are presented. The optimization horizon lasts 24 hours and the time step Δ is set to 15 min. For the base scenario, eight EVs are considered while the sensitivity analysis is conducted on a SPL with an increasing number of EVs to be charged. In order to represent a realistic framework, the EV fleet is composed by vehicles with different characteristics, reported in Table 5.3. As regards the energy buying price, a multi-tariff energy pricing is considered with three slots:

- 00:00 - 07:59 $\longrightarrow$ 0.56 [€/kWh]
- 08:00 - 15:59 $\longrightarrow$ 0.53 [€/kWh]
- 16:00 - 23:59 $\longrightarrow$ 0.54 [€/kWh]

The set of time instants when the DSO requires DR services S^{DR} is set from 12:00 to 14:00, and the reference power value is set to 40 kW in total (i.e., the sum of all phases) for the base scenario.

5.3.2 Optimization Results

This section presents the results concerning the base scenario, in which eight EVs (6 single-phase and 2 three-phase) are considered. The results relevant to the overall power exchange with the grid and the state of charge of the EVs are presented in Figure 5.2 and Figure 5.3, respectively. In Figure 5.3, the blue line represents the dynamics of each EV state of charge, while the desired state of charge is marked in red. From Figure 5.2, it is possible to see how the grid power exchange follows the DR request within S^{DR}. This figure also allows to appreciate that the balance between phases cannot be ensured, despite being included in the objective function, mainly because of the different deadlines of the vehicles charging processes.

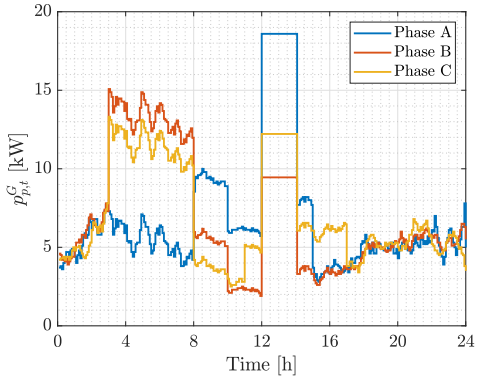

Figure 5.2: Power exchange with the main grid on each phase (Base Scenario)

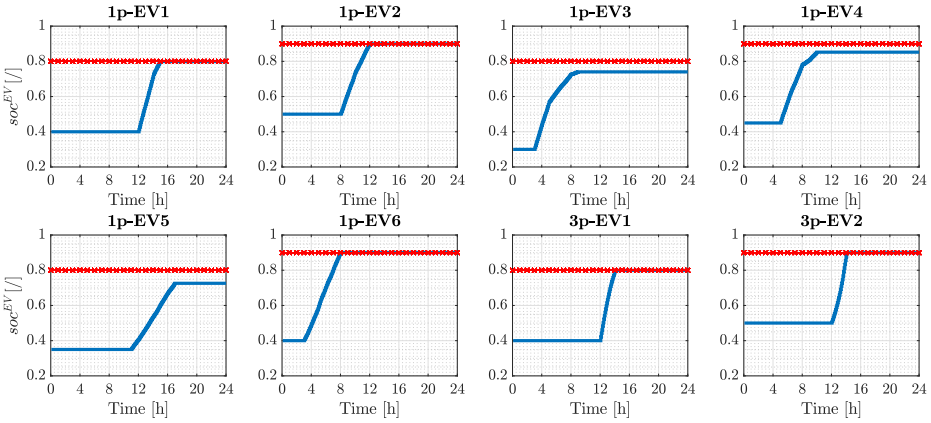

Figure 5.3: EV State of Charge

Table 5.4: Scalability analysis results

[#EVs]	*Single-phase [#EVs]*	*Three-phase [#EVs]*	*Runtime [s]*
8	6	2	0.59
16	10	6	2.14
32	20	12	12.84
40	20	20	25.43

5.3.3 Scalability Analysis

In this section, instances of increasing size (up to 40 EVs) are considered to demonstrate the scalability of the proposed approach. In this case, the data relevant to EVs and CSs are similar to those in Table 5.3. Concerning DR, the reference power value increases to be coherent with the larger power flows in the larger instances.
The results relevant to the runtime in each instance are reported in Table 5.4. The results indicate

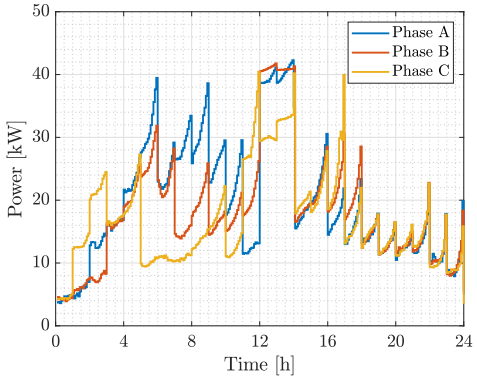

Figure 5.4: Power exchange with the main grid on each phase (Largest Instance)

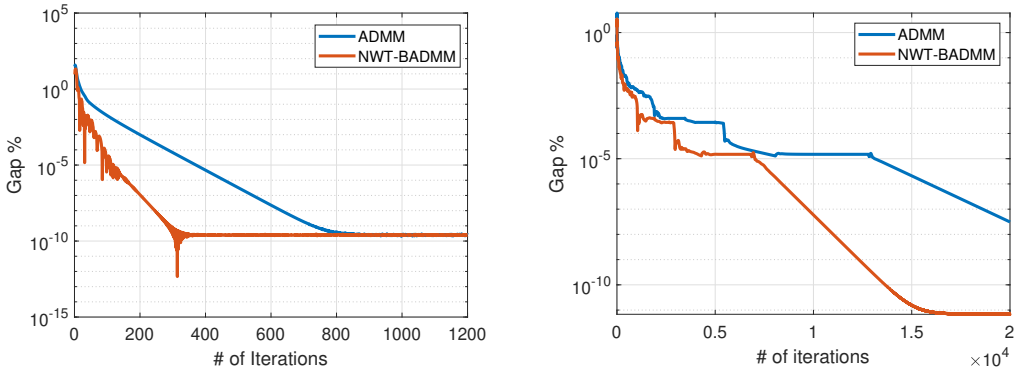

(a) 8 EVs (b) 40 EVs

Figure 5.5: Convergence plot

that the optimal solution can be obtained in a total runtime compatible with online operations, even for larger-size problems. It is relevant to remark that, even for the largest instance, the runtime is much lower than the selected time step, meaning that the designed algorithm allows for the integration of additional grid services and, eventually, REC features. Figure 5.4 depicts the optimal result for the largest instance where the P^{DR} value is 140 kW, still from 12:00 to 14:00. Then, to test the convergence of the proposed algorithm, a comparison with the standard ADMM is provided for the smallest and largest instances in Figure 5.5 *(a)* and *(b)*, respectively. From the results, it is evident that the Nwt-BADMM algorithm needs less than half of the iterations to reach the same precision.

5.3.4 Multi-objective Analysis

In this section, a multi-objective analysis is performed. Unlike single-objective formulations, which provide a unique optimal solution according to a predefined priority, multi-objective opti-

mization explicitly accounts for the coexistence of potentially conflicting goals. By varying the weighting coefficients α_i of the objective functions, a set of optimal solutions is obtained allowing for the analysis of the compromise space among the considered performance criteria.
The two-dimensional Pareto front in Figure 5.6 highlights the trade-off between the most relevant pairs of objectives. Before discussing the results in detail, it should be noted that objectives not explicitly represented in the plots are assigned zero weighting coefficients and are therefore excluded from the optimization in the corresponding scenario. The Pareto front between J_1 and J_3 exhibits a clear monotonically decreasing trend, highlighting the structural conflict between user satisfaction and grid cost minimization: specifically, the slope of the curve reflects the sensitivity of grid cost to incremental improvements in SOC tracking. The steeper portion of the curve near high J_3 values suggests that achieving very small tracking errors requires significant grid costs. The second plot in Figure 5.6 shows a strongly non-linear and convex behavior, revealing a conflict between accurate EV charging and three-phase power balance: achieving very low tracking errors requires disproportionately high phase imbalance, and vice versa. In particular, the knee region of the curve identifies an operational compromise where moderate relaxation of the SOC tracking constraint yields a significant reduction in phase imbalance. The Pareto front between the DR tracking objective J_2 and the grid-related cost J_3 exhibits an approximately linear decreasing trend, indicating a relatively proportional trade-off between the two objectives: incremental improvements in DR tracking result in almost proportional increases in grid cost. This indicates a strong coupling between flexibility provision and local grid constraints. The last plot in Figure 5.6 shows a non-linear decreasing curve, indicating that strict compliance with the DR reference signal may induce phase asymmetries in the three-phase system. The shape of the curve suggests that the conflict between DR compliance and phase balancing is not structurally severe: a small degradation in DR tracking accuracy allows the optimization to redistribute charging power across phases more effectively, substantially improving electrical symmetry.
All the considered objectives are jointly represented in Figure 5.7, where the complete set of combinations of the weighting coefficients α_i is reported; the coefficients are varied with a step of 0.1 under the constraint $\sum_i \alpha_i = 1$, resulting in a total of 286 points. This comprehensive representation allows a general visualization of the multi-objective response surface, complementing the pairwise Pareto analyses discussed above. Please note that in this figure only objectives J_1, J_2 and J_3 are explicitly represented as objectives J_3 and J_4 are strongly correlated and largely driven by the same underlying decision variables. For this reason, plotting both would not provide additional insight into the structure of the multi-objective trade-off.
Finally, the radar plot in Figure 5.8 is another way to represent multiple objectives. In this case, the plotted values correspond to the combinations of the weight coefficients α_i reported in Table 5.5. In this type of representation, the geometry of the polygons clearly highlights the structural conflicts among objectives: highly asymmetric shapes correspond to extreme optimization toward one specific criterion, whereas more compact shapes indicate balanced operational strategies. Four representative α_i combinations have been selected in order to illustrate different compromise solutions within the objective space. In particular, the configuration associated with $\boldsymbol{\alpha} = [0.1, 0.2, 0.2, 0.5]$ results in one of the most compact shapes, indicating a relatively bal-

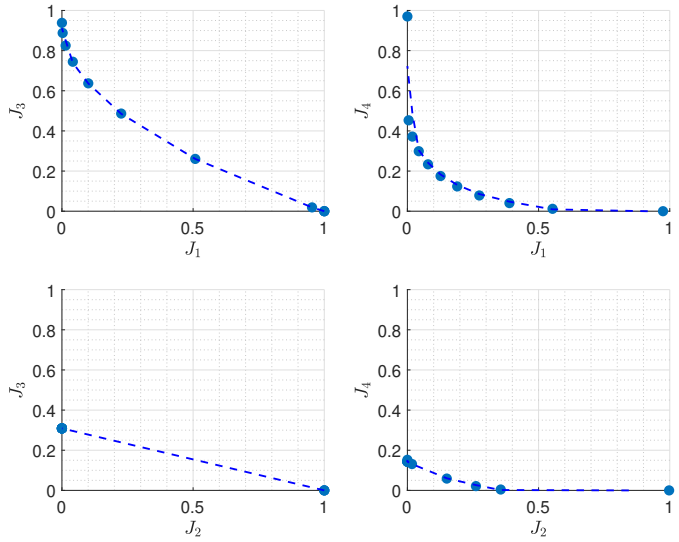

Figure 5.6: Pareto Front for objectives pairs

Table 5.5: Objective values for different α_i combinations

$[\alpha_1, \alpha_2, \alpha_3, \alpha_4]$	J_1	J_2	J_3	J_4
$[0.1, 0.2, 0.2, 0.5]$	0.745492	0.219054	0.265787	0.033643
$[0.1, 0.3, 0.4, 0.2]$	0.805825	3.68E-09	0.308863	0.143798
$[0.2, 0.2, 0.2, 0.4]$	0.410278	0.163897	0.464063	0.078582
$[0.6, 0.1, 0.1, 0.2]$	0.045972	0.12828	0.814565	0.318322

anced trade-off among the four objectives. Conversely, the combination $\boldsymbol{\alpha} = [0.6, 0.1, 0.1, 0.2]$ produces a wider polygon, mainly due to the large value of the grid-related objective J_3, highlighting the strong impact that prioritizing the J_1 objective can have on grid stress. Moreover, the radar representation shows that objectives J_1 and J_3 exhibit the largest variability across the considered weighting configurations, indicating that these performance indicators are the most sensitive to variations in the weighting coefficients compared to the other objectives. In contrast, J_2 remains relatively stable among the different solutions, while J_4 shows a moderate variation.

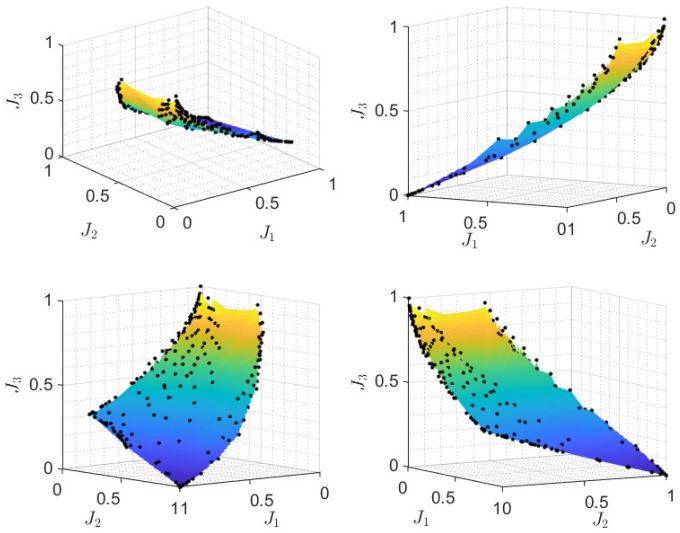

Figure 5.7: Overall Pareto Front

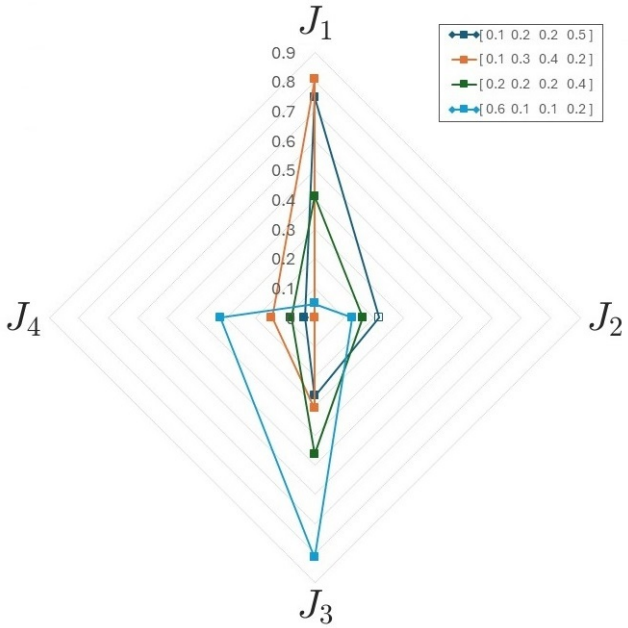

Figure 5.8: Star graph

Chapter 6

Optimal energy scheduling of multi-vector energy hubs with renewables and hydrogen-based components

This chapter focuses on the optimal energy scheduling of a multi-vector energy hub, integrating different energy carriers such as electricity, gas, and hydrogen. With the ongoing electrification of end-use sectors and the increasing complexity of modern infrastructures, energy systems are evolving toward integrated multi-vector configurations; such systems represent flexible yet complex entities within the overall energy grid, capable of significantly influencing local grid operation and energy flows [130]. When properly managed, multi-vector energy hubs can alleviate network congestion and balance renewable generation by coordinating the interaction among the different energy carriers [131]. Moreover, the inherent flexibility provided by the integration of multiple energy vectors can be exploited to enhance the microgrid ability to participate in renewable energy communities; indeed, through coordinated vector conversion and storage management, these systems can offer enhanced local balancing capabilities, increase local self-consumption, and more effectively contribute to the community's shared-energy objectives. Depending on the configuration, a multi-vector energy hub can either join an existing REC as an active participant or constitute a REC itself, aggregating various users and technologies under a unified management system. Within this framework, the hub manager/controller can also assume the role of ECM and coordinate the operation of distributed energy resources, storage systems, and conversion units to maximize shared energy and collective economic benefits.
The optimization problem presented in this chapter addresses the multi-energy dispatch problem for such systems, extending classical formulations to account for multi-vector efficient integration and coupled operational constraints. Moreover, it includes constraints on temperature ramp rates to limit component degradation. As concerns the solution method, the classical Augmented Lagrangian Method is enhanced with a switching matrix, which enables computationally efficient optimization by activating penalties only for binding constraints.

Polygenerative microgrids represent one of the most effective implementations of multi-vector energy systems, offering distributed renewable-powered generation, energy and thermal storage, and flexible demand management [132], [133]. Within multi-vector energy hubs, hydrogen is gaining significant attention as a complementary energy vector, especially in the form of green hydrogen, which enables deep carbonization [134], seasonal storage [135], and enhanced operational flexibility [136]. This growing interest has led to an increase of recent studies integrating electrolyzers, fuel cells and hydrogen storage into microgrid architectures. While several studies have explored hydrogen integration in multi-vector energy systems [137], most neglect detailed operational constraints critical to component longevity. For example, [138] studied hydrogen storage management in isolated microgrids using demand response strategies; the overall problem is decomposed into a master-slave structure in which the slave problem is kept fully linear and thus exchangeable by its Karush Kuhn Tucker conditions. In [139], authors developed a risk-constrained energy management model based on information gap decision theory to handle uncertainties in hydrogen systems; the resulting problem is a mixed integer nonlinear programming model, which is converted into a MILP model to ensure global optimality. The scheduling problem in [140] optimally manages a microgrid integrated with EV charging stations, an electrolyzer, and a hydrogen refueling station; the optimal solution, which aims to increase self-

consumption and the degree of autonomy of the microgrid, provides the optimal scheduling for hydrogen production and storage, which also enhances the use of local generation resources. The EMS proposed in [141] incorporates a hybrid hydrogen-battery energy storage system; to address the heterogeneous storage coordination, the developed model considers the characteristics of both short-term and long-term storage technologies. A hybrid hydrogen-battery energy storage is considered also in [142], where a two-stage optimization framework is developed: the offline stage generates the annual SoC reference for hydrogen storage, which are tracked in the online convex optimization problem. The work in [143] proposes a data-driven methodology for the coordinated operation of multi-energy microgrids, integrating electricity, natural gas, green hydrogen and thermal networks, with a focus on congestion management and secure resource optimization. Electricity, hydrogen and thermal systems are coordinated within a residential multi-energy microgrid, which is optimally controlled in [144] with a fuzzy-logic control method; the EMS, designed to dynamically manage the operational states of thermal sources in real-time, is evaluated through simulations and hardware-in-the-loop testing and the results show that the microgrid is capable of operating autonomously with effective storage coordination and accurate thermal regulation. A green hydrogen-based energy storage is designed in [145] as a service mode: the operator manages the system and allows microgrids to access the storage devices, while generating revenue through electricity and hydrogen trading; to ensure fair benefit distribution, the Nash bargaining method is exploited. In [146], the operating cost of a multi-energy microgrid and carbon emissions are minimized, while fully utilizing the electrolyzer potential integrating the water network to realize interdependence; McCormick envelope technique is utilized to manage the non-linear constraints and obtain a MILP problem solved using CPLEX. Authors in [147] propose an off-grid integrated electricity-hydrogen system in which all the needed energy is supplied by solar and hydroelectric renewable resources.
Notably, none of these works explicitly enforce operational temperature constraints, which are essential for preventing accelerated degradation of electrolyzers and fuel cells. In this context, the originality of this work lies in the detailed modeling of a hydrogen-based multi-vector energy hub with strict operational constraints on hydrogen components. The model explicitly includes bounds on the operating temperatures of both the electrolyzer and fuel cell, capturing the influence of thermal dynamics on component aging and system-level economics. This representation enables evaluation of trade-offs between operational efficiency and longevity, providing a robust and realistic framework for microgrid scheduling.

Modeling the interdependency among different energy carriers makes the optimal management problem more accurate and reliable; however, because of the tight coupling among multiple energy carriers, optimization problems for polygenerative or multi-vector systems become highly complex; as a result, high-performance mathematical models and computationally efficient solution algorithms are required to enable real-time or large-scale applications [148], [149]. The proposed framework adopts an Augmented Lagrangian Method (ALM) enhanced with a switching matrix to solve the resulting optimization problem. ALM-based techniques have been successfully applied in previous studies to manage complex energy systems. For instance, authors in [150] applied ALM to networked microgrids, achieving efficient decomposition into local sub-

Table 6.1: Comparison with state of the art works and their features

	Energy carrier			**H_2 safe operational limits**	**Solution method**
	Electricity	Gas	Hydrogen		
[138]	✓		✓		Constraint-and-Column Generation Algorithm
[139]	✓	✓	✓		CPLEX
[140]	✓		✓		Genetic Algorithm
[141]	✓		✓		Deep-reinforcement-learning algorithm
[142]	✓		✓		Adaptive virtual-queue-based OCO algorithm
[143]	✓	✓	✓		Reinforcement learning-based
[144]	✓	✓	✓		Fuzzy Logic EMS
[145]	✓	✓	✓		Nash bargaining-based
[146]	✓		✓		CPLEX
[147]	✓	✓	✓		CPLEX
This work	✓	✓	✓	✓	Augmented Lagrangian

problems with global consistency. In [151], authors used a Lagrange multiplier-based approach for real-time economic dispatch of microgrids comprising RES and battery ESS; inequality constraints are transformed into the corresponding equality constraints, allowing to achieve the solution analytically. Authors in [152] propose a distributed optimization method with weighted gradients, which can be applied to solve the economic dispatch problem of single microgrids or of multi-microgrid systems. Authors in [153] implemented bi-level distributed optimization for interconnected microgrids; ALM is incorporated to establish a fair price mechanism for the energy exchange and the marginal prices, represented by the optimal Lagrange multipliers, are obtained through parallel iteration. A bi-level model is also adopted in [154] to achieve coordination between the EV aggregators and the DSO, which is solve with an augmented Lagrangian-based safe DRL method. The optimal power allocation is achieved in [155] for DC microgrid with a novel distributed fixed-time control system. A distributed optimization algorithm is proposed in [156] for the day-ahead optimal scheduling of a virtual power plant; by temporally decoupling the charging and discharging model of the ESS, a distributed optimization algorithm is proposed for solving the large-scale optimization problem. The spatial-temporal interaction of multi-microgrids and the urban transportation system (coupled via fast charging stations) is investigated in [157], where a privacy-preserving multi-agent based optimal scheduling and trading scheme is adopted to allow each agent to independently determine its own operational schedule based on peer-to-peer communication.

The present work extends the conducted literature from both a modeling and a methodology point of view. From a modeling perspective, a tri-vector microgrid is modeled including electricity, syngas and hydrogen flows; several components are considered such as renewable generators, microturbines, energy storage systems, thermal boilers, and a hydrogen system comprising an electrolyzer, a fuel cell, a storage tank, and hydrogen fuel cell vehicles (HFCVs). The model accounts for the cogeneration capability of microturbines and fuel cells enabling simultaneous electricity and heat production, while gas boilers and microturbines are fueled by a hy-

drogen–methane blend, with an upper limit on the hydrogen share to reflect technical and safety constraints. The modeling novelty lies in the implementation of manufacturer-recommended operational limits, including temperature bounds and ramp rates, to preserve hydrogen system longevity while maintaining operational efficiency. From a methodology perspective, the linearized formulation of the overall problem is solved using the designed ALM algorithm. The methodological novelty instead lies in enhancing the algorithm with a switching matrix that applies penalties only to active constraints, ensuring computational efficiency while preserving fidelity of thermo-electro-chemical couplings.
Summarizing, the main contributions of this chapter are:

- A detailed modelling of a hydrogen-based multi-vector energy hub that integrates electricity, heat, and hydrogen flows, with a realistic representation of component interactions and thermal dynamics, with implementation on a real case study.
- Direct incorporation of manufacturer-recommended operational limits, including temperature bounds and ramp rates, to preserve hydrogen system longevity while maintaining operational efficiency.
- Development and application of an enhanced ALM with a switching matrix, which enables computationally efficient optimization of the multi-vector system by activating penalties only for binding constraints.

6.1 Decision problem definition

This section describes the optimization problem of the considered tri-vector energy hub, depicted in Figure 6.1. Energy flows among components are optimized under physical and operational constraints, whereas the final goal is to ensure an efficient and sustainable energy supply that meets electrical, thermal, and hydrogen demands while minimizing operational costs and CO_2 emissions.

Before starting to define the overall problem, Table 6.2 reports problem variables and parameters. Moreover, in the formalization that follows, upper and lower bounds are not explicitly defined as they are well recognizable from notation: they are characterized by an upper bar ($\bar{\cdot}$) and lower bar ($\underline{\cdot}$), respectively. For a clearer reading, the objective function is firstly introduced, then all constraints are presented divided by component.

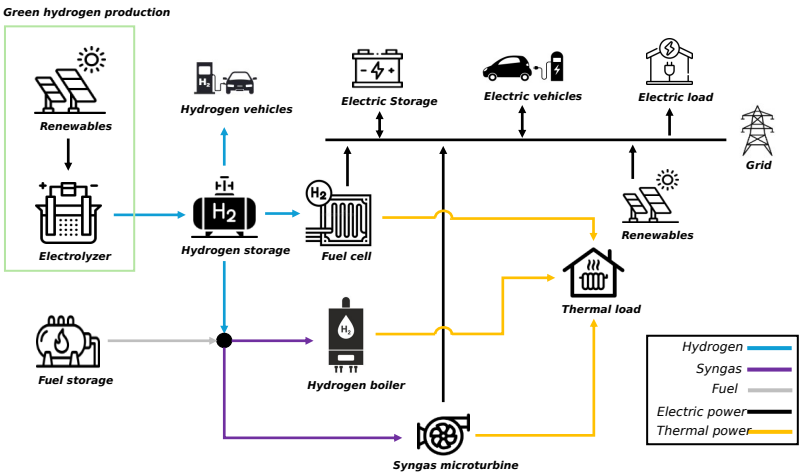

Figure 6.1: The studied energy hub with multiple components

Table 6.2: Nomenclature

Symbol	Unit	Description
Sets		
$S^T = \{1, \ldots, T\}$		Set of time instants
$S^R = \{1, \ldots, R\}$		Set of RES production plants
$S^S = \{1, \ldots, S\}$		Set of electric storage systems
$S^M = \{1, \ldots, M\}$		Set of syngas microturbines
$S^B = \{1, \ldots, B\}$		Set of syngas boilers
$S^F = \{1, \ldots, F\}$		Set of hydrogen fuel cell vehicles
$S^E = \{1, \ldots, E\}$		Set of electric vehicles
Variables		
p_t^G	[kW]	Power exchange with the grid at time t
$p_t^{G,in}$	[kW]	Grid power withdrawal
$p_t^{G,out}$	[kW]	Grid power injection
$p_{s,t}^S$	[kW]	Power exchange with the storage system s at time t
$p_{s,t}^{S,ch}$	[kW]	Charging power of ESS s
$p_{s,t}^{S,dch}$	[kW]	Discharging power of ESS s
$x_{s,t}^S$	[/]	State of charge of ESS s
$p_t^{el,FC}$	[kW]	Electric power produced by fuel cell
$p_t^{th,FC}$	[kW]	Thermal power produced by fuel cell (cogeneration)
p_t^{EZ}	[kW]	Electric power consumed by the electrolyzer
m_t^{EZ}	[kg]	Hydrogen mass produced by electrolyzer
m_t^{FC}	[kg]	Hydrogen mass consumed by fuel cell

Symbol	Unit	Description
δp_t^{EZ}, δp_t^{FC}	[kW]	EZ and FC power variations between t-1 and t
δT_t^{EZ}, δT_t^{FC}	[°C]	EZ and FC temperature deviations
$x_t^{H_2}$	[/]	Hydrogen tank level
$p_{m,t}^{el,\mu GT}$	[kW]	Electric power produced by microturbine m
$p_{m,t}^{th,\mu GT}$	[kW]	Thermal power produced by microturbine m
$m_{m,t}^{H_2,\mu GT}$	[kg]	H_2 mass feeding microturbine m
$m_{m,t}^{CH_4,\mu GT}$	[kg]	CH_4 mass to microturbine m
$m_{b,t}^{\mu GT}$	[kg]	Total fuel consumption of microturbine m at time t
$p_{b,t}^{boil}$	[kW]	Thermal power produced by boiler b
$m_{b,t}^{H_2,boil}$	[kg]	H_2 mass feeding boiler b
$m_{b,t}^{CH_4,boil}$	[kg]	CH_4 mass to boiler b
$m_{b,t}^{boil}$	[kg]	Total fuel consumption of hydrogen boiler b at time t
$m_t^{CH_4}$	[kg]	Total methane consumption (system-wide)
$m_{f,t}^{HFCV}$	[kg]	H_2 mass charged into HFCV vehicle f
$x_{f,t}^{HFCV}$	[/]	Tank level of HFCV vehicle f
$p_{e,t}^{EV}$	[kW]	Charging power of EV e
$x_{e,t}^{EV}$	[/]	State of charge of EV e
Parameters		
Δ	[h]	Time step
C_t^{buy}	[€/kWh]	Electricity purchasing price
C_t^{sell}	[€/kWh]	Electricity selling price
α_k	[/]	Weights of multi-objective terms
$P_{r,t}^{PV}$	[kW]	Power production from RES plant r at time t
$P_t^{el,L}$	[kW]	Electric load demand
$P_t^{th,L}$	[kW]	Thermal load demand
$\overline{P}^G$	[kW]	Maximum power exchange with the main grid
CAP_s^S	[kWh]	Capacity of storage system s
$\Gamma_s^{S,ch}$	[/]	Charging efficiency of storage system s
$\Gamma_s^{S,dch}$	[/]	Discharging efficiency of storage system s
$\overline{P}_s^S$	[kW]	Maximum power exchange with ESS s
$\underline{X}_s^S$, $\overline{X}_s^S$	[/]	Minimum/Maximum ESS state of charge
Γ^{EZ}	[/]	Electrolyzer efficiency
Γ^{FC}	[/]	Fuel cell efficiency
Φ^{FC}	[/]	FC heat-to-electricity coefficient
$\overline{P}^{EZ}$, $\overline{P}^{FC}$	[kW]	Maximum power consumed/produced by EZ / FC
$\overline{M}^{EZ}$, $\overline{M}^{FC}$	[kg]	Maximum hydrogen mass produced/consumed by EZ / FC

Symbol	Unit	Description
$\overline{P}^{th,FC}$	[kW]	Maximum thermal power produced by the FC
Υ^{EZ}, Υ^{FC}	[°C/kW]	Temperature–power coefficients for EZ and FC
$\underline{\Delta T}^{EZ}$, $\overline{\Delta T}^{EZ}$	[°C]	Safety temperature operating range for EZ
$\underline{\Delta T}^{FC}$, $\overline{\Delta T}^{FC}$	[°C]	Safety temperature operating range for FC
Σ^{H_2}	[/]	Hydrogen tank leakage factor
CAP^{H_2}	[kg]	Hydrogen tank capacity
$\underline{X}_t^{H_2}$, $\overline{X}_t^{H_2}$	[/]	Minimum/Maximum H_2 tank level
LHV^{H_2}	[kWh/kg]	H_2 lower heating value
LHV^{CH_4}	[kWh/kg]	CH_4 lower heating value
$\Gamma_m^{\mu GT}$	[/]	Microturbine efficiency
$\Phi_m^{\mu GT}$	[/]	Microturbine heat-to-electricity ratio
$\Theta_m^{\mu GT}$	[/]	Max allowed H_2/CH_4 ratio for microturbine m
$\overline{P}_m^{el,\mu GT}$	[kW]	Maximum microturbine electric power
$\overline{P}_m^{th,\mu GT}$	[kW]	Maximum microturbine thermal power
$\overline{M}_b^{\mu GT}$	[kg]	Maximum fuel mass that can be feed in the microturbine
Γ_b^{boil}	[/]	Boiler efficiency
Θ_b^{boil}	[/]	Max allowed H_2/CH_4 ratio for boiler b
$\overline{P}_b^{boil}$	[kW]	Maximum boiler thermal power
$\overline{M}_b^{boil}$	[kg]	Maximim fuel mass that can be feed in the hydrogen boiler
CAP_f^{HFCV}	[kg]	Tank capacity of HFCV vehicle f
$\overline{M}_f^{HFCV}$	[kg]	Maximum charging H_2 mass for HFCV f
$\underline{X}_f^{HFCV}$, $\overline{X}_f^{HFCV}$	[/]	Minimum/Maximum storage level for HFCV f
X_f^{HFCV*}	[/]	Desired final H_2 level for HFCV f
T_f^{HFCV*}	[h]	Deadline to reach the desired final tank level for HFCV f
Γ_e^{EV}	[/]	EV charging efficiency
CAP_e^{EV}	[kWh]	EV battery capacity
$\overline{P}_e^{EV}$	[kW]	Maximum charging power of EV e
$\underline{X}_e^{EV}$,$\overline{X}_e^{EV}$	[/]	Minimum/Maximum EV state of charge
X_e^{EV*}	[/]	Desired final SoC EV e
T_e^{EV*}	[h]	Deadline to reach the desired final SoC level for EV e

6.1.1 Objective function

The proposed formulation takes into account a multiobjective formulation with two terms. In particular, operational costs (J^1) and CO_2 emissions (J^2) are minimized. Operational costs are

given by exchanging power with the main grid and fuel cost, while CO_2 emissions are calculated based on emission factors for grid power, and microturbine and boiler fuel usage. Moreover, the environmental benefit associated with the use of innovative and alternative energy sources is also considered. Therefore, it is possible to write the objective function as follows

$$\min f(x) = \alpha_1 J^1 + \alpha_2 J^2 \tag{6.1}$$

where

$$J^1 = \min \sum_{t \in S^T} \left\{ \left(C_t^{buy} p_t^{G,in} - C_t^{sell} p_t^{G,out} \right) \Delta + C_t^{CH4} m_t^{CH_4} \right\} \tag{6.2}$$

$$J^2 = \min \sum_{t \in S^T} \left\{ C^{\mathrm{CO_2}} \left[F^G p_t^{G,in} + F^{\mu GT} \sum_{m \in S^M} p_{m,t}^{el,\mu GT} \right] - \sum_{i \in \{fc, H_2 boil, PV\}} \left(S^i + E^i \right) p_t^i \right\} \tag{6.3}$$

In equation (6.2), C_t^{buy} and C_t^{sell} [€/kWh] are the electricity buying and selling price respectively, whereas C_t^{CH4} [€/kg] is the fuel cost. In equation (6.3), $C^{CO_2}[€/t_{CO_2}]$ is the CO_2 unit cost, F^G and $F^{\mu GT}[€/t_{CO_2}]$ are emission factors. Then, S^i, E^i [€/kW] are cost savings and environmental benefits for system i.

6.1.2 Constraints

The problem analyzed in this chapter models several components, each of them characterized by specific constraints. For a better understanding and smoother reading, each of the following paragraphs is dedicated to one specific component and its constraints.

6.1.2.1 The electric power balance

The power balance ensures that the total power generated by the microgrid components equals the total load demand. The general electric power balance equation is given by

$$\sum_{m \in S^M} p_{m,t}^{el,\mu GT} + \sum_{r \in S^R} P_{r,t}^{PV} + \sum_{s \in S^S} p_{s,t}^{S} + p_t^{el,FC} + p_t^G = P_t^{el,L} + p_t^{EZ} + \sum_{e \in S^E} p_{e,t}^{EV} \quad t \in S^T \tag{6.4}$$

$$p_t^G = P_t^{G,in} - p_t^{G,out} \quad t \in S^T \tag{6.5}$$

$$0 \leq p_t^{G,in} \leq \overline{P}^G \quad t \in S^T \tag{6.6}$$

$$0 \leq p_t^{G,out} \leq \overline{P}^G \quad t \in S^T \tag{6.7}$$

Power generation is given by the contribution of all microturbines ($p_{m,t}^{el,\mu GT}$), all photovoltaic units ($P_{r,t}^{PV}$), all energy storage systems ($p_{s,t}^{S}$), the fuel cell ($p_t^{el,FC}$) and the power exchanged

with the main grid (p_t^G). On the right side of equation (6.3), the electric load demand ($P_t^{el,L}$), the power consumed by the electrolyzer (p_t^{EZ}) and the charging power of all electric vehicles ($p_{e,t}^{EV}$) represent the power consumption. In (6.5), the power exchange with the grid is defined as the difference between the power imported from ($p_t^{G,in}$) and exported to ($p_t^{G,out}$) the grid. Then, the overall power exchange with the grid is constrained in (6.6) and (6.7).

6.1.2.2 The thermal power balance

The thermal power balance ensures that the thermal load is satisfied at any time. For this to happen, the thermal power generated by all system components able to produce some thermal power (boilers, microturbines and fuel cell) must be greater than or equal to the thermal load at each time step. The general thermal power balance equation is given by

$$\sum_{b \in S^B} p_{b,t}^{boil} + \sum_{m \in S^M} p_{m,t}^{th,\mu GT} + p_t^{th,FC} \geq P_t^{th,L} \quad t \in S^T \tag{6.8}$$

where $p_{b,t}^{boil}$ is the thermal power produced by the hydrogen boiler b, and $p_{m,t}^{th,\mu GT}$ and $p_t^{th,FC}$ are the thermal power produced thanks to the cogenerative capacity of microturbines and fuel cell, respectively. On the right side of equation (6.8), $P_t^{th,L}$ is the thermal load demand at time t.

6.1.2.3 The electric storage systems

The constraints relevant to the energy storage system are here described. The electric storage system allows to store (charging) and release (discharging) energy according to the ESS state of charge and depending on electricity prices, giving the system greater flexibility.

$$x_{s,t+1}^S = x_{s,t}^S + \frac{\Delta}{CAP_s^S}\left(\Gamma_s^{S,ch} p_{s,t}^{S,ch} - \frac{1}{\Gamma_s^{S,dch}} p_{s,t}^{S,dch}\right) \quad s \in S^S, t \in S^T \tag{6.9}$$

$$p_{s,t}^S = p_{s,t}^{S,dch} - p_{s,t}^{S,ch} \quad s \in S^S, t \in S^T \tag{6.10}$$

$$0 \leq p_{s,t}^{S,ch} \leq \overline{P}_s^S \quad s \in S^S, t \in S^T \tag{6.11}$$

$$0 \leq p_{s,t}^{S,dch} \leq \overline{P}_s^S \quad s \in S^S, t \in S^T \tag{6.12}$$

$$\underline{X}_s^S \leq x_{s,t}^S \leq \overline{X}_s^S \quad s \in S^S, t \in S^T \tag{6.13}$$

Equation (6.9) is the dynamic equation of each ESS $s \in S^S$, where $x_{s,t}^S$ is its state of charge, CAP_s^S its capacity, $\Gamma_s^{S,ch}$ and $\Gamma_s^{S,dch}$ its charging and discharging efficiencies, respectively. In (6.10), the power exchanged with the electric storage is split into charging ($p_{s,t}^{S,ch}$) and discharging ($p_{s,t}^{S,dch}$) power, which are bounded in (6.11) and (6.12), respectively. Lastly, the storage state of charge is constrained in (6.13).

6.1.2.4 The hydrogen system

The hydrogen system includes several components: an electrolyzer, a fuel cell and a hydrogen tank. The hydrogen tank is modeled as a storage system, while electrolyzer and fuel cell are modeled with their respective efficiency, power and mass flow constraints. The possibility of recovering heat from the fuel cell, thanks to the highly exothermic electrochemical reactions that take place inside it, is taken into consideration and therefore the cogenerative capacity of the fuel cell is modeled. Moreover, some constraints are implemented to keep electrolyzer and fuel cell temperature variations within manufacturer-prescribed operating range and to ensure safe operations. Indeed, when transitioning between different power levels, electrolyzers and fuel cells exhibit significant temperature fluctuations [158], that need to be controlled to stay within safe operating limits as recommended by manufacturers [159, 160].

$$m_t^{EZ} = \frac{\Gamma^{EZ} p_t^{EZ}}{LHV^{H_2}} \quad t \in S^T \tag{6.14}$$

$$m_t^{FC} = \frac{p_t^{el,FC}}{\Gamma^{FC} LHV^{H_2}} \quad t \in S^T \tag{6.15}$$

$$0 \leq m_t^{EZ} \leq \overline{M}^{EZ} \quad t \in S^T \tag{6.16}$$

$$0 \leq p_t^{EZ} \leq \overline{P}^{EZ} \quad t \in S^T \tag{6.17}$$

$$0 \leq m_t^{FC} \leq \overline{M}^{FC} \quad t \in S^T \tag{6.18}$$

$$0 \leq p_t^{FC} \leq \overline{P}^{FC} \quad t \in S^T \tag{6.19}$$

$$p_t^{th,FC} = \Phi^{FC} p_t^{el,FC} \quad t \in S^T \tag{6.20}$$

$$0 \leq p_t^{th,FC} \leq \overline{P}th, FC, \; t \in S^T \tag{6.21}$$

$$\delta T_t^{EZ} = \Upsilon^{EZ} \delta p_t^{EZ} \quad t \in S^T \tag{6.22}$$

$$\delta T_t^{FC} = \Upsilon^{FC} \delta p_t^{FC} \quad t \in S^T \tag{6.23}$$

$$\delta p_t^{EZ} = p_t^{EZ} - p_{t-1}^{EZ} \quad t \in S^T \tag{6.24}$$

$$\delta p_t^{FC} = p_t^{FC} - p_{t-1}^{FC} \quad t \in S^T \tag{6.25}$$

$$\underline{\Delta T}^{EZ} \leq \delta T_t^{EZ} \leq \overline{\Delta T}^{EZ} \quad t \in S^T \tag{6.26}$$

$$\underline{\Delta T}^{FC} \leq \delta T_t^{FC} \leq \overline{\Delta T}^{FC} \quad t \in S^T \tag{6.27}$$

$$x_{t+1}^{H_2} = \Sigma^{H_2} x_t^{H_2} + \frac{\Delta}{CAP^{H_2}} \left(m_t^{EZ} - m_t^{FC} - \sum_{f \in S^F} m_{f,t}^{HFCV} - \sum_{m \in S^M} m_{m,t}^{H_2,\mu GT} - \sum_{b \in S^B} m_{b,t}^{H_2,boil} \right) t \in S^T \tag{6.28}$$

$$\underline{X}^{H_2} \leq x_t^{H_2} \leq \overline{X}^{H_2} \quad t \in S^T \tag{6.29}$$

The mass of hydrogen produced/consumed by electrolyzer/fuel cell are defined in (6.14) and (6.15), respectively. In these equations, Γ^{EZ} is the electrolyzer efficiency, Γ^{FC} is the fuel cell efficiency, and LHV^{H_2} is the hydrogen lower heating value. Recalling the operations of these devices, p_t^{EZ} is the power consumed by the electrolyzer at time t, while p_t^{FC} is the electric power produced by the fuel cell. Masses and powers are bounded in (6.16)-(6.19). While generating electric power, the fuel cell can also produce thermal power acting as a cogenerator. The relation between electric and thermal power can be modeled by a linear coefficient Φ^{FC} as in (6.20). The temperature deviations that electrolyzers and fuel cells experience when moving from one power level to another can be modeled as proportional to the changes in power between two consecutive operations, as shown in equations (6.21) and (6.22), where Υ^{EZ} and Υ^{FC} are proper coefficients relating temperature and power variations. These power variations δp_t are computed as the difference between the power at the current time step t and the power at the previous time step t-1, for both the electrolyzer (6.24) and fuel cell (6.25). To ensure that the temperature deviation stays within the manufacturer-prescribed safe operating range, constraints (6.26) and (6.27) are introduced. Finally, the dynamic equation of the hydrogen tank is given by (6.28), where $x_t^{H_2}$ is the hydrogen storage level in the tank at time t, Σ^{H_2} is the hydrogen storage leakage factor (to be considered as hydrogen is an extremely volatile gas), and CAP^{H_2} is the storage capacity. Regarding inlet and outlet contributions, in addition to the hydrogen mass produced by the electrolyzer and consumed by the fuel cell, $m_{f,t}^{HFCV}$ is the mass of hydrogen charged into fuel cell vehicle f, $m_{m,t}^{H_2,\mu GT}$ is the hydrogen consumed by microturbine m, and $m_{b,t}^{H_2,boil}$ is the hydrogen consumed by boiler b. The hydrogen storage level is also subject to upper and lower bounds specified by the manufacturer to ensure that the system operates within safe limits (6.29).

6.1.2.5 Syngas microturbines

The microturbines considered in this problem are assumed to operate with a mixture of hydrogen (H_2) and methane (CH_4) to produce both electrical and thermal power (cogeneration). The model includes mass balance for fuel consumption, power production efficiency, and microturbines operational limits.

$$p_{m,t}^{el,\mu GT} = \Gamma_m^{\mu GT}\Big(m_{m,t}^{H_2,\mu GT} LHV^{H_2} + m_{m,t}^{CH_4,\mu GT} LHV_{CH_4}\Big) \quad m \in S^M,\ t \in S^T \tag{6.30}$$

$$0 \leq P_{m,t}^{el,\mu GT} \leq \overline{P}_m^{el,\mu GT} \quad m \in S^M,\ t \in S^T \tag{6.31}$$

$$p_{m,t}^{th,\mu GT} = \Phi_m^{\mu GT} p_{m,t}^{el,\mu GT} \quad m \in S^M,\ t \in S^T \tag{6.32}$$

$$0 \leq p_{m,t}^{th,\mu GT} \leq \overline{P}_m^{th,\mu GT} \quad m \in S^M,\ t \in S^T \tag{6.33}$$

$$m_{m,t}^{H_2,\mu GT} \leq \Theta_m^{\mu GT}\, m_{m,t}^{CH_4,\mu GT} \quad m \in S^M,\ t \in S^T \tag{6.34}$$

$$m_{b,t}^{\mu GT} = m_{b,t}^{H_2,\mu GT} + m_{b,t}^{CH_4,\mu GT} \quad b \in S^B,\ t \in S^T \tag{6.35}$$

$$0 \leq m_{b,t}^{\mu GT} \leq \overline{M}_{b}^{\mu GT} \quad b \in S^B, t \in S^T \tag{6.36}$$

The electrical power produced by microturbine m at time t is defined in (6.30), where $m_{m,t}^{CH_4,\mu GT}$ and $m_{m,t}^{H_2,\mu GT}$ are the masses of methane and hydrogen feeding the microturbine, respectively. In this equation, $\Gamma_{m}^{\mu GT}$ is the microturbine efficiency, and LHV^{CH_4} and LHV^{H_2} are the lower heating values of methane and hydrogen, respectively. The electrical power produced by this device is upper and lower bounded in (6.31). Since exhaust gasses leave the turbine at a significant temperature, this thermal power can be recovered with cogenerative techniques. The thermal power output of the microturbine is modeled as proportional to the electrical power through a heat-to-electricity ratio coefficient $\Phi_{m}^{\mu GT}$ in (6.32) and is bounded in (6.33). To ensure safe operation and account for hydrogen-related technical limits, the hydrogen-to-methane ratio is constrained in (6.34), where $\Theta_{m}^{\mu GT}$ is the maximum hydrogen fraction, relative to methane, that is allowed to feed the microturbine. The total fuel consumption of microturbine m at time t is calculated in (6.35) and bounded in (6.36).

6.1.2.6 Hydrogen boilers

The hydrogen boilers considered in this problem are assumed to consume a mixture of hydrogen and methane for thermal energy production.

$$p_{b,t}^{boil} = \Gamma_{b}^{boil}\left(m_{b,t}^{H_2,boil} LHV^{H_2} + m_{b,t}^{CH_4,boil} LHV^{CH_4}\right) \quad b \in S^B,\ t \in S^T \tag{6.37}$$

$$m_{b,t}^{H_2,boil} \leq \Theta_{b}^{boil} m_{b,t}^{CH_4,boil} \quad b \in S^B, t \in S^T \tag{6.38}$$

$$0 \leq p_{b,t}^{boil} \leq \overline{P}_{b}^{boil} \quad b \in S^B, t \in S^T \tag{6.39}$$

$$m_{b,t}^{boil} = m_{b,t}^{H_2,boil} + m_{b,t}^{CH_4,boil} \quad b \in S^B,\ t \in S^T \tag{6.40}$$

$$0 \leq m_{b,t}^{boil} \leq \overline{M}_{b}^{boil} \quad b \in S^B, t \in S^T \tag{6.41}$$

$$m_{t}^{CH_4} = m_{t}^{CH_4,\mu GT} + m_{t}^{CH_4,boil} \quad t \in S^T \tag{6.42}$$

The thermal power produced by each boiler is a function of the amount of consumed fuel and its lower heating value, considering that two different gases are burnt in the boiler (6.37). Equation (6.38) constrains the hydrogen-to-methane ratio of the fuel mixture, though coefficient Θ_{b}^{boil}. The thermal power output from the hydrogen boiler is bounded in (6.39). Equation (6.40) determines the total fuel consumption of hydrogen boiler b at time t as the sum of the mass of hydrogen and methane consumed. The boiler fuel consumption is bounded in (6.41). Finally, the overall methane consumption of the system is calculated in (6.42).

6.1.2.7 Hydrogen vehicles

The considered system includes hydrogen electric vehicles, which consume hydrogen as fuel and need their tank to be recharged.

$$x_{f,t+1}^{HFCV} = x_{f,t}^{HFCV} + \frac{\Delta}{CAP_f^{HFCV}} m_{f,t}^{HFCV} \quad f \in S^F, t \in S^T \tag{6.43}$$

$$\underline{X}_f^{HFCV} \leq x_{f,t}^{HFCV} \leq \overline{X}_f^{HFCV} \quad f \in S^F, t \in S^T \tag{6.44}$$

$$\underline{M}_f^{HFCV} \leq m_{f,t}^{HFCV} \leq \overline{M}_f^{HFCV}, f \in S^F, t \in S^T \tag{6.45}$$

$$x_{f,t}^{HFCV} = X_f^{HFCV*} \quad f \in S^F, t \geq T_f^{HFCV*} \tag{6.46}$$

The hydrogen storage level of HFCV vehicle f is defined by the dynamic equation in (6.43), where CAP_f^{HFCV} is the storage capacity, and $m_{f,t}^{HFCV}$ is the mass of hydrogen charged into the vehicle. Hydrogen tank levels and charging hydrogen mass are bounded in (6.44) and (6.45), respectively. Finally, each HFCV vehicle is required to reach a target storage level X_f^{HFCV*} by time T_f^{HFCV*} (6.46).

6.1.2.8 Electric vehicles

In addition to HFCVs, the system also considers electric vehicles that arrive at the energy hub needing to be charged.

$$x_{e,t+1}^{EV} = x_{e,t}^{EV} + \frac{\Delta}{CAP_e^{EV}} \Gamma_e^{EV} p_{e,t}^{EV} \quad e \in S^E,\ t \in S^T \tag{6.47}$$

$$0 \leq p_{e,t}^{EV} \leq \overline{P}_e^{EV} \quad e \in S^E, t \in S^T \tag{6.48}$$

$$\underline{X}_e^{EV} \leq x_{e,t}^{EV} \leq \overline{X}_e^{EV} \quad e \in S^E, t \in S^T \tag{6.49}$$

$$x_{e,t}^{EV} = X_e^{EV*} \quad e \in S^E, t \geq T^{EV*} \tag{6.50}$$

The dynamic equation of the battery of each EV is given in equation (6.47), where $p_{e,t}^{EV}$ is the charging power, Γ_e^{EV} is the charging efficiency, and CAP_e^{EV} is the battery capacity. EV charging power and state of charge are bounded in (6.48) and (6.49), respectively; please note that imposing $p_{e,t}^{EV}$ to be positive implies that vehicle-to-grid mode is discarded. Finally, starting from time T^{EV*}, vehicles must reach the desired state of charge X_e^{EV*} as imposed in (6.50).

Summarizing, the overall optimization problem is given by (6.1) subject to (6.3)-(6.50).

6.2 Optimization Algorithm

In this section, the proposed optimization algorithm is described. Before that, the problem just described must be formulated in its canonical form; then, the proposed algorithm is presented.

6.2.1 Problem Reformulation

The system model previously described is reformulated into a mathematical optimization problem suitable for the proposed ALM enhanced with the switching matrix framework. To apply this method, all equations are expressed in the canonical form

$$\begin{aligned} \min \quad & \mathbf{c}^T \mathbf{u} \\ s.t. \quad & \mathbf{A}\mathbf{u} \leq \mathbf{b} \end{aligned} \tag{6.51}$$

where $\mathbf{u}$ is the vector of decision variables, $\mathbf{c}$ contains linear cost coefficients, $\mathbf{A}$ is the constraint matrix, and $\mathbf{b}$ is the bound vector. All equality constraints are transformed into inequalities. For instance, constraints such as (6.22) and (6.23) are substituted in bounds (6.26) and (6.27). State equations can be rewritten in matrix form; for example, by expanding the ESS dynamic equation in (6.9) over all time steps, the following form is obtained.

$$\mathbf{x}^S = \mathbf{1}\, X_0^S + \mathbf{K}^{S,ch}\, \mathbf{p}^{S,ch} - \mathbf{K}^{S,dch}\, \mathbf{p}^{S,dch} \tag{6.52}$$

where $\mathbf{K}^{S,ch}$ and $\mathbf{K}^{S,dch}$ are lower-triangular matrices encoding the cumulative effect of charging and discharging powers over time. Then, the matrix form of each state equation is substituted into the original bound constraints, effectively removing the explicit state equations; returning to the ESS example, equation (6.52) can be substituted in (6.29).

6.2.2 Optimization algorithm

In this section, a novel ALM is proposed to optimize the overall multi-vector energy microgrid. This approach is particularly effective for handling large-scale systems with many constraints. Considering the convex optimization problem in (6.51), inequality constraints can be transformed into equalities by introducing positive slack variables $\mathbf{s}$.

$$\begin{aligned} \min_{\mathbf{u},\,\mathbf{s}\geq 0} \quad & f(\mathbf{u}) \\ s.t. \quad & \mathbf{A}\mathbf{u} - \mathbf{b} + \mathbf{s} = 0 \end{aligned} \tag{6.53}$$

The augmented Lagrangian for the problem in (6.53) is

$$L(\mathbf{u}, \mathbf{s}, \boldsymbol{\mu}) = f(\mathbf{u}) + \boldsymbol{\mu}^T(\mathbf{A}\mathbf{u} - \mathbf{b} + \mathbf{s}) + \frac{\rho}{2} \left\| \mathbf{A}\mathbf{u} - \mathbf{b} + \mathbf{s} \right\|_2^2 \tag{6.54}$$

where $\boldsymbol{\mu}$ is the vector of Lagrange multipliers associated with equality constraints. For fixed $\mathbf{u}$, the minimization of $L(\mathbf{u}, \mathbf{s}, \boldsymbol{\mu})$ with respect to $\mathbf{s}$ can be performed element-wise

$$\min_{s_j \geq 0} \quad \left[\mu_j s_j + \frac{\rho}{2} \left\| \mathbf{A}_j \mathbf{u} - b_j + s_j \right\|_2^2 \right] \tag{6.55}$$

whose explicit solution is

$$s_j = \max \left\{ 0, \, - \left(\mathbf{A}_j \mathbf{u} - b_j + \frac{\mu_j}{\rho} \right) \right\} \tag{6.56}$$

Adding $\mathbf{A}_j \mathbf{u} - b_j$ to both sides, we get

$$s_j + \mathbf{A}_j \mathbf{u} - b_j = \max \left\{ \mathbf{A}_j \mathbf{u} - b_j, \, - \frac{\mu_j}{\rho} \right\} \tag{6.57}$$

Applying the column operator $\mathbf{y} = \text{col}\{y_j, \forall j\}$, we obtain

$$\mathbf{s} + \mathbf{A}\mathbf{u} - \mathbf{b} = \max \left\{ \mathbf{A}\mathbf{u} - \mathbf{b}, \, - \frac{\boldsymbol{\mu}}{\rho} \right\} \tag{6.58}$$

Substituting into (6.54), the augmented Lagrangian becomes

$$L(\mathbf{u}, \boldsymbol{\mu}) = f(\mathbf{u}) + \boldsymbol{\mu}^T \max \left(\mathbf{A}\mathbf{u} - \mathbf{b}, - \frac{\boldsymbol{\mu}}{\rho} \right) + \frac{\rho}{2} \left\| \max \left(\mathbf{A}\mathbf{u} - \mathbf{b}, - \frac{\boldsymbol{\mu}}{\rho} \right) \right\|_2^2 \tag{6.59}$$

The ALM implementation is

$$\mathbf{u}_{\tau+1} = \arg\min_{\mathbf{u}} \left\{ f(\mathbf{u}) + \boldsymbol{\mu}_\tau^T \max \left(\mathbf{A}\mathbf{u} - \mathbf{b}, - \frac{\boldsymbol{\mu}_\tau}{\rho} \right) + \frac{\rho}{2} \left\| \max \left(\mathbf{A}\mathbf{u} - \mathbf{b}, - \frac{\boldsymbol{\mu}_\tau}{\rho} \right) \right\|_2^2 \right\} \tag{6.60}$$

$$\boldsymbol{\mu}_{\tau+1} = \boldsymbol{\mu}_\tau + \rho \, \max \left(\mathbf{A}\mathbf{u}_{\tau+1} - \mathbf{b}, - \frac{\boldsymbol{\mu}_\tau}{\rho} \right) \tag{6.61}$$

Problem (6.60) is difficult to solve due to the $\max$ operator, since this operator leads to the introduction of binary variables. Nevertheless, its solution can be simplified by noticing that problem (6.60) depends on the value of the Lagrange multipliers computed at the previous iteration $\boldsymbol{\mu}_\tau \geq 0$. Two different cases are possible:

1. $\boldsymbol{\mu}_\tau = \mathbf{0}$ for inactive constraints ($\mathbf{A}\mathbf{u} \leq \mathbf{b}$ strictly satisfied)
2. $\boldsymbol{\mu}_\tau > \mathbf{0}$ for active constraints ($\mathbf{A}\mathbf{u} = \mathbf{b}$)

Based on the previous consideration, we introduce a diagonal *switching matrix* $\mathbf{I}_\rho$, whose diagonal elements are ρ for active constraints. According to this, problem (6.60) is reformulated as follows

$$\mathbf{u}_{\tau+1} = \arg\min_{\mathbf{u}} \Big\{ f(\mathbf{u}) + \boldsymbol{\mu}_\tau^T(\mathbf{A}\mathbf{u} - \mathbf{b}) + \frac{\rho}{2}(\mathbf{A}\mathbf{u} - \mathbf{b})^T \mathbf{I}_\rho (\mathbf{A}\mathbf{u} - \mathbf{b}) \Big\} \tag{6.62}$$

Different from (6.60), the new augmented Lagrangian does not include any $\max$ operator, so no binary variables are needed. Finally, to ensure strong convexity, a proximal augmentation term $\frac{1}{2\rho}\|\mathbf{u} - \mathbf{u}_\tau\|_2^2$ is added, where $\mathbf{u}_\tau$ denotes the solution at the previous iteration. Thus, the final algorithm can be expressed as

$$\mathbf{u}_{\tau+1} = \arg\min_{\mathbf{u}} \Big\{ f(\mathbf{u}) + \boldsymbol{\mu}_\tau^T(\mathbf{A}\mathbf{u} - \mathbf{b}) + \frac{\rho}{2}(\mathbf{A}\mathbf{u} - \mathbf{b})^T \mathbf{I}_\rho (\mathbf{A}\mathbf{u} - \mathbf{b}) + \frac{1}{2\rho}\|\mathbf{u} - \mathbf{u}_\tau\|_2^2 \Big\} \tag{6.63}$$

$$\boldsymbol{\mu}_{\tau+1} = \boldsymbol{\mu}_\tau + \rho \max\{\mathbf{A}\mathbf{u}_{\tau+1} - \mathbf{b}, \mathbf{0}\} \tag{6.64}$$

6.3 Application to a case study

In this section, the optimal energy scheduling problem just formalized is tested on a case study and the main results are discussed.

6.3.1 Problem Data

Here, the main data of the optimization problem are presented. The proposed energy scheduling model is tested considering a 24-hour optimization horizon ($T = 24$) with a time step of 15 minutes ($\Delta = 0.25$ [h]) and an energy hub whose main parameters are reported in Table 6.3. Data related to the electrical and thermal networks and storage systems have been taken from a real case study, namely the Savona Campus Smart polygeneration Microgrid [161]. The bound on the temperature ramp rate, introduced to preserve hydrogen devices and limit their degradation over time, is set to ± 2°C for both the electrolyzer and the fuel cell.

6.3.2 Optimization results

The proposed methodology is tested on the case study just described and a detailed description of the results is provided in this section. The problem is implemented in Python and solved using the enhanced Lagrangian method of multipliers with the introduction of the switching matrix.
Figure 6.2 shows the electric power balance and provides an overview of the interaction between the different components over the 24-hour period within the microgrid system. Positive values represent power generation, while negative values indicate consumption. Microturbines dominate generation from midnight to noon, providing a steady supply. Solar PV contributes

Table 6.3: Problem data

$\overline{P}^{G}$[kW]	CAP_s^S[kWh]	$\Gamma_s^{S,ch}$[/]	$\Gamma_s^{S,dch}$[/]	$\overline{P}_s^{S,ch}$[kW]	$\overline{P}_s^{S,dch}$[kW]	$\underline{X}_s^S$[/]
141	0.9	1.1	35	35	0.1	0.9
$\overline{X}_s^{\mathrm{S}}$[/]	Γ^{EZ}[/]	$\overline{P}^{EZ}$[kW]	Γ^{FC}[/]	$\overline{P}^{el,FC}$[kW]	CAP^{H_2}[kg]	$\underline{X}^{H_2}$[/]
100	0.75	50	0.55	50	15	0.2
$\overline{X}^{H_2}$[kW]	$\Gamma_m^{\mu GT}$[/]	$\Theta_m^{\mu GT}$[/]	$\overline{P}_m^{el,\mu GT}$[kW]	$\overline{P}_m^{th,GT}$[kW]	Γ_b^{boil}[/]	Θ_b^{boil}[/]
0.9	0.35	0.8	65	52	0.85	0.8
$\overline{P}_b^{boil}$[kW]	LHV_{H_2}[kWh/kg]	LHV_{CH_4}[kWh/kg]	CAP_f^{HFCV}[kg]	$\underline{X}_f^{HFCV}$[/]	$\overline{X}_f^{HFCV}$[/]	X_f^{HFCV*}[/]
250	33.33	50	5	0.1	0.9	0.9
CAP_e^{EV}[kWh]	Γ_e^{EV}[/]	$\overline{P}_e^{EV,ch}$[kW]	$\overline{P}_e^{EV,dch}$[kW]	$\underline{X}_e^{EV}$[/]	$\overline{X}_e^{EV}$[/]	X_e^{EV*}[/]
60	0.9	50	50	0.2	0.9	0.9

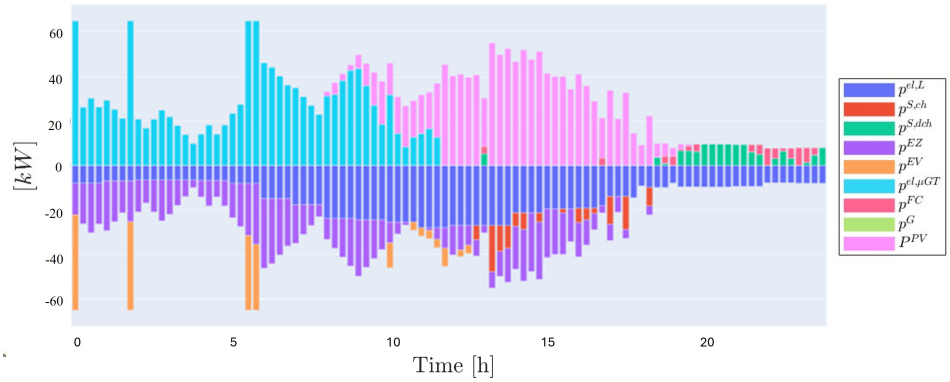

Figure 6.2: Electric power balance

significantly around midday, when sunlight is abundant. The fuel cell and the ESS discharge provide supplemental electricity in the evening and night. On the consumption side, the electrical load represents the base demand, while the electrolyzer consumes power dynamically depending on the available RES surplus. EV and ESS charging occur mainly during high PV-generation periods, efficiently using renewable energy. The thermal power balance, shown in Figure 6.3, illustrates how system components interact to satisfy thermal demand. The boiler serves as the main source during the night and evening hours, while the microturbines contribute modestly during periods of moderate demand. The thermal output of the fuel cell is negligible, highlighting its secondary role in thermal power provision. Figure 6.4 shows the hydrogen balance, which shows the integration of hydrogen production and consumption. The electrolyzer operates primarily during the first half of the day, converting excess electricity from microturbines and PV into hydrogen for storage. The fuel cell consumes hydrogen only occasionally to complement electricity demand. Figure 6.5 shows the temperature deviations for the electrolyzer and fuel cell. The electrolyzer exhibits dynamic temperature fluctuations throughout the day, reflecting its active operation and effective thermal management. The fuel cell shows deviations mainly in the evening, corresponding to its limited electricity generation. These patterns indicate effective

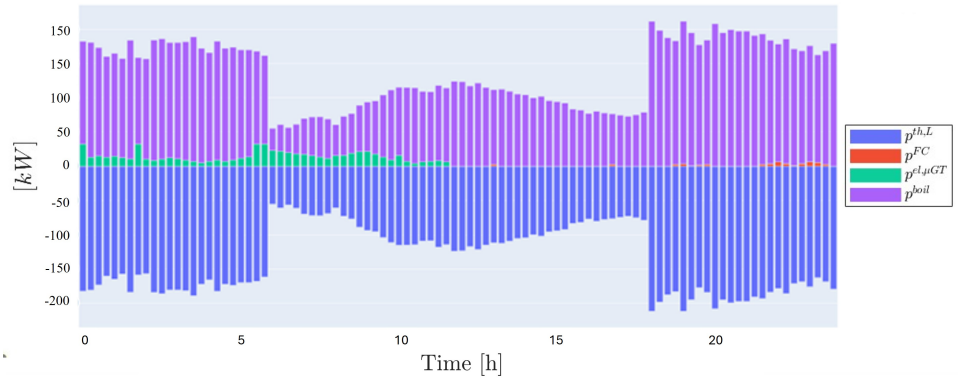

Figure 6.3: Thermal power balance

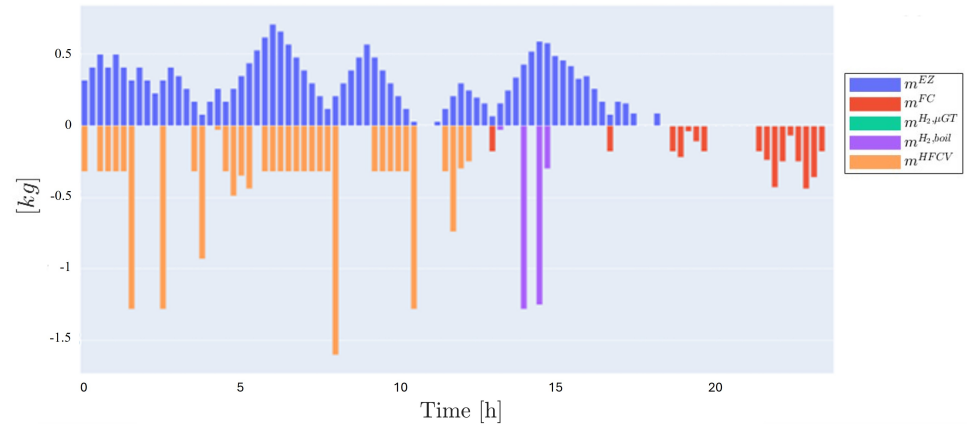

Figure 6.4: Hydrogen balance

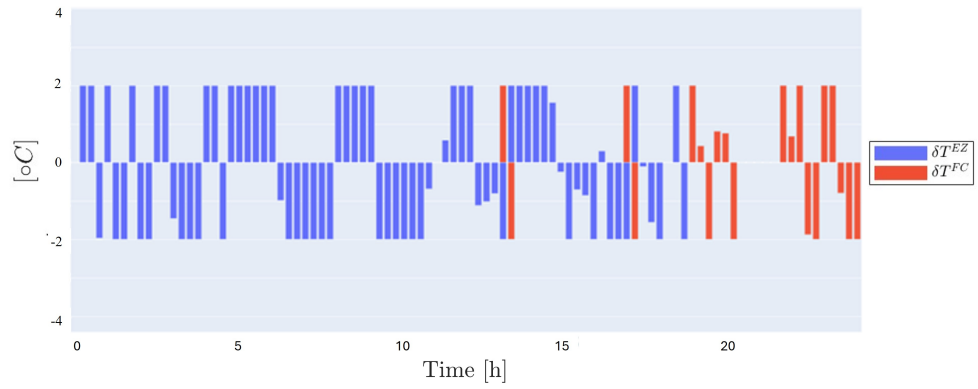

Figure 6.5: Temperature deviation of electrolyzer and fuel cell

thermal regulation within the $\pm 2°C$ tolerance.

On the computational side, the enhanced ALM achieves convergence in 45.3 seconds, with the optimality gap rapidly decreasing to below $10^{-6}\%$ after about 5500 iterations (Figure 6.6).

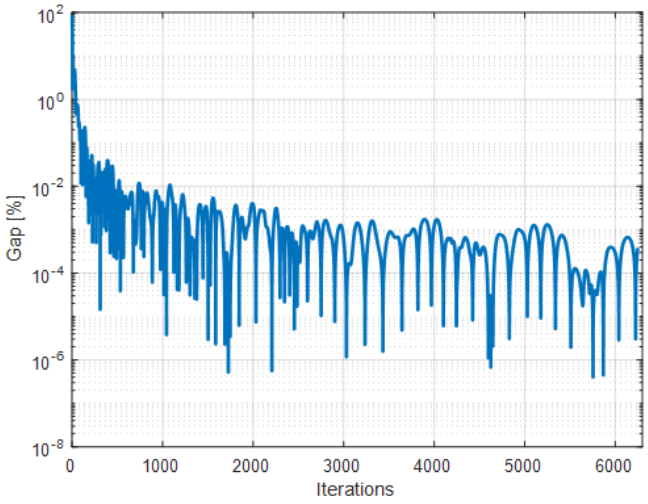

Figure 6.6: Convergence of the enhanced ALM approach using the switch matrix

Chapter 7

Conclusions and Future Developments

This thesis has investigated the role of energy management systems for the optimal management of renewable energy communities within the Italian legislative framework. Starting from the challenges posed by the large-scale integration of renewable energy sources, renewable energy communities have established themselves in recent years because they promote local production from renewable plants while enhancing the local consumption of that same renewable energy. This energy sharing is a key concept when it comes to RECs, as it represents the technical foundation for community operations as well as the basis for economic incentives. Therefore, maximizing the so-called shared energy is crucial to develop community-based projects that implement regulation-aware constraints and pursue community-level objectives. In this sense, in the beginning this thesis deals with the optimal management of a REC internal operations, where the community manager aims to maximize energy sharing among members, who in turn want to minimize their own costs. In this framework, two different problems have been developed: the first one models the real incentive scheme recently introduced by the Italian legislation, while the second problem adds the possibility that the REC participates in the balancing market by offering demand response services. Therefore, this thesis has further extended the analysis beyond internal community management by addressing the participation of RECs in flexibility and balancing mechanisms. Indeed, providing flexibility services to the grid would allow to exploit the REC inherent flexibility and would improve the economic benefit of a REC, currently relying only on the incentive for energy sharing. The results highlight that, thanks to the aggregation of multiple heterogeneous and flexible resources, RECs are well suited to provide demand response services. Nevertheless, to intensify impact and benefit of these services, a cluster of several communities could participate in the market as a single entity offering a level of operational flexibility that cannot be achieved by an individual RECs acting independently: this is possible thanks to the emerging figure of the aggregator who can manage the flexibility of several RECs and offer it to the system operator. This specific problem is addressed in a dedicated Chapter of this thesis and the coordination of multiple RECs through an aggregator has been shown to significantly enhance the available flexibility capacity, enabling effective tracking of reference power signals and improving the reliability of service provision to system operators.

Despite RECs are often associated with domestic users such as individual households or residential condominiums, the current regulatory framework also allows the participation of more complex and structured entities and aggregated energy systems. In this context, RECs can naturally extend beyond purely domestic settings to include infrastructures characterized by high power demand, flexible operation, and advanced energy management capacity. A distinctive contribution of this thesis lies in the modeling and optimal management of complex REC participants, such as smart parking lots and hydrogen-based multi-vector energy hubs which have a huge potential as RECs or REC participants. If properly managed and controlled, this potential can be further enhanced: the results indicate that integrating efficient energy management strategies at the grassroots level provides a solid foundation for the subsequent integration of community-level constraints, regulation-aware equations and energy sharing maximization objectives to encourage sustainable cooperation.

From a methodological perspective, the thesis has demonstrated that optimization models traditionally developed for microgrids can be effectively extended to renewable energy communities, provided that community-level objectives and regulatory constraints are explicitly embedded in the formulation. In particular, the maximization of shared energy has been shown to be a central objective that fundamentally shapes operational decisions, influencing load scheduling, storage utilization, and power exchange profiles with the grid. By integrating this objective alongside cost minimization and technical constraints, the proposed models capture the distinctive operational logic of RECs compared to conventional energy systems. As in microgrid applications, the choice of the optimization architecture depends on the size of the system, the heterogeneity of its assets, and the degree of coordination required. In this thesis, different optimization architectures have been explored to address the optimal management problem of RECs. Specifically, to encode the presence of multiple actors with distinct and potentially conflicting objectives and different operational constraints, multi-level optimization approaches have been applied: two levels are always developed but, depending on which level (internal or external) is considered, the formulation of each level. For internal operations, the high-level focus on shared energy maximization, while at the low-level ECPs want to minimize cost; when dealing with external operations, at the high level the aggregator tracks the reference power value from the DSO, while at the low level each REC is modeled considering ECM and ECP's objective together. When multi-level programming is not adopted, a decentralized algorithm able to exploit the structure of the problem is developed to solve the problem efficiently and effectively for real-time applications. Specifically, a new decentralized algorithm that exploits second order information to achieve fast convergence by keeping privacy among ECPs is developed in Chapter 3. For the optimal management in smart parking lots, the proposed method integrates a second-order Newton step into the dual update, thereby accelerating convergence without imposing strict convexity or Hessian invertibility constraints. Finally, the solution to the hydrogen-based multi-vector MG problem is obtained using an enhanced Augmented Lagrangian Method with a switching matrix for selective constraint enforcement.

As regards possible future developments, despite the proven potential of RECs in providing services to the grid, the presence of multiple PODs complicates activation and coordination of flexibility services, as system operators must account for spatially distributed responses rather than a single aggregated interface. Therefore, a possible future work would be investigate regulatory adaptations and aggregation mechanisms, and develop suitable control architectures able to ease REC participation in flexibility markets while ensuring reliable and verifiable service provision. Always concerning the benefits to the grid, it would be interesting to quantify how energy sharing affects the grid in terms of reverse power flow decrease and transmission/distribution losses reduction. Another possible future research direction concerns the allocation of economic benefits within renewable energy communities, with particular focus on the distribution of the incentives associated with shared energy. While existing regulatory frameworks define how incentives are calculated at the community level, the internal allocation of revenues among members is not explicitly addressed. Future works could therefore focus on the integration of incentive allocation

mechanisms within community-tailored EMS: this would include the investigation of fair and transparent allocation criteria that account for individual contributions to shared energy, flexibility provision, and community objectives. Addressing this aspect is essential to ensure long-term participation, social acceptance, and economic sustainability of renewable energy communities.

Overall, the findings of this thesis confirm that optimization-based EMS represent a powerful and necessary tool to translate the potential of renewable energy communities into operational reality. By jointly addressing several aspects, such as economic efficiency, regulatory compliance, energy sharing maximization and flexibility provision, the proposed methods contribute to REC real-world effective deployments.

Appendix

An optimization problem is characterized by three main components: decision variables, objective function, and constraints. Decision variables are those entities that represent the decisions of a specific decision problem (for example power produced by some production plant, the number and the size of charging stations in a territory, the path of a vehicle, etc.). The objective function represents the target (or the key performance indicators) of the decision problem to be minimized or maximized (like for example costs, revenues, emissions, temperature and state of charge levels); it should be a function of the decision variables and it is generally an algebraic equation. Constraints represent restrictions such as the size of production plants, emission levels from regulation, etc. An optimization problem is generally expressed by:

$$\min_{x} f(x) \tag{7.1}$$

$$s.t.$$

$$h(x) = 0 \tag{7.2}$$

$$g(x) \leq 0 \tag{7.3}$$

where $x \in \mathbb{R}^n$ is the decision variable vector, $f(x) : \mathbb{R}^n \to \mathbb{R}$ is the objective function to be minimized, $h(x) : \mathbb{R}^n \to \mathbb{R}^{n_E}$ are the functions for the equality constraints and $g(x) : \mathbb{R}^n \to \mathbb{R}^{n_I}$ for the inequality constraints. It is important to note that:

- A feasible solution is any $x \in \mathbb{R}^n$ that respects constraints (7.2)-(7.3).
- If a feasible solution minimizes (7.1), it is an optimal solution, which then provides the objective function optimal value
- Minimizing $f(x)$ is equivalent to maximizing $-f(x)$.

Example: Linear optimization problem A Linear Programming (LP) problem is a mathematical programming problem in which functions f, g and h are all linear functions (or affine functions) of the vector x of the decision variables. An affine function is a linear function plus a constant. Any LP problem can be put in the *standard form*

$$\max \quad x_0 = c^T x \tag{7.4}$$

$$s.t.$$

$$Ax = b \tag{7.5}$$

$$x \geq 0 \tag{7.6}$$

$$\tag{7.7}$$

where

$$x \in R^n$$
$$c^T \in R^n$$
$$b \in R^m$$
$$\dim [A] = m \cdot n$$

Besides, it is supposed that $m < n$ and that $rank[A] = m$. Note that c^T, A, b are the known parameters of the optimization problem.

Regarding the standard form of an LP problem,

- A vector x satisfying the matrix equality $Ax = b$ is said to be a solution.
- The solution x is said *feasible* if it also satisfies the non-negativity constraint $x > 0$.
- A feasible solution x^* is *optimal* if no other feasible solution $x^{'}$ exists such that $c^T x^{'} > c^T x^*$ (that is if no better feasible solution exists).

Bibliography

[1] H. Ritchie, "Sector by sector: where do global greenhouse gas emissions come from?," *Our World in Data*, 2020. https://archive.ourworldindata.org/20251125-173858/ghg-emissions-by-sector.html.

[2] REScoop.eu, "Transposition tracker of rec and cec." Online policy tracker, 2024. Qualitative assessment of national transposition frameworks.

[3] GSE Gestore Servizi Energetici, "Gse website." https://www.gse.it/servizi-per-te/autoconsumo.

[4] C. of European Energy Regulators, "Report on regulatory aspects of self-consumption and energy communities," Tech. Rep. C18-CRM9$_D$S7 $-$ 05 $-$ 03, $(CEER)$, $June$2019. $Accessed$: 2025 $-$ 12 $-$ 22.

[5] A. T. T. Karameros, A.I.; Chassiakos, "A novel community energy projects governance model and support ecosystem framework based on heating and cooling projects enabled by energy communities," *Sustainability*, vol. 17, 2025.

[6] E. Commission, "The european green deal." COM(2019) 640 final, Dec. 2019. Accessed: YYYY-MM-DD.

[7] Q. Hassan, P. Viktor, T. J. Al-Musawi, B. M. Ali, S. Algburi, H. M. Alzoubi, A. K. Al-Jiboory, A. Z. Sameen, H. M. Salman, and M. Jaszczur, "The renewable energy role in the global energy transformations," *Renewable Energy Focus*, vol. 48, p. 100545, 2024.

[8] I. E. Agency, "Electricity 2025, analysis and forecast to 2027," tech. rep., 2025.

[9] J. Ali, Y. Qiblawey, A. Alassi, A. Massoud, S. Muyeen, and H. Abu-Rub, "Power system stability with high penetration of renewable energy sources: Challenges, assessment, and mitigation strategies," *IEEE Access*, vol. PP, pp. 1–1, 01 2025.

[10] V. M. K. Hamed H. Pourasl, Reza Vatankhah Barenji, "Solar energy status in the world: A comprehensive review," *Energy Reports*, vol. 10, pp. 3474–3493, 2023.

[11] E. Commission, “Clean energy for all europeans,” Communication from the Commission COM(2016) 860 final, European Commission, Brussels, Nov. 2016.

[12] A. Caramizaru and A. Uihlein, “Energy communities: An overview of energy and social innovation,” Tech. Rep. JRC119433, European Commission, Joint Research Centre (JRC), Luxembourg, 2020.

[13] REScoop.eu, “Energy communities under the clean energy package: Transposition guidance,” 2020.

[14] European Parliament and Council of the European Union, “Directive (eu) 2019/944 of the european parliament and of the council of 5 june 2019 on common rules for the internal market for electricity and amending directive 2012/27/eu,” June 2019. OJ L 158, 14.6.2019, pp. 125–199.

[15] European Union, “Directive (eu) 2018/2001 of the european parliament and of the council of 11 december 2018 on the promotion of the use of energy from renewable sources,” 2018.

[16] Repubblica Italiana, “Decreto-legge 30 dicembre 2019, n. 162 (milleproroghe), art. 42-bis,” 2019. Introduzione sperimentale di autoconsumo collettivo e comunità di energia rinnovabile.

[17] Ministero dello Sviluppo Economico, “Decreto ministeriale 16 settembre 2020,” 2020. Regime incentivante sperimentale per autoconsumo collettivo e comunità energetiche.

[18] ARERA, “Delibera 318/2020/r/eel,” 2020. Regole tecniche per autoconsumo collettivo e comunità energetiche.

[19] Repubblica Italiana, “Decreto legislativo 8 novembre 2021, n. 199,” 2021. Recepimento della Direttiva (UE) 2018/2001 (RED II).

[20] ARERA, “Delibera 727/2022/r/eel,” 2022. Testo Integrato dell’Autoconsumo Diffuso (TIAD).

[21] Ministero dell’Ambiente e della Sicurezza Energetica, “Decreto ministeriale n. 414 del 7 dicembre 2023,” 2023. Schema di decreto attuativo per CER e autoconsumo diffuso.

[22] ARERA, “Delibera 15/2024/r/eel,” 2024. Aggiornamento del TIAD in attuazione del DM MASE 414.

[23] G. dei Servizi Energetici, “Regole tecniche per l’accesso al servizio di valorizzazione e incentivazione dell’energia elettrica condivisa,” 2025.

[24] G. dei Servizi Energetici, “Configurazioni per l’autoconsumo diffuso – corrispettivi e tariffa,” 2025. Accessed: 2025-12-02.

[25] IEA, “Global ev outlook 2024, moving towards increased affordability,” tech. rep., https://www.iea.org/reports/global-ev-outlook-2024/trends-in-electric-vehicle-charging, 2024.

[26] IEA, IRENA, and UN Climate Change High-Level Champions, "Breakthrough agenda report 2023," 2023. Accessed: 2025-05-15.

[27] S.-G. European Commission, "The european green deal," 2019.

[28] V. Casella, D. Fernandez Valderrama, G. Ferro, R. Minciardi, M. Paolucci, L. Parodi, and M. Robba, "Towards the integration of sustainable transportation and smart grids: A review on electric vehicles' management," *Energies*, vol. 15, no. 11, p. 4020, 2022.

[29] O. Sadeghian, A. Oshnoei, B. Mohammadi-Ivatloo, V. Vahidinasab, and A. Anvari-Moghaddam, "A comprehensive review on electric vehicles smart charging: Solutions, strategies, technologies, and challenges," *Journal of Energy Storage*, vol. 54, p. 105241, 2022.

[30] R. Kakkar, S. Agrawal, and S. Tanwar, "A systematic survey on demand response management schemes for electric vehicles," *Renewable and Sustainable Energy Reviews*, vol. 203, p. 114748, 2024.

[31] T. Harighi, A. Borghetti, F. Napolitano, and F. Tossani, "Flexibility modeling for parking lots with multiple ev charging stations," *Electric Power Systems Research*, vol. 234, p. 110732, 2024.

[32] M. Nazari-Heris, M. Abapour, and B. Mohammadi-Ivatloo, "An updated review and outlook on electric vehicle aggregators in electric energy networks," *Sustainability*, vol. 14, no. 23, p. 15747, 2022.

[33] G. Wang, Z. Zhang, and J. Lin, "Multi-energy complementary power systems based on solar energy: A review," *Renewable and Sustainable Energy Reviews*, vol. 199, p. 114464, 2024.

[34] M. Swadi, D. J. Kadhim, M. Salem, F. M. Tuaimah, A. S. Majeed, and A. J. Alrubaie, "Investigating and predicting the role of photovoltaic, wind, and hydrogen energies in sustainable global energy evolution," *Global Energy Interconnection*, vol. 7, no. 4, pp. 429–445, 2024.

[35] H. H. Pourasl, R. V. Barenji, and V. M. Khojastehnezhad, "Solar energy status in the world: A comprehensive review," *Energy Reports*, vol. 10, pp. 3474–3493, 2023.

[36] M. Jayachandran, R. K. Gatla, K. P. Rao, G. S. Rao, S. Mohammed, A. H. Milyani, A. A. Azhari, C. Kalaiarasy, and S. Geetha, "Challenges in achieving sustainable development goal 7: Affordable and clean energy in light of nascent technologies," *Sustainable Energy Technologies and Assessments*, vol. 53, p. 102692, 2022.

[37] R. Faia, F. Lezama, J. Soares, T. Pinto, and Z. Vale, "Local electricity markets: A review on benefits, barriers, current trends and future perspectives," *Renewable and Sustainable Energy Reviews*, vol. 190, p. 114006, 2024.

[38] E. Barabino, D. Fioriti, E. Guerrazzi, I. Mariuzzo, D. Poli, M. Raugi, E. Razaei, E. Schito, and D. Thomopulos, "Energy communities: A review on trends, energy system modelling, business models, and optimisation objectives," *Sustainable Energy, Grids and Networks*, vol. 36, p. 101187, 2023.

[39] C. P. S. H. A.E.H. Berjawi, S.L. Walker, "An evaluation framework for future integrated energy systems: A whole energy systems approach," *Renewable and Sustainable Energy Reviews*, vol. 145, 2021.

[40] OECD, "Global hydrogen review 2021," 2021.

[41] S. E. Hosseini, "Hydrogen fuel, a game changer for the world's energy scenario," *International Journal of Green Energy*, vol. 21, no. 6, pp. 1366–1382, 2024.

[42] E. H. T. M. A. B. Y. Erfan Abbasian Hamedani, Pooriya Khodaparast, "A mini-review of energy hub: concept, components, classifications, and applications," *Energy Reports*, vol. 15, 2026.

[43] G. Bianco, S. Bracco, F. Delfino, G. Ferro, L. Parodi, M. Robba, and M. Rossi, "A demand response energy management system (dr-ems) for sustainable district," in *2020 7th International Conference on Control, Decision and Information Technologies (CoDIT)*, vol. 1, pp. 551–556, 2020.

[44] A. P. M. R. M. R. Virginia Casella, Giulio Ferro, "A novel decentralized cooperative architecture for energy storage systems providing frequency support services," *Control Engineering Practice*, vol. 156, 2025.

[45] G. Ferro, R. Minciardi, M. Robba, and M. . Rossi, "Optimal voltage control and demand response: Integration between distribution system operator and microgrids," in *2017 IEEE 14th International Conference on Networking, Sensing and Control (ICNSC)*, pp. 435–440, 2017.

[46] C. of European Energy Regulators (CEER), "Flexibility use at distribution level: Ceer guidelines of good practice," tech. rep., CEER, 2024.

[47] I. Bouloumpasis and et al., "Local flexibility market framework for grid support services in distribution networks," *Mathematical and Computer Modelling of Dynamical Systems (or relevant journal)*, 2022.

[48] V. Talaeizadeh, "Day-ahead flexibility market clearing mechanism for distribution network congestion management," *IET Generation, Transmission Distribution*, 2022.

[49] F. Gulotta, A. Rossi, F. Bovera, D. Falabretti, A. Galliani, M. Merlo, and G. Rancilio, "Opening of the italian ancillary service market to distributed energy resources: Preliminary results of uvam project," in *2020 IEEE 17th International Conference on Smart Communities: Improving Quality of Life Using ICT, IoT and AI (HONET)*, pp. 199–203, 2020.

[50] E. Mohammadi, M. Alizadeh, M. Asgarimoghaddam, X. Wang, and M. G. Simões, "A review on application of artificial intelligence techniques in microgrids," *IEEE Journal of Emerging and Selected Topics in Industrial Electronics*, vol. 3, no. 4, pp. 878–890, 2022.

[51] A. Parisio, E. Rikos, and L. Glielmo, "A model predictive control approach to microgrid operation optimization," *IEEE Transactions on Control Systems Technology*, vol. 22, no. 5, pp. 1813–1827, 2014.

[52] E. Espina, J. Llanos, C. Burgos-Mellado, R. Cárdenas-Dobson, M. Martínez-Gómez, and D. Sáez, "Distributed control strategies for microgrids: An overview," *IEEE Access*, vol. 8, pp. 193412–193448, 2020.

[53] A. Cortés and S. Martínez, "On distributed reactive power and storage control on microgrids," *International Journal of Robust and Nonlinear Control*, vol. 26, pp. n/a–n/a, 09 2016.

[54] R. Scattolini, "Architectures for distributed and hierarchical model predictive control – a review," *Journal of Process Control*, vol. 19, no. 5, pp. 723–731, 2009.

[55] S. A. Gabriel, A. J. Conejo, J. D. Fuller, B. F. Hobbs, and C. Ruiz, *Complementarity modeling in energy markets*, vol. 180. Springer Science & Business Media, 2012.

[56] S. Ahmed, A. Ali, and A. D'Angola, "A review of renewable energy communities: Concepts, scope, progress, challenges, and recommendations," *Sustainability*, vol. 16, p. 1749, Feb. 2024.

[57] F. Vecchi, R. Stasi, and U. Berardi, "Modelling tools for the assessment of renewable energy communities," *Energy Reports*, vol. 11, pp. 3941–3962, June 2024.

[58] B. Laurini, B. Bonvini, and S. Bracco, "Optimal design model for a public-private renewable energy community in a small italian municipality," *Sustainable Energy, Grids and Networks*, vol. 40, p. 101545, 2024.

[59] G. G. Zanvettor, M. Casini, A. Giannitrapani, S. Paoletti, and A. Vicino, "Optimal management of energy communities hosting a fleet of electric vehicles," *Energies*, vol. 15, p. 8697, Nov. 2022.

[60] F. Conte, F. D'Antoni, G. Natrella, and M. Merone, "A new hybrid ai optimal management method for renewable energy communities," *Energy and AI*, vol. 10, p. 100197, Nov. 2022.

[61] J. Li and et al., "Cuems: Deep reinforcement learning for community energy management system," *Applied Energy*, 2024.

[62] J. Faraji, Z. De Grève, and F. Vallée, "Hierarchical energy sharing management for a renewable energy community with heterogeneous end-users," in *2023 IEEE Belgrade PowerTech*, (Belgrade, Serbia), pp. 1–8, IEEE, June 2023.

[63] G. Barone, A. Buonomano, C. Forzano, A. Palombo, and G. Russo, "The role of energy communities in electricity grid balancing: A flexible tool for smart grid power distribution optimization," *Renewable and Sustainable Energy Reviews*, vol. 187, p. 113742, Nov. 2023.

[64] A. Cosic, M. Stadler, M. Mansoor, and M. Zellinger, "Mixed-integer linear programming based optimization strategies for renewable energy communities," *Energy*, vol. 235, p. 121345, 2021.

[65] S. Mohsen Hosseini, R. Carli, J. Jantzen, and M. Dotoli, "Multi-block admm approach for decentralized demand response of energy communities with flexible loads and shared energy storage system," in *2022 30th Mediterranean Conference on Control and Automation (MED)*, pp. 67–72, 2022.

[66] P. Scarabaggio, R. Carli, J. Jantzen, and M. Dotoli, "Stochastic model predictive control of community energy storage under high renewable penetration," in *2021 29th Mediterranean Conference on Control and Automation (MED)*, pp. 973–978, 2021.

[67] M. Calefati, S. Proia, P. Scarabaggio, R. Carli, and M. Dotoli, "A decentralized noncooperative control approach for sharing energy storage systems in energy communities," in *2021 IEEE International Conference on Systems, Man, and Cybernetics (SMC)*, pp. 1430–1435, 2021.

[68] L. Gomes and Z. Vale, "Costless renewable energy distribution model based on cooperative game theory for energy communities considering its members' active contributions," *Sustainable Cities and Society*, vol. 101, p. 105060, Feb. 2024.

[69] N. Mignoni, J. Martinez-Piazuelo, R. Carli, C. Ocampo-Martinez, N. Quijano, and M. Dotoli, "A game-theoretical control framework for transactive energy trading in energy communities," in *2024 European Control Conference (ECC)*, pp. 786–791, 2024.

[70] M. Stephant, D. Abbes, K. Hassam-Ouari, A. Labrunie, and B. Robyns, "Distributed optimization of energy profiles to improve photovoltaic self-consumption on a local energy community," *Simulation Modelling Practice and Theory*, vol. 108, p. 102242, 2021.

[71] L. Zhang, S. Li, Q. Nie, and Y. Hu, "A two-stage benefit optimization and multi-participant benefit-sharing strategy for hybrid renewable energy systems in rural areas under carbon trading," *Renewable Energy*, vol. 189, pp. 744–761, 2022.

[72] M. A. M. Messilem, D. Deplano, M. Franceschelli, E. Usai, and R. Carli, "Distributed optimization for networks of battery energy storage systems in energy communities with shared energy incentives," in *2024 IEEE 20th International Conference on Automation Science and Engineering (CASE)*, (Bari, Italy), pp. 2745–2751, IEEE, Aug. 2024.

[73] J. J. Moré, D. Deplano, A. Pilloni, A. Pisano, and M. Franceschelli, "Online coordination of bess and thermostatically control loads for shared energy optimization in energy communities," in *2024 IEEE 20th International Conference on Automation Science and Engineering (CASE)*, (Bari, Italy), pp. 2738–2744, IEEE, Aug. 2024.

[74] F. R. Bianchi *et al.*, "Modelling and optimal management of renewable energy communities using reversible solid oxide cells," *Applied Energy*, vol. 334, p. 120657, Mar. 2023.

[75] G. Talluri, G. M. Lozito, F. Grasso, C. Iturrino Garcia, and A. Luchetta, "Optimal battery energy storage system scheduling within renewable energy communities," *Energies*, vol. 14, p. 8480, Dec. 2021.

[76] M. Stentati, S. Paoletti, and A. Vicino, "Optimization of energy communities in the italian incentive system," in *2022 IEEE PES Innovative Smart Grid Technologies Conference Europe (ISGT-Europe)*, (Novi Sad, Serbia), pp. 1–5, IEEE, Oct. 2022.

[77] M. Di Somma, D. Cimmino, M. Dolatabadi, N. Bianco, A. Burgio, and P. Siano, "Optimizing virtual energy sharing in renewable energy communities of residential users for incentives maximization," *Sustainable Energy, Grids and Networks*, vol. 39, p. 101492, 2024.

[78] F. D'Amico, L. De Santoli, and L. Martirano, "Analyzing wind and photovoltaic plant development toward the energy transition in italy," *Energy Reports*, vol. 16, p. 102345, 2025. Accessed October 2025.

[79] T. S.p.A., "Electricity consumption and installed capacity in italy, 2024." Press release, 2025. Accessed October 2025.

[80] NextGenerationEU and GSE Gestore Servizi Elettrici, "Regole operative per l'accesso al servizio per l'autoconsumo diffuso e al contributo pnrr." `https://www.mase.gov.it/sites/default/files/ALLEGATO%201%20Regole%20operative%20CACER%20def.pdf`, Feb. 2024. MASE - Ministero dell'Ambiente e della Sicurezza Energetica.

[81] K. Biswas, S. Kumar, S. Banerjee, and A. K. Pandey, "Smooth maximum unit: Smooth activation function for deep networks using smoothing maximum technique," in *2022 IEEE/CVF Conference on Computer Vision and Pattern Recognition (CVPR)*, (New Orleans, LA, USA), pp. 784–793, IEEE, June 2022.

[82] J. Lofberg, "Yalmip: A toolbox for modeling and optimization in matlab," in *2004 IEEE international conference on robotics and automation (IEEE Cat. No. 04CH37508)*, pp. 284–289, IEEE, 2004.

[83] G. Ferro, M. Robba, R. Haider, and A. M. Annaswamy, "A second-order dual update approach for the decentralized optimal scheduling of polygenerative microgrids," *IEEE Transactions on Control Systems Technology*, pp. 1–13, 2025.

[84] V. Casalicchio, G. Manzolini, M. G. Prina, and D. Moser, "From investment optimization to fair benefit distribution in renewable energy community modelling," *Applied Energy*, vol. 310, p. 118447, 2022.

[85] I. Aranzabal and et al., "Optimal management of an energy community with pv + bess including aggregated afrr market participation," *LAPSE:2023.20639*, 2023.

[86] H. Chamandoust, S. Bahramara, and G. Derakhshan, "Day-ahead scheduling problem of smart micro-grid with high penetration of wind energy and demand side management strategies," *Sustainable Energy Technologies and Assessments*, vol. 40, p. 100747, 2020.

[87] R. Tutunov, H. Bou-Ammar, and A. Jadbabaie, "Distributed newton method for large-scale consensus optimization," *IEEE Transactions on Automatic Control*, vol. 64, no. 10, pp. 3983–3994, 2019.

[88] M. Wu, N. Xiong, A. V. Vasilakos, V. C. Leung, and C. P. Chen, "Rnn-k: A reinforced newton method for consensus-based distributed optimization and control over multiagent systems," *IEEE Transactions on Cybernetics*, vol. 52, no. 5, pp. 4012–4026, 2020.

[89] H. Ye, C. He, and X. Chang, "Accelerated distributed approximate newton method," *IEEE Transactions on Neural Networks and Learning Systems*, 2022.

[90] M. Zarghamy, A. Ribeiroy, and A. Jadbabaiey, "Accelerated dual descent for constrained convex network flow optimization," in *52nd IEEE Conference on Decision and Control*, pp. 1037–1042, IEEE, 2013.

[91] R. Hult, M. Zanon, S. Gros, and P. Falcone, "Energy-optimal coordination of autonomous vehicles at intersections," in *2018 European control conference (ECC)*, pp. 602–607, IEEE, 2018.

[92] A. Kozma, E. Klintberg, S. Gros, and M. Diehl, "An improved distributed dual newton-cg method for convex quadratic programming problems," in *2014 American Control Conference*, pp. 2324–2329, IEEE, 2014.

[93] E. Klintberg and S. Gros, "A parallelizable interior point method for two-stage robust mpc," *IEEE Transactions on Control Systems Technology*, vol. 25, no. 6, pp. 2087–2097, 2016.

[94] H. Firoozi, H. Khajeh, and H. Laaksonen, "Optimized operation of local energy community providing frequency restoration reserve," *IEEE Access*, vol. 8, pp. 180558–180575, 2020.

[95] T. A. Howell, B. E. Jackson, and Z. Manchester, "Altro: A fast solver for constrained trajectory optimization," in *2019 IEEE/RSJ International Conference on Intelligent Robots and Systems (IROS)*, pp. 7674–7679, IEEE, 2019.

[96] B. E. Jackson, T. Punnoose, D. Neamati, K. Tracy, R. Jitosho, and Z. Manchester, "Altro-c: A fast solver for conic model-predictive control," in *2021 IEEE International Conference on Robotics and Automation (ICRA)*, pp. 7357–7364, IEEE, 2021.

[97] M. Caliano, F. Delfino, M. Di Somma, G. Ferro, G. Graditi, L. Parodi, M. Robba, and M. Rossi, "An energy management system for microgrids including costs, exergy, and stress indexes," *Sustainable Energy, Grids and Networks*, vol. 32, p. 100915, 2022.

[98] A. A. di Regolazione per Energia Reti e Ambiente, "Analisi dei consumi dei clienti domestici," 2023.

[99] V. Casella, G. Ferro, L. Parodi, and M. Robba, "Energy community optimal management: A bilevel approach," in *2024 IEEE 20th International Conference on Automation Science and Engineering (CASE)*, pp. 2720–2725, IEEE, 2024.

[100] S. Boyd, N. Parikh, E. Chu, B. Peleato, J. Eckstein, *et al.*, "Distributed optimization and statistical learning via the alternating direction method of multipliers," *Foundations and Trends® in Machine learning*, vol. 3, no. 1, pp. 1–122, 2011.

[101] J. Sheikh Ali, Y. Qiblawey, A. Alassi, A. M. Massoud, and S. M. Muyeen, "Power system stability with high penetration of renewable energy sources: Challenges, assessment and mitigation strategies," *IEEE Access*, 2025. Survey on stability issues in power systems with high RES penetration.

[102] A. Dimovski, M. Moncecchi, and M. Merlo, "Impact of energy communities on the distribution network: An italian case study," *Sustainable Energy, Grids and Networks*, vol. 35, p. 101148, 2023.

[103] A. Dimovski, C. M. Caminiti, G. Rancilio, M. Ricci, B. Di Pietra, and M. Merlo, "A focus on reverse power flow and energy balance," *Energies*, vol. 18, no. 5, p. 1255, 2025.

[104] S. Mocci, S. Ruggeri, and F. Pilo, "Low-voltage renewable energy communities' impact on the distribution networks," *Energies*, vol. 18, no. 1, p. 126, 2024.

[105] European Commission, "The european green deal." `https://eur-lex.europa.eu/legal-content/EN/TXT/?uri=CELEX:52019DC0640`, 2019. COM(2019) 640 final, Brussels, 11 December 2019.

[106] A. available on ScienceDirect, "Multi-objective optimization for renewable energy communities: From design to operation," *Sustainable Energy, Grids and Networks*, vol. 28, p. 100551, 2021.

[107] A. available on ScienceDirect, "Energy community models for residential prosumers: A review and future trends," *Energy and Buildings*, vol. 210, p. 109817, 2020.

[108] S. Gabriel, A. Conejo, J. Fuller, B. Hobbs, and C. Ruiz, *Complementarity Modeling in Energy Markets*, vol. 180. Springer Nature, 01 2013.

[109] GSE - Gestore dei Servizi Energetici, "Renewable energy communities and self-consumer groups: Published 2024 standard profiles for withdrawal and injection," 2024. Italian Energy Service Agency (GSE) official communication.

[110] M. Caliano, F. Delfino, M. Di Somma, G. Ferro, G. Graditi, L. Parodi, M. Robba, and M. Rossi, "An energy management system for microgrids including costs, exergy, and stress indexes," *Sustainable Energy, Grids and Networks*, vol. 32, p. 100915, 2022.

[111] U.S. Department of Energy, Office of Electricity, "Impact of electric vehicles on the grid," report to congress, U.S. Department of Energy, June 2024. Prepared in response to H. Rept. 117-394 – Energy and Water Development and Related Agencies Appropriations Bill, 2023.

[112] Q. Fu, Y. Ding, Y. Wang, and L. Yu, "Goal-oriented heuristic dynamic programming for scheduling of virtual energy hubs with management of intelligent parking lot," *Sustainable Energy, Grids and Networks*, p. 101718, 2025.

[113] A. Varone, Z. Heilmann, G. Porruvecchio, and A. Romanino, "Solar parking lot management: An iot platform for smart charging ev fleets, using real-time data and production forecasts," *Renewable and Sustainable Energy Reviews*, vol. 189, p. 113845, 2024.

[114] A. Leippi, M. Fleschutz, K. Davis, A.-L. Klingler, and M. D. Murphy, "Optimizing electric vehicle fleet integration in industrial demand response: Maximizing vehicle-to-grid benefits while compensating vehicle owners for battery degradation," *Applied Energy*, vol. 374, p. 123995, 2024.

[115] İ. Şengör, S. Güner, and O. Erdinç, "Real-time algorithm based intelligent ev parking lot charging management strategy providing pll type demand response program," *IEEE Transactions on Sustainable Energy*, vol. 12, no. 2, pp. 1256–1264, 2020.

[116] M. Alinejad, O. Rezaei, A. Kazemi, and S. Bagheri, "An optimal management for charging and discharging of electric vehicles in an intelligent parking lot considering vehicle owner's random behaviors," *Journal of Energy Storage*, vol. 35, p. 102245, 2021.

[117] Z. Yang, X. Huang, T. Gao, Y. Liu, and S. Gao, "Real-time energy management strategy for parking lot considering maximum penetration of electric vehicles," *IEEE Access*, vol. 10, pp. 5281–5291, 2022.

[118] M. Shariatzadeh, C. H. Antunes, and M. A. Lopes, "Charging scheduling in a workplace parking lot: Bi-objective optimization approaches through predictive analytics of electric vehicle users' charging behavior," *Sustainable Energy, Grids and Networks*, vol. 39, p. 101463, 2024.

[119] I. Chandra, N. K. Singh, P. Samuel, M. Bajaj, and I. Zaitsev, "Coordinated charging of ev fleets in community parking lots to maximize benefits using a three-stage energy management system," *Scientific Reports*, vol. 14, no. 1, p. 32026, 2024.

[120] M. Valizadeh, F. Moradi, A. K. Sarvenoee, M. Kohzadipour, N. Gowtham, and K. M. Aboras, "Economic management of an intelligent parking lot using a time-based load response program," *IEEE Access*, 2024.

[121] T. Gökçek, A. R. Boynueğri, S. Güner, O. Erdinç, and J. Sadreddini, "A new distributed charge approach for the electric vehicle parking lots considering coordination between dso and ev operators," *Applied Energy*, vol. 390, p. 125780, 2025.

[122] W. Wang and L. Wu, "A semi-decentralized real-time charging scheduling scheme for large ev parking lots considering uncertain ev arrival and departure," *IEEE Transactions on Smart Grid*, 2024.

[123] D. Yan, C. Ma, and Y. Chen, "Distributed coordination of charging stations considering aggregate ev power flexibility," *IEEE Transactions on Sustainable Energy*, vol. 14, no. 1, pp. 356–370, 2022.

[124] V. Casella, G. Ferro, and M. Robba, "A decentralized optimization approach to the power management of electric vehicles parking lots," *Sustainable Energy, Grids and Networks*, vol. 38, p. 101301, 2024.

[125] M. Aicardi and G. Ferro, "A newton-based dual update framework for admm in convex optimization problems," *IEEE Control Systems Letters*, 2024.

[126] A. Bemporad, M. Morari, V. Dua, and E. N. Pistikopoulos, "The explicit linear quadratic regulator for constrained systems," *Automatica*, vol. 38, no. 1, pp. 3–20, 2002.

[127] S. Boyd, N. Parikh, E. Chu, B. Peleato, and J. Eckstein, "Distributed optimization and statistical learning via the alternating direction method of multipliers," *Foundations and Trends® in Machine Learning*, vol. 3, no. 1, pp. 1–122, 2011.

[128] T. V. Dang, K. V. Ling, and J. M. Maciejowski, "Embedded admm-based qp solver for mpc with polytopic constraints," in *2015 European Control Conference (ECC)*, pp. 3446–3451, IEEE, 2015.

[129] D. P. Bertsekas, *Constrained optimization and Lagrange multiplier methods*. Academic press, 2014.

[130] I. E. Agency, "Empowering electricity markets: How sector coupling and flexibility are reshaping energy systems," tech. rep., IEA, 2024. Accessed: 2025-01.

[131] M. Marzband, M. Savaghebi, J. M. Guerrero, M. Shafie-khah, and J. P. Catalão, "A hybrid energy management system for multi-vector microgrids: Optimal scheduling of electricity, heating, cooling and gas resources," *Applied Energy*, vol. 344, p. 120246, 2023.

[132] M. Ghofrani and et al., "A comprehensive review on multi-energy systems: Architectures, optimization, and energy management," *Renewable and Sustainable Energy Reviews*, vol. 192, p. 113128, 2024.

[133] N. Ghadimi and et al., "Hydrogen-integrated multi-energy microgrids: A systematic review of technologies, control, and optimization," *Energy Conversion and Management*, vol. 281, p. 116774, 2023.

[134] International Energy Agency, "Global hydrogen review 2023," 2023.

[135] R. Khakimov, A. Moskvin, and O. Zhdaneev, "Hydrogen as a key technology for long-term and seasonal energy storage applications," *International Journal of Hydrogen Energy*, vol. 68, pp. 374–381, 2024.

[136] Y. Zhao, C. Wang, Z. Zhang, and H. Lv, "Flexibility evaluation method of power system considering the impact of multi-energy coupling," *IEEE Transactions on Industry Applications*, vol. 57, no. 6, pp. 5687–5697, 2021.

[137] M. Zarei and et al., "A review on multi-energy microgrids with hydrogen storage systems," *International Journal of Hydrogen Energy*, 2024.

[138] M. Tostado-Véliz, A. R. Jordehi, L. Fernández-Lobato, and F. Jurado, "Robust energy management in isolated microgrids with hydrogen storage and demand response," *Applied Energy*, vol. 345, p. 121319, 2023.

[139] V. Khaligh, M. K. Ghasemnejad, A. Ghezelbash, J. Liu, and W. Won, "Risk-constrained energy management of an isolated multi-energy microgrid enhanced with hydrogen storage," *Journal of Energy Storage*, vol. 63, p. 107103, 2023.

[140] J. Massana, L. Burgas, S. Herraiz, J. Colomer, and C. Pous, "Multi-vector energy management system including scheduling electrolyzer, electric vehicle charging station and other assets in a real scenario," *Journal of Cleaner Production*, vol. 380, p. 134996, 2022.

[141] Y. Zheng, J. Jia, and D. An, "Energy management for microgrids with hybrid hydrogen-battery storage: A reinforcement learning framework integrated multi-objective dynamic regulation," *Processes*, vol. 13, no. 8, p. 2558, 2025.

[142] Z. F. B. X. Ning Qi, Kaidi Huang, "Long-term energy management for microgrid with hybrid hydrogen-battery energy storage: A prediction-free coordinated optimization framework," *Applied Energy*, vol. 377, no. Part B, p. 124485, 2025.

[143] X. Jia, Z. Li, Y. Xia, Z. Yan, H. Gao, D. Qiu, and J. M. Guerrero, "Coordinated operation of multi-energy microgrids considering green hydrogen and congestion management via a safe policy learning approach," *Applied Energy*, vol. 401, p. 126611, 2025.

[144] P. Horrillo-Quintero, P. García-Triviño, E. Hosseini, C. A. G. Vázquez, H. Sánchez-Sainz, and L. M. Fernández-Ramírez, "Coordinated operation of electricity, hydrogen, and thermal systems in a residential multi-energy microgrid," *IEEE Transactions on Industry Applications*, pp. 1–17, 2025.

[145] G. W. Y. L. J. Y. Rui Qiu, Haoran Zhang, "Green hydrogen-based energy storage service via power-to-gas technologies integrated with multi-energy microgrid," *Applied Energy*, vol. 350, no. 121716, 2023.

[146] H.-M. K. Muhammad Ahsan Khan, Talha Rehman, "Optimal operation of hydrogen-based multi-energy microgrid integrating water network and transportation sector," *International Journal of Hydrogen Energy*, vol. 97, pp. 501–515, 2025.

[147] H. S. Reza Hemmati, Seyyed Mohammad Bornapour, "Standalone hybrid power-hydrogen system incorporating daily-seasonal green hydrogen storage and hydrogen refueling station," *Energy*, vol. 295, 2024.

[148] G. Mancò and et al., "A review on multi energy systems modelling and optimization," *Renewable and Sustainable Energy Reviews*, 2024.

[149] P. Sasidhar and et al., "Multi-energy microgrid design and the role of coupling components – a review," *Energy*, 2025.

[150] N. Nikmehr, "Distributed robust operational optimization of networked microgrids embedded interconnected energy hubs," *Energy*, vol. 199, p. 117440, 2020.

[151] F. J. Lin, J. C. Liao, Y. M. Zhang, and Y. C. Huang, "Optimal economic dispatch and power generation for microgrid using novel lagrange multipliers-based method with hil verification," *IEEE Systems Journal*, vol. 17, no. 3, pp. 4533–4544, 2023.

[152] K. Wu, Q. Li, Z. Chen, J. Lin, Y. Yi, and M. Chen, "Distributed optimization method with weighted gradients for economic dispatch problem of multi-microgrid systems," *Energy*, vol. 222, p. 119898, 2021.

[153] X. Kong, D. Liu, C. Wang, F. Sun, and S. Li, "Optimal operation strategy for interconnected microgrids in market environment considering uncertainty," *Applied Energy*, vol. 275, 2020.

[154] X. Shi, Y. Xu, G. Chen, and Y. Guo, "An augmented lagrangian-based safe reinforcement learning algorithm for carbon-oriented optimal scheduling of ev aggregators," *IEEE Transactions on Smart Grid*, vol. 15, no. 1, pp. 795–809, 2024.

[155] M. Zaery, P. Wang, W. Wang, and D. Xu, "A novel fully distributed fixed-time optimal dispatch of dc multi-microgrids," *International Journal of Electrical Power and Energy Systems*, vol. 129, p. 106792, 2021.

[156] J. Li, H. Mo, Q. Sun, W. Wei, and K. Yin, "Distributed optimal scheduling for virtual power plant with high penetration of renewable energy," *International Journal of Electrical Power and Energy Systems*, vol. 160, 2024.

[157] Y. Liu, Y. Wang, Y. Li, H. B. Gooi, and H. Xin, "Multi-agent based optimal scheduling and trading for multi-microgrids integrated with urban transportation networks," *IEEE Transactions on Power Systems*, vol. 36, no. 3, pp. 2197–2210, 2021.

[158] Y. Ennassiri, G. Ferro, D. Bellotti, L. Magistri, and M. Robba, "Optimal scheduling and real-time control of a microgrid with an electrolyzer and a fuel cell systems using a reference governor approach," *Sustainable Energy, Grids and Networks*, vol. 36, p. 101218, 2023.

[159] J. Mao, Z. Li, J. Xuan, X. Du, M. Ni, and L. Xing, "A review of control strategies for proton exchange membrane (pem) fuel cells and water electrolyzers: From automation to autonomy," *Energy and AI*, vol. 17, p. 100406, 2024.

[160] C. Haoran, Y. Xia, W. Wei, Z. Yongzhi, Z. Bo, and Z. Leiqi, "Safety and efficiency problems of hydrogen production from alkaline water electrolyzers driven by renewable energy sources," *International Journal of Hydrogen Energy*, vol. 54, pp. 700–712, 2024.

[161] S. Bracco, F. Delfino, F. Pampararo, M. Robba, and M. Rossi, "The university of genoa smart polygeneration microgrid test-bed facility: The overall system, the technologies and the research challenges," *Renewable and sustainable energy reviews*, vol. 18, pp. 442–459, 2013.